NASA Contractor Report 177597

A Study of the Control Problem of the Shoot Side Environment Delivery System of a Closed Crop Growth Research Chamber

C. C. Blackwell and A. L. Blackwell, The University of Texas at Arlington, Arlington, Texas

June 1992

National Aeronautics and
Space Administration

Ames Research Center
Moffett Field, California 94035-1000

CONTENTS

CONTENTS iii

LIST OF FIGURES AND TABLES vi

ABBREVIATIONS, ACRONYMS, DEFINITIONS, AND SYMBOLS vii

1 - INTRODUCTION 1

1.1 - Organization of the Report 4

2 - DESCRIPTION OF THE SHOOT ENVIRONMENT DELIVERY SYSTEM 4

3 - PERFORMANCE AND PHYSICAL CONFIGURATION REQUIREMENTS 7

4 - PURPOSE OF THE MODEL 8

5 - THE MATHEMATICAL MODEL OF THE CROP SHOOT ENVIRONMENT DELIVERY SYSTEM 9

5.1 - SUMMARY OF THE PHASES OF THE MODEL GENERATION PROCEDURE 10

5.2 - THE MODELING PROCESSES 12

5.3 - THE MODELING SYSTEM 15

5.4 - THE PRIMITIVE EQUATIONS 16

5.5 - THE MODELED SCENARIO 41

PRECEDING PAGE BLANK NOT FILMED

CONTENTS (Continued)

5.6 - NOMINAL VALUES OF THE POINT VARIABLES AND THE PATH VARIABLES 42

5.7 - THE CONDENSED PRIMITIVE EQUATIONS 46

5.8 - THE STATE VARIABLE FORM OF THE LINEARIZED MATHEMATICAL MODEL 50

6 - SOME PROPERTIES OF THE LINEARIZED STATE VARIABLE MODEL 53

6.1 - A REAL JORDAN CANONICAL FORM OF THE LINEAR TIME INVARIANT STATE VARIABLE REPRESENTATION 54

7 - AN ELEMENTARY CONTROL STUDY 63

8 - CONCLUDING REMARKS 71

ACKNOWLEDGEMENTS 72

REFERENCES 72

APPENDICES 74

A1. A formal symbology and structure for generating the mathematical model of mixed energy systems; A. L. Blackwell and C. C. Blackwell. 1990. A modeling system for control of the thermal and fluid dynamics of the NASA CELSS Crop Growth Research Chamber, *SAE Transactions: J. Aerospace*, 90(1):1073-1089. ..... A1.1

CONTENTS (Continued)

A2. A brief summary of some of the results obtained in the study; A. L. Blackwell and C. C. Blackwell. 1990. Development of a model for control of the NASA CELSS Crop Growth Research Chamber. *Proceedings of the 1990 American Control Conference.* San Diego, California, USA 23 - 25 May, 3:2113-2114. ..... A2.1

A3. The linear state variable representation coefficient matrices. A3.1

LIST OF FIGURES AND TABLES

FIGURES

Figure 1. Diagram of a CELSS 2

Figure 2. Diagram of the Crop Shoot Side Environment Delivery System: overall system visualization emphasized 5

Figure 3. Diagram of the Crop Shoot Side Environment Delivery System: visualization needed for model synthesis emphasized 6

Figure 4. The fluid flow portion of the CSSEDS modeling system 13

Figure 5. The thermal portion of the CSSEDS modeling system 14

TABLES

Table 1. Assignment of the Perturbation Primitive Variables to the Fundamental Variables. 47

Table 2. Assignment of the Fundamental Variables to the Perturbation Primitive Variables. 48

ABBREVIATIONS, ACRONYMS, DEFINITIONS, AND SYMBOLS

ABBREVIATIONS AND ACRONYMS

AC/HS - Airflow cooling/heating system.

CELSS - Controlled ecological life support system.

CGC - Crop growth chamber.

CGRC - Crop growth research chamber.

CJEM - Complex Jordan eigenvalue matrix.

CJMM - Complex Jordan modal matrix.

CSSEDS - Crop Shoot Side Environmental Delivery System.

GIMC - Gas injection and mixing chamber.

JCT - Jordan canonical transformation.

MMA&S - Mathematical modeling, analysis, and simulation.

RJCT - Real Jordan canonical transformation.

RJEM - Real Jordan eigenvalue matrix.

RJMM - Real Jordan modal matrix.

SVD - the Singular Value Decomposition.

DEFINITIONS

$(\dot{\cdot}) \triangleq d(\cdot)/dt$

$\partial f/\partial x$ the partial derivative of f with respect to x

SYMBOLS

$\mathcal{A}$	state coefficient matrix of the linear state variable format model of a system
$A_1, \cdots A_5$	coefficient matrices of linear model primary equations.
A_i	duct cross sectional area in flow path i (m^2)
A_i	area of surface i (m^2)
A_{pf}	crop growth platform area (m^2)
A_v	valve flow area (m^2)
air	dry air
$\mathcal{B}$	control variable coefficient matrix of the linear state variable format model of a system
b_1	rotational bearing linear drag coefficient (N-m/(rad/sec))
b_2	motor and blower windage coefficient (N-m/(rad/sec)^2)
$B_1, \cdots B_4$	coefficient matrices of linear model secondary equations
$\mathcal{C}$	disturbance variable coefficient matrix of the linear state variable format model of a system
c_{p_i}	molar specific heat for a constant pressure process of the gas flowing in volume i (Joules mol^{-1} K^{-1})
c_{v_i}	molar specific heat for a constant volume process of the gas flowing in volume i (Joules mol^{-1} K^{-1})
$Cc_{j,k}$	molar concentration of constituent k at the point j
CO_2	carbon dioxide
d(t)	the vector of modeled system disturbances
$d_{PPF_{ref}}$	distance from lamps at which PPF is at the required value (m)
d_{pf}	thickness of plant root chamber (m)

SYMBOLS (continued)

$\mathfrak{D}$	state variable matrix coefficient of the secondary variable output equation of the linear state variable format model of a system
D	duct diameter (m)
$\mathfrak{E}$	control variable matrix coefficient of the secondary variable output equation of the linear state variable format model of a system
$\dot{E}_j$	rate of energy accumulation at point i (Watts)
$\mathfrak{F}$	disturbance variable matrix coefficient of the secondary variable output equation of the linear state variable format model of a system
$f_{fan}(\cdot)$	fan total pressure increment function
f_i	Moody friction factor of the fluid flowing on the i^{th} path
g_c	units resolution constant for Newton's mass acceleration law (Newton-meters/kg-sec^2)
h_{canopy}	height of the plant canopy (m)
$h_{chamber}$	height of the growth chamber (m)
h_{ci}	convective heat transfer coefficient on path i (Watts m^{-2} K^{-1})
h_i	local static enthalpy transport rate in path i (Watts)
h_i^o	total enthalpy transport rate in path i (Watts)
$h_{j,k}$	specific enthalpy of the k^{th} constituent at point j (Joules mol^{-1})
J	moment of inertia of motor and impeller (kg m^2)
k_j	thermal conductivity of air mixture at point j (Watts/(m^2- K))
K_i	pressure loss coefficient for path i (unitless)
K_i	pressure loss coefficient for path i (Newtons/m^2/(mole/sec)^2)
L_i	effective duct length of path i (m)
LAI	leaf area index (actual leaf area/crop growth platform area)

SYMBOLS (continued)

MW_j	molecular weight of the air mixture at point j (g mol^{-1})
n_i	total molar flow rate in path i (moles sec^{-1})
$n_{i,k}$	molar flow rate of constituent k in path i (moles sec^{-1})
N_j	total molar presence of material in volume marked by j
$N_{j,k}$	moles of constituent k contained in volume marked by point j
$Nu_{L,i}$	Nusselt number based on length L_i
$P_1\dot{V}_g$	power expended in the upper chamber by the system when glove intrusion is changed (Watts)
P_j	static pressure at point j (Pa)
P_j^o	total pressure at point j (Pa)
PPF	photosynthetic photon flux (μmol m^{-2} sec^{-1})
Pa	Pascals (Newtons/m^{-2})
P_r	Prandtl number
$\dot{Q}$	heat flow rate (Watts)
resp	respiration
R	universal gas constant (Joules mol^{-1} K^{-1})
Re_{Lj}	Reynolds' number based on length of the j^{th} path (unitless)
SH_j	specific humidity at point j (moles water vapor /mole dry air)
t	time (seconds)
T_j	temperature at point j (K)
u(t)	the vector of system control variables
U_i	overall heat transfer coefficient on the i^{th} path (Joules m^{-2} K^{-1})
V_i	speed of airflow in path i (meters/second)
$\dot{V}_g$	glove port volume change rate (m^3/sec)

SYMBOLS (continued)

V_j	value of the volume marked as point j (m^3)
$\dot{W}$	rate of doing work. Power (Watts)
x(t)	the vector of system dynamically independent (state) variables
$\delta(\cdot)$	denotation of a variation of $(\cdot)$ from some (specified) reference value
$\eta(t)$	the vector of primary primitive variables (modeled system dynamically determined variables)
η_o	overall efficiency of the air mover
μ_i	absolute viscosity of the air at point i ((Newtons/m^2)/((m/s)/m)
ν	light frequency (Hz)
ρ_j	air density at point j (moles/m^3)
$\rho_{m,j}$	mass density of air at point j (kg/m^3)
$\sigma(t)$	the vector of secondary primitive variables (modeled system algebraically determined variables)
τ	torque (Newton-meters).
τ_c	torque exerted on the motor rotor - fan rotor unit (Newton-meters)
ω_{37}	angular speed of the motor rotor - blower rotor unit; inertial coordinates (radians/second)
χ_i	by-pass fraction of path i: the fraction of the flow in path i which is diverted to flow around the heat exchanger which is in one of the following flow paths.

1 - INTRODUCTION

It is widely understood that the use of mathematical modeling, analysis, and simulation (MMA&S), when used wisely, is of great value as a means to gain early insights into the nature of a proposed engineering system and to enhance the probability of anticipating problem areas early in the program. It is also now widely understood that MMA&S, when properly integrated into a system development program, can result in a system development cost which is orders of magnitude less expensive than the cost of development via the once traditional strategy of rushing through the preliminary design in an *ad lib* fashion to the early fabrication of the physical system, testing, changing design, rebuilding, retesting, etc. A combination of MMA&S, design, fabrication, and testing will minimize total system development cost. Systems control is an area of one of the earliest applications of MMA&S, possibly because of the subtle and often counter-intuitive nature of the dynamic stability problem. Results have been extraordinarily successful in many cases.

The Controlled Ecological Life Support System (CELSS) concept presents a prospective application of this system development strategy. It is interdisciplinary in its scientific and technological span and, of necessity, contains dynamic processes of wide diversity of physical origin. Such a system would contain at least a crop growth subsystem, a personnel subsystem, a waste treatment subsystem (Figure 1), and a management, automation, and control subsystem. Systems characterized by

this level of complexity and diversity almost always have the potential for counter-intuitive behavior which, at best, results in unacceptable performance of the controlled system, and, at worst, results in self-destructive behavior when improperly chosen feedback control is imposed on the system.

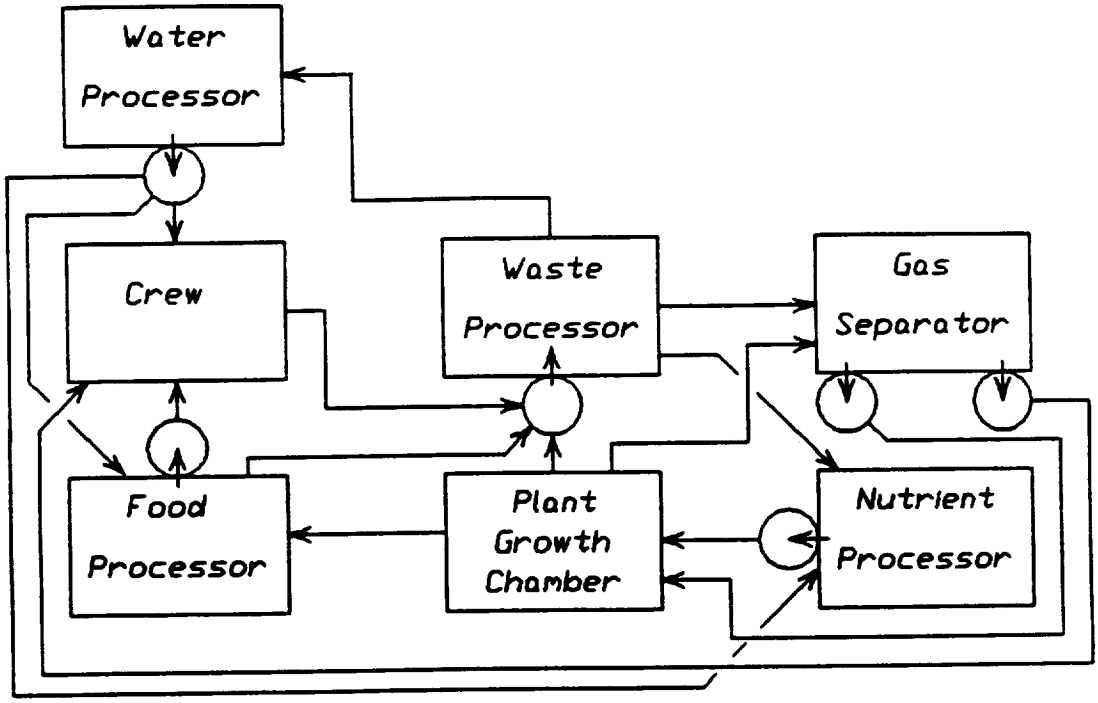

Figure 1. Schematic showing the primary functional subsystems of a CELSS. Data acquisition, data processing, and control subsystems are not shown.

The Crop Growth Research Chamber (CGRC) project, an element of the CELSS program, can itself be profitably subjected to the MMA&S treatment. (As pointed out earlier, CELSS must contain a crop growth subsystem, but its required envelope of operating conditions is much smaller than that of a CGRC.) The CGRC is intended to be a precision research apparatus to support research in crop growth science and technology and must provide a precisely controlled environment for this purpose. The performance requirements include

providing satisfactory (prescribed) time histories of fluid flows, concentrations of gases and liquids, temperatures, and pressures at designated points within the CGRC system, a scenario which is referred to as the multi-input, multi-output tracking problem in the field of systems control. Even a subsystem of a CGRC, such as the shoot side environmental control system, is sufficiently complex to present a challenging but clearly tractable and almost ideal subject for MMA&S attention.

The development of a system to control the environmental conditions within the shoot side chamber of the CGRC involves (1) the selection of component devices (i.e. actuators) which will affect the environmental variables that are to be controlled, (2) the selection of component devices which will provide suitable measurements of the environmental variables (i.e. measurement instruments), and (3) the development of control algorithms which utilize the outputs of the measurement instruments to provide the necessary combinations and time sequencing of inputs to the actuators so that the required performance characteristics of the environmental variables within the CGRC are met.

The process of control system synthesis almost always involves a familiarization process, and the familiarization process almost always involves a process of starting with great but meaningful simplifications and moving in some rational sequence of stages to a stage in which sufficient complexity and detail is addressed. The conscious pursuit of this strategy and what it implies is apparently not generally intuitive.

The purpose of this report is to present the results of the authors' initial examination of the control problem related to the provision of the required

environment of the plant shoots of a hypothetical CGRC configuration. This configuration was thought to be consistent with the requirements of a CGRC but not expected to be the final configuration. Figure 2 is a minimally annotated schematic representation of the object of study, and is provided to help the reader gain insights into the relative positions of the major components and their sequence in the air flowstream.

1.1 ORGANIZATION OF THE REPORT

In the sequel, we describe the crop shoot side environmental delivery system (CSSEDS), define the specific purpose of the model, characterize the model in terms of the processes of which it is composed and how they interact, present the natural equations in both linear and nonlinear forms, extract the state variable representation of the model, present a canonical form of the state variable form, and present the results of a cursory study of the problem of choosing feedback control gains so that one of the unstable modes of the system is replaced by a stable mode.

2 - DESCRIPTION OF THE SHOOT ENVIRONMENT DELIVERY SYSTEM

Figure 3 is also a representation of the CSSEDS but is configured to be very useful to the modeling process and displays much more detail than does Figure 2. In Figure 3, large circled numbers indicate points (nodes) at which it is anticipated that the potential variables are important to the control and performance problem, and small numbers beside arrows with

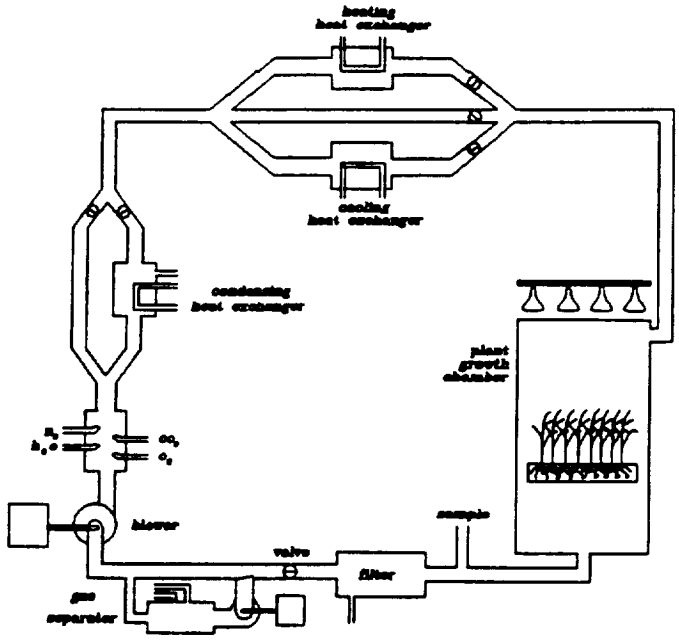

Figure 2. Diagram of the crop shoot side environment delivery system. Relative position of primary functional subsystems and fluid flow paths are emphasized.

one-sided heads indicate flow paths for which it is anticipated that the flow variables will have similar importance. The function of the components of the CSSEDS will be explained by tracing the airflow clockwise around the circuit beginning with its entrance into the upper chamber. The plants receive radiant energy from a light source above (and external to) the chamber after it emerges from an electromagnetic radiation filter which removes most of the long-wave (IR) radiation from the spectrum. Water and nutrients are supplied to the roots by means of a nutrient delivery system that is materially isolated from the shoot side environment. The flow path for the air entering the chamber is assumed to be designed to assure that uniform conditions exist in the shoot side chamber.

Air enters near the top of the upper chamber and is thoroughly mixed with the air in the upper portion of the chamber. As the air moves from the upper chamber inlet to its exit, gaseous exchange of carbon dioxide, water vapor and

oxygen occurs between the crop canopy and the atmosphere. The resulting mixture exits the upper chamber via a flow path provided between the chamber walls and the plant support surface into the lower chamber and then into the ducting via an entrance located in the bottom. The flow is then directed through a pre-filter and a HEPA filter to remove particulates from the air as it leaves the chamber. Upon exiting the filter, the air sustains a pressure loss imposed by a valve. By means of a valve and fan, a portion of the air flow is diverted into a gas separator which removes excess oxygen and/or carbon dioxide as required. The required air movement around the flow path is accomplished by employing an air mover (e.g., a centrifugal pump or a blower), and at the discharge of the air mover, makeup gases are injected into the flow stream to maintain the required atmospheric

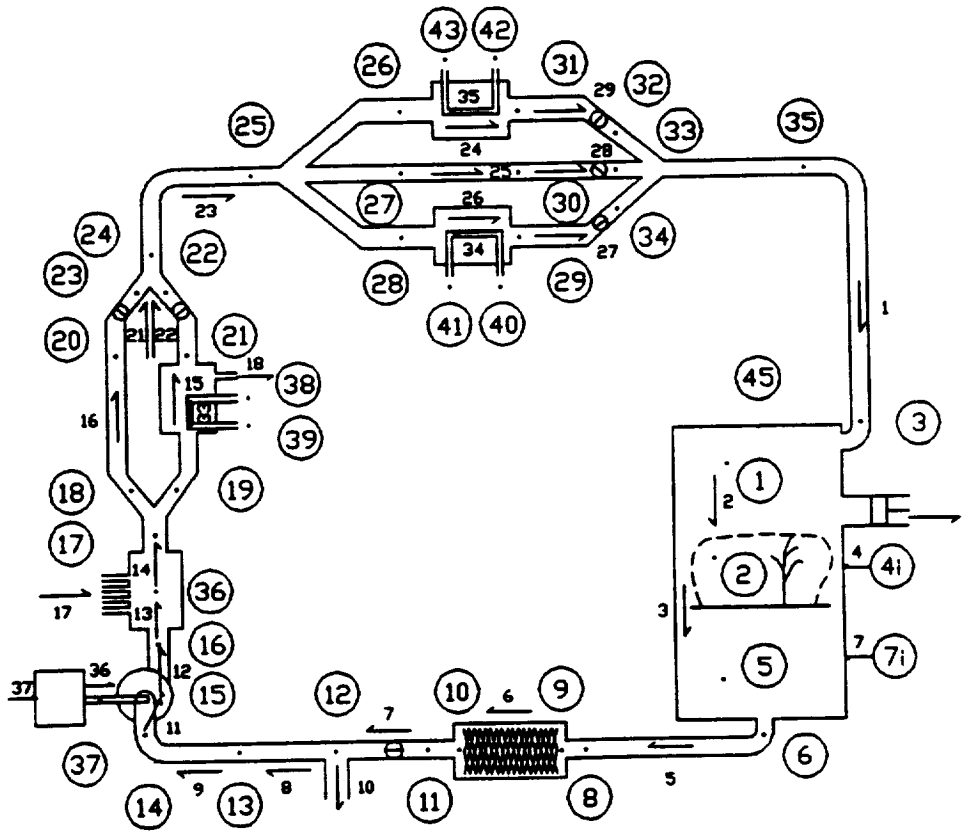

Figure 3. Schematic of the crop shoot side environment delivery system. Includes detail necessary for model synthesis.

composition. The water which is transpired by the plants is removed from the system airflow stream in the form of condensate by diverting a portion of the flow through a condensing heat exchanger. Two valves, one in the flow path through the condensing heat exchanger and one in the condensing heat exchanger bypass regulate the mass flow ratio of the paths. The flow is recombined and enters the cooling/heating subsystem. A portion of the flow can be diverted through either a heater or a cooling heat exchanger. Valves control the flow distribution among the three possible flow paths. Again, the flows are combined and the mixture is ducted to the chamber inlet, completing the traverse of the circuit.

3 - PERFORMANCE AND PHYSICAL CONFIGURATION REQUIREMENTS

It was established by a science advisory group that a CGRC which could be useful for their research would of necessity have certain performance capabilities and would have certain physical characteristics. The group limited itself to describing these capabilities and characteristics and left the details of how they might be obtained to the designers.

(1). Crop growth platform area - 2.0 m^2

(2). Minimum upper crop shoot volume - 2.0 m^3.

(3). With the lights on and no plants in the CGRC, the temperature rise of the air exiting the upper chamber must not be greater than 2 C.

(4). The CGRC must be able to provide a quantum light intensity of as much as 2000 μmoles/(m^2-sec).

(5). The airflow speed must not exceed 2 m/s in the shoot upper chamber

(7). It is not permissible for the pressure within the shoot and root environments to be less than 0.5 mm Hg higher than the CGRC surroundings.

(8). The chamber walls must be kept at least 2 C higher than the air within the chamber.

(9). Water must not precipitate from the air anywhere other than in the water removal subsystem.

4 - PURPOSE OF THE MODEL

We consider the scenario in which the growth chamber contains a crop of plants forming a closed canopy and the system goal is to maintain temperature, relative humidity, pressure, carbon dioxide concentration, oxygen concentration, and mean air velocity in the chamber within set tolerances about constant operating points. The formal purpose of the model is to support the exploration of the generic stability properties of the system in the neighborhood of an operating condition of specific interest to members of a science advisory group, but it also played an important role in the process of familiarization. Of course, the scientists who expect to do research with this type of chamber are concerned about a great deal more than simple stability, but stability is a logical starting point for performance studies. The details of the operating condition for which the study was done are presented in Sections 3, 7.4, and 7.5.

5 - THE MATHEMATICAL MODEL OF THE CROP SHOOT ENVIRONMENT DELIVERY SYSTEM

The philosophy and procedure with which the mathematical model of the CGRC system was developed is documented in [1] (see Appendix A1). Here, we present a summary of the procedure at the level of detail necessary for purposes of continuity of thought.

The initial stage of the modeling process, the conceptualization of (1) which processes within the system are to be addressed, (2) how they interact with one another, (3) how the system interacts with the surroundings, and (4) how each process is to be characterized mathematically/numerically is a purely abstract process. To make each of these decisions tangibly available for the modeler's utility, as well as the equally important responsibility of communicating the details of the model to others, preparing an adequately annotated list suffices effectively for the first purpose, constructing a "modeling system" diagram is very useful for the second and third purposes, and listing the "natural equations" of the system is very effective for the fourth.

The behavior of any system is the resultant of the nature of the processes contained by the system, their interaction, the conditions at the time the system is set free, and the interaction of the the system with its surroundings. The use of mathematical modeling to predict the behavior of the system in the context of some question or questions requires (1) the recognition that these processes are in action, that they interact with one another and the details of those interactions, and that they interact with the surroundings and the details of those interactions, and (2) committing this recognition to a prescription of mathematical operations and parameter values. The intellectual process of accomplishing these actions is

called mathematical modeling.

In the course of generating a system representation, one synthesizes an idealized conceptual system (the "modeling system") of idealized processes ("modeling processes") which mimic the actual system's physical processes to an adequate degree. In this procedure, it is implicit that by contemplation of the actual system, one must correctly infer how the idealized processes must be arranged to interact so that the modeling system will emulate the actual system's behavior in the context of the problem being addressed to a degree of adequate accuracy. In Appendix A.1 the reader can find a set of facts and thoughts about the CSSEDS which shape the contemplation. Logically, one first identifies the processes and then establishes how they interact.

5.1 - SUMMARY OF THE PHASES OF THE MODEL GENERATION PROCEDURE

In the sequel, the description of the stages of the model generation procedure will be found;

(1) List the physical processes which are to be represented by model processes

(2) Declare the interpretation of how the processes interact, sign conventions, point identities and path identities. This is done via process interaction diagrams Figures 4 and 5.

(3) Write the primitive equations; the mathematical model of each process in terms of the point variables and path variables associated with that process in Figures 4 and 5, and the compatibility equations (those which express constraints among the point and path variables). In this phase, the linearized form of the equation is also developed.

(4) Solve the primitive equations for the nominal values of the variables at the experimental operating condition.

(5) Write the linear primary equations. Take advantage of opportunities to eliminate variables *ad lib* using some of the equations. The object of this action is to reduce the number of equations which must be manipulated.

(6) Substitute nominal values into linearized equations to obtain equation forms which have numerical coefficients. This form is characterized by the linear equations:

$$A_1\dot{\eta} = A_2\eta + A_3\sigma + A_4u + A_5d \tag{5.1.1}$$

and

$$B_1\sigma = B_2\eta + B_3u + B_4d \tag{5.1.2}$$

The state variable format can then be determined, using, e.g., MATLAB

$$\dot{x} = A_1^{-1}(A_2 + A_3B_1^{-1}B_2)x + A_1^{-1}(A_4 + A_3B_1^{-1}B_3)u + A_1^{-1}(A_5 + A_3B_1^{-1}B_4)d \tag{5.1.3}$$

and

$$\sigma = B_1^{-1}(B_2x + B_3u + B_4d) \tag{5.1.4}$$

(generalized inverse is implied) which is of the simple form

$$\dot{x} = \mathcal{A}x + \mathcal{B}u + \mathcal{C}d \tag{5.1.5}$$

and

$$\sigma = \mathcal{D}x + \mathcal{E}u + \mathcal{F}d \tag{5.1.6}$$

(7) Analyze the state variable representation for the purpose of familiarization

with its dynamical properties and its controllability properties. There is a great variety of choices of what might be done and it varies with the application and the investigator. In the sequel, we present the results of:

1. the Jordan canonical transformation
2. the Real Jordan transformation
3. eigenvalue assessment
4. controllability assessment, and
5. an elementary feedback control study.

5.2 - THE MODELING PROCESSES.

It was anticipated that the following physical processes would have to be included in the modeling system in order for the representation to be useful:

(1). Fluid inertance in upper duct.

(2). Radiant energy flow from the light source into the upper shoot chamber (source of PAR).

(3). Molar storage of N_2 in upper chamber.

(4). Molar storage of O_2 in the upper chamber.

(5). Molar storage of CO_2 in upper chamber.

(6). Molar storage of H_2O vapor in the upper chamber.

(7). O_2 flux from crop into the upper chamber air.

(7). CO_2 flux from the upper chamber air into the crop.

(8). H_2O flux from the crop into the upper chamber air.

(9). Upper chamber gas state.

(10). Thermal energy of gas in upper chamber.

(11). Volume change of the upper chamber due to glove port activity.

(12). Heat exchange between walls of upper chamber and upper chamber air.

(13). Heat exchange between crop canopy and upper chamber air.

(14). Flow energy loss; airflow past plant platform.

(15). Molar storage of N_2 in lower chamber.

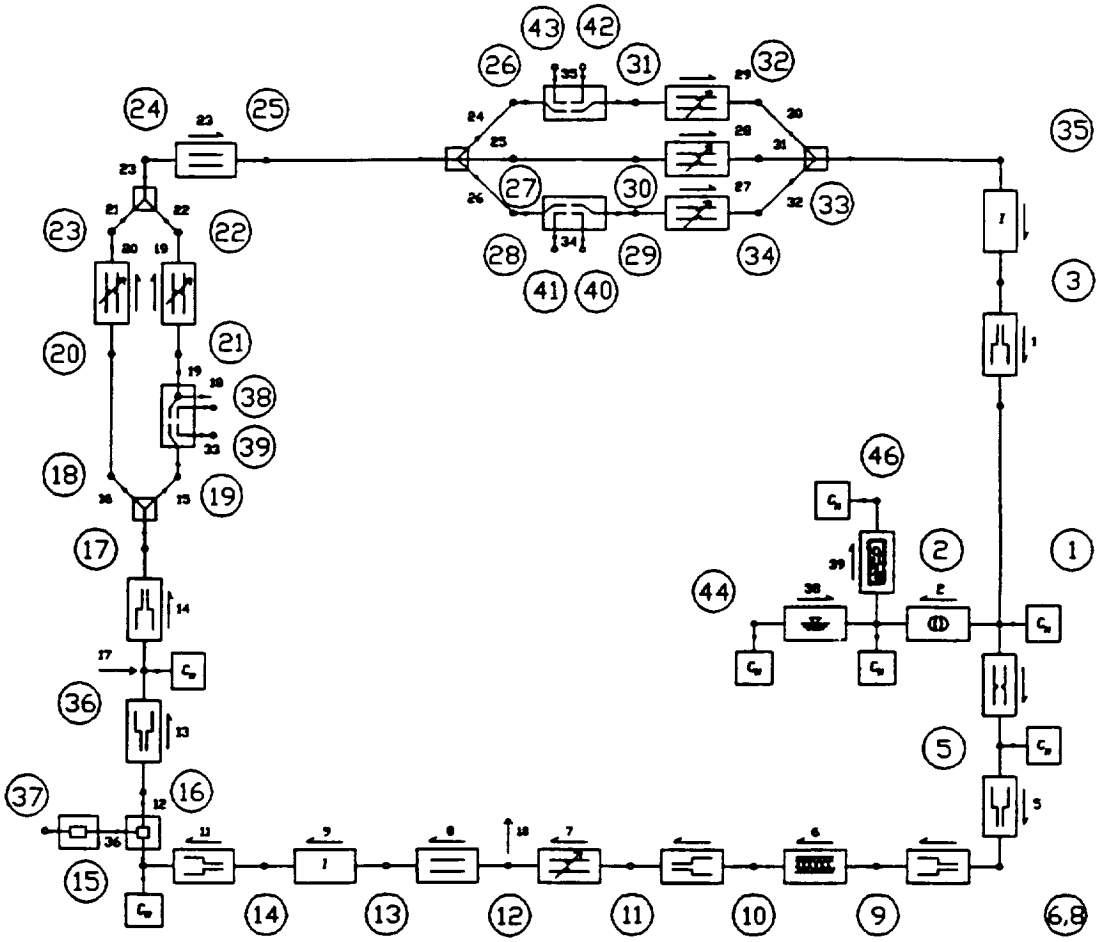

Figure 4. The fluid flow modeling system. Only paths and points utilized in the model we present here are indicated. The fluid and thermal modeling systems are not isolated from each other. They exchange power.

(16). Molar storage of O_2 in the lower chamber.

(17). Molar storage of CO_2 in lower chamber.

(18). Molar storage of H_2O in the lower chamber.

(19). Heat exchange between walls of lower chamber and lower chamber air.

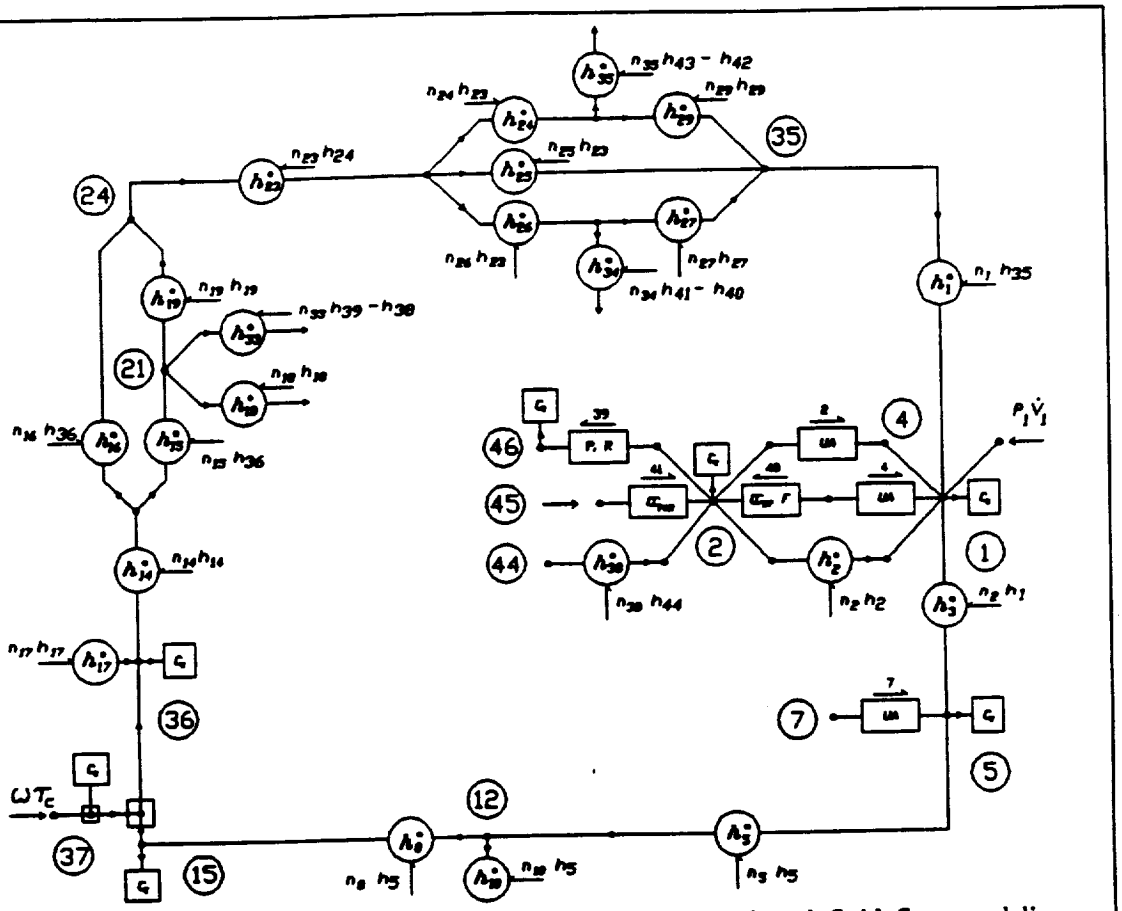

Figure 5. The thermal exchange modeling system. The thermal and fluid flow modeling systems are not isolated from each other. They exchange power.

(20). Flow energy loss; exit from lower chamber.

(21). Flow energy loss; filter and lower valve.

(22). Extraction of excess oxygen; lower duct section.

(23). Fluid inertance; lower duct section.

(24). Flow energy loss; lower duct section.

(25). Energy conversion by the pump.

(26). Motor and pump rotor rotational inertia.

(27). Control moment on the motor armature.

(28). Motor and blower friction.

(29). Injection of CO_2 into the gas addition mixing section.

(30). Molar storage of N_2 in the gas addition mixing section.

(31). Molar storage of O_2 in the gas addition mixing section.

(32). Molar storage of CO_2 in the gas addition mixing section.

(33). Molar storage of H_2O in the gas addition mixing section.

(34). Thermal energy storage in the gas addition mixing section.

(35). Flow energy loss; condensing heat exchanger bypass control valve.

(36). Flow energy loss; condensing heat exchanger air side flow control valve.

(37). Liquid water precipitation; condensing heat exchanger

(38). Thermal energy exchange; condensing heat exchanger.

(39). Flow energy loss; duct from condensing to heating/cooling system.

(40). Flow energy loss; air heater flow control valve.

(41). Flow energy loss; air cooler flow control valve.

(42). Flow energy loss; air heater/air cooler bypass flow control valve.

(43). Thermal energy exchange; air cooler heat exchanger.

(44). Flow energy loss; heater flow control valve.

(45). Volume change of the shoot upper chamber due to glove port activity.

The entire CSSEDS is assumed to be adiabatic with respect to its surroundings. All ducts are assumed to be of the same cross-sectional area for flow.

5.3 - THE MODELING SYSTEM

In the coherent process of generating a system representation, one synthesizes an idealized conceptual system, the modeling system, of idealized processes. In the contemplation of the actual system, one must correctly infer which processes are at work and how the idealized processes must be arranged to

interact so that the modeling system will emulate the behavior of the actual system in the context of the problem being addressed to a degree of adequate accuracy. Logically, one first perceives the processes that are in action and then how they interact. Figures 4 and 5 together display the results of this activity. In Figure 4, the fluid flow processes and their interactions are declared and in Figure 5 the thermal processes and their interactions are displayed. It is important to note that they are not separate, they interact significantly. It is only for convenience in the presentation that they are placed in different figures.

5.4 - THE PRIMITIVE EQUATIONS.

The modeling system provides a basis for ordering the equations and labeling the variables of the model. First, for the matter exchange and storage portion of the modeling system, and then for the thermal exchange and storage portion of the system, we will list the primitive equations in the sequential order of the point numbers and/or path number(s) to which they refer. Reference to Figures 4 and 5 should be made as needed. The choice of representation of the flow processes via "compressible" or "incompressible" flow models is made based on the process being described. In the present case, the pressure variations across the modeled processes are rather small, and thus incompressible representations are appropriate.

The procedure is the same for each of the processes. First, the process is identified and then the modeling process equation which is needed is stated, first in its typically standard form. In many cases, these expressions are nonlinear. Next, supplementary equations are presented in order to demonstrate how relations

among the variables may be brought in to convert the expressions to relate only the selected set of variables. After this is done, the individual expressions are linearized about the prescribed operating condition. Then we move on to the next process or conservation constraint. In some cases, a process which might very well be included is stated, but because of the early phase nature of this study, insufficient physical configuration definition has been done, and it is judged that a meaningful study can be conducted though it is not included. "Meaningful" is a quality that is in the mind of the investigator; here we mean that we judge that a majority of the knowledgeable persons in the field would agree that it was a reasonable and understandable thing to do and that a worthwhile study could be conducted without accounting for the process.

5.4.1 - SOME BASIC EQUATIONS.

Some frequently used models of commonly encountered physical processes are listed for easy reference.

Ideal gas law: $P_j V_j = N_j R T_j$

First law of thermodynamics for steady state, steady flow: $h_{out} - h_{in} = \dot{Q} + \dot{W}$

Molar density: $\rho_j = \frac{N_j}{V_j}$

Molar flow rate: $n_i = V_i \rho_i A_i$

Total pressure loss model: ideal gas, steady, adiabatic, no-work flow: flow from point 3 to point 1

$(P_3 + \frac{1}{2}\rho_{m_3} V_3^2) - (P_1 + \frac{1}{2}\rho_{m_1} V_1^2) = \Delta P^o_{3\to 1}$

$n_i = \sum_{k=1}^{4} n_{i,k}$; $k = 1 \Rightarrow$ nitrogen, $k = 2 \Rightarrow$ oxygen, $k = 3 \Rightarrow$ carbon dioxide, and $k = 4 \Rightarrow$ water vapor

Molar content of the j^{th} volume:

$$N_j = \sum_{k=1}^{4} N_{j,k}$$

Molar concentration: of the k^{th} constituent in the j^{th} volume:

$$Cc_{j,k} = \frac{N_{j,k}}{N_j}$$

5.4.2 - THE MATHEMATICAL MODEL OF THE INDIVIDUAL PHYSICAL PROCESSES IN THE MODELING SYSTEM AND OF THE CONSERVATION CONSTRAINTS

Fluid inertance of the air column in the upper duct system (path 1):

$$\dot{n}_1 = \frac{1000\, g_c\, A_1}{MW_1 L_{23}} (P_{35} - P_3)$$

$$A_1 = A_{23}$$

with linearization:

$$\delta\dot{n}_1 = \frac{1000\, g_c\, A_1}{MW_1 L_{23}} (\delta P_{35} - \delta P_1)$$

Rate of accumulation of the air constituents in the shoot upper chamber (point 1):

Using the relations

$$n_{3,k} = \frac{N_{1,k}}{N_1}\ n_3,\ k = 1,2,3,4$$

$$n_{1,k} = \frac{N_{36,k}}{N_{36}}\ n_{14},\ k = 1,2,3\ ;\ n_{1,k} = \frac{N_{36,k}}{N_{36}}\ n_{14} - n_{18},\ k = 4$$

$$n_{14} = n_1 + n_{18}$$

one obtains:

Nitrogen.

$$\dot{N}_{1,1} = n_{1,1} - n_{3,1}$$

$$\dot{N}_{1,1} = (n_1 + n_{18}) \frac{N_{36,1}}{N_{36}} - n_3\ \frac{N_{1,1}}{N_1}$$

with linearization:

$$\delta\dot{N}_{1,1} = (\delta n_1 + \delta n_{18})\ \frac{N_{36,1}}{N_{36}} + (n_1 + n_{18})\ \frac{\delta N_{36,1}}{N_{36}} - (n_1 + n_{18})\ \frac{N_{36,1}}{N_{36}^2} \sum_{k=1}^{4} \delta N_{36,k}$$

$$- \delta n_3\ \frac{N_{1,1}}{N_1} - n_3\ \frac{\delta N_{1,1}}{N_1} + n_3\ \frac{N_{1,1}}{N_1^2} \sum_{k=1}^{4} \delta N_{1,k}$$

Oxygen.

$$\dot{N}_{1,2} = n_{1,2} - n_{2,2}[\hbar\nu] - n_{2,2}[\text{resp}] - n_{3,2}$$

$$\dot{N}_{1,2} = (n_1 + n_{18})\ \frac{N_{36,2}}{N_{36}} - n_{2,2}[\hbar\nu] - n_{2,2}[\text{resp}] - n_3\ \frac{N_{1,2}}{N_1}$$

with linearization:

$$\delta\dot{N}_{1,2} = (\delta n_1 + \delta n_{18})\ \frac{N_{36,2}}{N_{36}} + (n_1 + n_{18})\ \frac{\delta N_{36,2}}{N_{36}} - (n_1 + n_{18})\ \frac{N_{36,2}}{N_{36}^2} \sum_{k=1}^{4} \delta N_{36,k}$$

$$- \delta n_3\ \frac{N_{1,2}}{N_1} - n_3\ \frac{\delta N_{1,2}}{N_1} + n_3\ \frac{N_{1,2}}{N_1^2} \sum_{k=1}^{4} \delta N_{1,k} - \delta n_{2,2}$$

Carbon dioxide.

$$\dot{N}_{1,3} = n_{1,3} - n_{2,3}[\hbar\nu] - n_{2,3}[\text{resp}] - n_{3,3}$$

$$\dot{N}_{1,3} = (n_1 + n_{18})\ \frac{N_{36,3}}{N_{36}} - n_{2,3}[\hbar\nu] - n_{2,3}[\text{resp}] - n_3\ \frac{N_{1,3}}{N_1}$$

with linearization:

$$\delta\dot{N}_{1,3} = (\delta n_1 + \delta n_{18})\ \frac{N_{36,3}}{N_{36}} + (n_1 + n_{18})\ \frac{\delta N_{36,3}}{N_{36}} - (n_1 + n_{18})\ \frac{N_{36,3}}{N_{36}^2} \sum_{k=1}^{4} \delta N_{36,k}$$

$$- \delta n_3\ \frac{N_{1,3}}{N_1} - n_3\ \frac{\delta N_{1,3}}{N_1} + n_3\ \frac{N_{1,3}}{N_1^2} \sum_{k=1}^{4} \delta N_{1,k} - \delta n_{2,3}$$

Water.

$$\dot{N}_{1,4} = n_{1,4} - n_{2,4} - n_{3,4}$$

$$\dot{N}_{1,4} = (n_1 + n_{18})\ \frac{N_{36,4}}{N_{36}} - n_{18} - n_{2,4} - n_3\ \frac{N_{1,4}}{N_1}$$

with linearization:

$$\delta\dot{N}_{1,4} = (\delta n_1 + \delta n_{18})\ \frac{N_{36,4}}{N_{36}} + (n_1 + n_{18})\ \frac{\delta N_{36,4}}{N_{36}} - (n_1 + n_{18})\ \frac{N_{36,4}}{N_{36}^{\ 2}} \sum_{k=1}^{4} \delta N_{36,k} - \delta n_{18}$$

$$- \delta n_3\ \frac{N_{1,4}}{N_1} - n_3\ \frac{\delta N_{1,4}}{N_1} + n_3\ \frac{N_{1,4}}{N_1^{\ 2}} \sum_{k=1}^{4} \delta N_{1,k} - \delta n_{2,4}$$

Total molar content of the upper chamber air.

$$N_1 = \sum_{i=1}^{4} N_{1,i}$$

with linearization:

$$\delta N_1 = \sum_{i=1}^{4} \delta N_{1,i}$$

Energy accumulation in the shoot side upper chamber.

$$\dot{E}_1 = \sum_{k=1}^{4} \dot{h}_{1,k} - \sum_{k=1}^{4} \dot{h}_{3,k} - \sum_{k=2}^{4} \dot{h}_{2,k} + (UA)_2\,(T_2 - T_1) + (UA)_4\,(T_4 - T_1) - P_1\,\dot{V}_1$$

where

$$(UA)_2 = h_{c_2} A_{pf}$$

$$h_{c_2} = 11.30 \left(\frac{n_3}{0.1 \rho_2 (A_{pf} + A_3)} \right)^{0.5}$$

$$(UA)_4 = h_{c_4} A_4$$

$$h_{c_4} = \frac{2\ Nu_{x=L_1}\ k_1}{L_1}$$

$$Nu_{x=L_1} = 0.332\ Re_{L_1}^{\ 1/2}\ Pr_1^{\ 1/3}$$

$$Pr_1 = \frac{c_{p_1}\ \mu_1}{k_1}$$

$$Re_{L_1} = \frac{\rho_2\ MW_1\ V_1\ L_1}{1000\ \mu_1}$$

Inserting equivalent thermodynamic properties;

$$(N_{1,1}\, c_{v_{1,1}} + N_{1,2}\, c_{v_{1,2}} + N_{1,3}\, c_{v_{1,3}} + N_{1,4}\, c_{v_{1,4}})\, \dot{T}_1 =$$
$$(n_{1,1}\, c_{p_{35,1}} + n_{1,2}\, c_{p_{35,2}} + n_{1,3}\, c_{p_{35,3}} + n_{1,4}\, c_{p_{35,4}})\, (T_{35} - 273.15)$$
$$- (n_{3,1}\, c_{p_{1,1}} + n_{3,2}\, c_{p_{1,2}} + n_{3,3}\, c_{p_{1,3}} + n_{3,4}\, c_{p_{1,4}})\, (T_1 - 273.15)$$
$$- n_{2,2}[\hbar\nu]\, c_{p_{2,2}}\, (T_2 - 273.15) - n_{2,2}[\text{resp}]\, c_{p_{1,2}}\, (T_1 - 273.15)$$
$$- n_{2,3}[\hbar\nu]\, c_{p_{1,3}}\, (T_1 - 273.15) - n_{2,3}[\text{resp}]\, c_{p_{2,3}}\, (T_2 - 273.15)$$
$$- n_{2,4}\, c_{p_{2,4}}\, (T_2 - 273.15) + h_{c_2}\, 2\, \text{LAI}\, A_{pf}\, (T_2 - T_1) + \bar{h}_{c_4} A_4\, (T_4 - T_1) - P_1\, \dot{V}_1$$

Using

$$n_1\, c_{p_{35}} \doteq \sum_{k=1}^{4} n_{1,k}\, c_{p_{35,k}}$$
$$n_3\, c_{p_1} \doteq \sum_{k=1}^{4} n_{3,k}\, c_{p_{1,k}}$$

and linearizing gives:

$$(N_{1,1}\, c_{v_{1,1}} + N_{1,2}\, c_{v_{1,2}} + N_{1,3}\, c_{v_{1,3}} + N_{1,4}\, c_{v_{1,4}})\, \delta\dot{T}_1 =$$
$$n_1\, c_{p_{35}} \delta T_{35} + \delta n_1\, c_{p_{35}} (T_{35} - 273.15) - n_3\, c_{p_1} \delta T_1 + \delta n_3\, c_{p_1} (T_1 - 273.15)$$
$$- n_{2,2}[\hbar\nu]\, c_{p_{2,2}}\, \delta T_2 - \delta n_{2,2}[\hbar\nu]\, c_{p_{2,2}}\, (T_2 - 273.15)$$
$$- n_{2,2}[\text{resp}]\, c_{p_{1,2}}\, \delta T_1 - \delta n_{2,2}[\text{resp}]\, c_{p_{1,2}}\, (T_1 - 273.15)$$
$$- n_{2,3}[\hbar\nu]\, c_{p_{1,3}}\, \delta T_1 - \delta n_{2,3}[\hbar\nu]\, c_{p_{1,3}}\, (T_1 - 273.15)$$
$$- n_{2,3}[\text{resp}]\, c_{p_{2,3}}\, \delta T_2 - \delta n_{2,3}[\text{resp}]\, c_{p_{2,3}}\, (T_2 - 273.15)$$
$$- n_{2,4}\, c_{p_{2,4}}\, \delta T_2 - \delta n_{2,4}\, c_{p_{2,4}}\, (T_2 - 273.15)$$
$$+ h_{c_2}\, 2\, \text{LAI}\, A_{pf}\, (\delta T_2 - \delta T_1) + h_{c_4} A_4\, (\delta T_4 - \delta T_1) - P_1\, \delta\dot{V}_1$$

Equation of state of the air in the shoot upper chamber.

$$P_1\, V_1 = N_1\, R\, T_1$$

with linearization

$$\delta P_1\, V_1 + P_1\, \delta V_1 = \delta N_1\, R\, T_1 + N_1\, R\, \delta T_1$$

Airflow total pressure loss: from shoot upper chamber to shoot lower chamber (path 3):

$$P_1 - P_5 = K_3\, \frac{\rho_1 \text{MW}_3}{1000\, g_c}\, \frac{V_3^2}{2} = K_3\, \frac{\text{MW}_3}{2000\, \rho_1\, A_3^2\, g_c}\, n_3^2$$

with linearization:

$$\delta P_1 - \delta P_5 = \frac{2\, n_3\, MW_3}{2000\, \rho_1\, A_3^{\,2}\, g_c}\, \delta n_3$$

$$MW_3 \doteq \sum_{k=1}^{4} MW_{,k}\, \frac{N_{1,k}}{N_1}$$

$$K_3 \triangleq K_3\, \frac{2\, n_3\, MW_3}{2000\, \rho_1\, A_3^{\,2}\, g_c}$$

$$\delta P_1 - \delta P_5 = K_3\, \delta n_3$$

$$A_5 = A_1$$

Rate of accumulation of the air constituents in the shoot lower chamber (point 5):

Using the relations

$$n_{5,k} = \frac{N_{5,k}}{N_5}\, n_5,\ k = 1,2,3,4$$

and

$$n_5 = n_9 + n_{10,2}$$

one can obtain the following expressions for the accumulation of material in the lower shoot growth chamber.

Nitrogen.

$$\dot{N}_{5,1} = n_{3,1} - n_{5,1}$$

$$\dot{N}_{5,1} = n_3\, \frac{N_{1,1}}{N_1} - n_5\, \frac{N_{5,1}}{N_5}$$

$$\dot{N}_{5,1} = n_3\, \frac{N_{1,1}}{N_1} - (n_9 + n_{10,2})\, \frac{N_{5,1}}{N_5}$$

with linearization:

$$\delta\dot{N}_{5,1} = \delta n_3\, \frac{N_{1,1}}{N_1} + n_3\, \frac{\delta N_{1,1}}{N_1} - n_3\, \frac{N_{1,1}}{N_1^{\,2}} \sum_{k=1}^{4} \delta N_{1,k} - (\delta n_9 + \delta n_{10,2})\, \frac{N_{5,1}}{N_5}$$

$$- (n_9 + n_{10,2})\, \frac{\delta N_{5,1}}{N_5} + (n_9 + n_{10,2})\, \frac{N_{5,1}}{N_5^{\,2}} \sum_{k=1}^{4} \delta N_{5,k}$$

Oxygen.

$$\dot{N}_{5,2} = n_3 \frac{N_{1,2}}{N_1} - n_5 \frac{N_{5,2}}{N_5}$$

$$\dot{N}_{5,2} = n_{3,2} - n_{5,2}$$

$$\dot{N}_{5,2} = n_3 \frac{N_{1,2}}{N_1} - (n_9 + n_{10,2}) \frac{N_{5,2}}{N_5}$$

with linearization:

$$\delta\dot{N}_{5,2} = \delta n_3 \frac{N_{1,2}}{N_1} + n_3 \frac{\delta N_{1,2}}{N_1} - n_3 \frac{N_{1,2}}{{N_1}^2} \sum_{k=1}^{4} \delta N_{1,k} - (\delta n_9 + \delta n_{10,2}) \frac{N_{5,2}}{N_5}$$

$$- (n_9 + n_{10,2}) \frac{\delta N_{5,2}}{N_5} + (n_9 + n_{10,2}) \frac{N_{5,2}}{{N_5}^2} \sum_{k=1}^{4} \delta N_{5,k}$$

Carbon dioxide:

$$\dot{N}_{5,3} = n_3 \frac{N_{1,3}}{N_1} - n_5 \frac{N_{5,3}}{N_5}$$

$$\dot{N}_{5,3} = n_{3,3} - n_{5,3}$$

$$\dot{N}_{5,3} = n_3 \frac{N_{1,3}}{N_1} - (n_9 + n_{10,2}) \frac{N_{5,3}}{N_5}$$

with linearization:

$$\delta\dot{N}_{5,3} = \delta n_3 \frac{N_{1,3}}{N_1} + n_3 \frac{\delta N_{1,3}}{N_1} - n_3 \frac{N_{1,3}}{{N_1}^2} \sum_{k=1}^{4} \delta N_{1,k} - (\delta n_9 + \delta n_{10,2}) \frac{N_{5,3}}{N_5}$$

$$- (n_9 + n_{10,2}) \frac{\delta N_{5,3}}{N_5} + (n_9 + n_{10,2}) \frac{N_{5,3}}{{N_5}^2} \sum_{k=1}^{4} \delta N_{5,k}$$

Water.

$$\dot{N}_{5,4} = n_{3,4} - n_{5,4}$$

$$\dot{N}_{5,4} = n_3 \frac{N_{1,4}}{N_1} - n_5 \frac{N_{5,4}}{N_5}$$

$$\dot{N}_{5,4} = n_3 \frac{N_{1,4}}{N_1} - (n_9 + n_{10,2}) \frac{N_{5,4}}{N_5}$$

with linearization:

$$\delta\dot{N}_{5,4} = \delta n_3 \frac{N_{1,4}}{N_1} + n_3 \frac{\delta N_{1,4}}{N_1} - n_3 \frac{N_{1,4}}{{N_1}^2} \sum_{k=1}^{4} \delta N_{1,k} - (\delta n_9 + \delta n_{10,2}) \frac{N_{5,4}}{N_5}$$

$$- (n_9 + n_{10,2}) \frac{\delta N_{5,4}}{N_5} + (n_9 + n_{10,2}) \frac{N_{5,4}}{{N_5}^2} \sum_{k=1}^{4} \delta N_{5,k}$$

Total molar content of the shoot side lower chamber:

The total molar content of the shoot side lower chamber is given by

$$N_5 = \sum_{i=1}^{4} N_{5,i}$$

with linearization:

$$\delta N_5 = \sum_{i=1}^{4} \delta N_{5,i}$$

Energy accumulation in the shoot side lower chamber.

$$\dot{E}_5 = \sum_{k=1}^{4} \overset{\circ}{h}_{3,k} - \sum_{k=1}^{4} \overset{\circ}{h}_{5,k} + (UA)_7 \, (T_7 - T_5)$$

$$\downarrow$$

$$(N_{5,1} \, c_{v_{5,1}} + N_{5,2} \, c_{v_{5,2}} + N_{5,3} \, c_{v_{5,3}} + N_{5,4} \, c_{v_{5,4}}) \, \dot{T}_5 =$$

$$(n_{3,1} \, c_{p_{1,1}} + n_{3,2} \, c_{p_{1,2}} + n_{3,3} \, c_{p_{1,3}} + n_{3,4} \, c_{p_{1,4}}) \, (T_1 - 273.15)$$

$$- (n_{5,1} \, c_{p_{5,1}} + n_{5,2} \, c_{p_{5,2}} + n_{5,3} \, c_{p_{5,3}} + n_{5,4} \, c_{p_{5,4}}) \, (T_5 - 273.15)$$

$$+ UA_7 \, (T_7 - T_5)$$

Including the simplification

$$(n_9 + n_{10,2}) \, c_{p_5} \doteq n_{5,1} \, c_{p_{5,1}} + n_{5,2} \, c_{p_{5,2}} + n_{5,3} \, c_{p_{5,3}} + n_{5,4} \, c_{p_{5,4}}$$

along with linearization gives:

$$(N_{5,1} \, c_{v_{5,1}} + N_{5,2} \, c_{v_{5,2}} + N_{5,3} \, c_{v_{5,3}} + N_{5,4} \, c_{v_{5,4}}) \, \delta\dot{T}_5 =$$

$$n_3 \, c_{p_1} \delta T_1 + \delta n_3 \, c_{p_1} (T_1 - 273.15) - (n_9 + n_{10,2}) \, c_{p_5} \delta T_5$$

$$- (\delta n_9 + \delta n_{10,2}) \, c_{p_5} (T_5 - 273.15) + UA_7 \, (\delta T_7 - \delta T_5)$$

$$MW_5 = MW_1$$

$$(UA)_7 = h_{c_7} \, A_7$$

$$h_{c_7} = \frac{2 \, Nu_{x=L_5} \, k_5}{L_5}$$

$$Nu_{x=L_5} = 0.332 \, Re_{L_5}^{1/2} \, Pr_5^{1/3}$$

$$Re_{L_5} = \frac{\rho_5 \, MW_5 \, V_5 \, L_5}{1000 \, \mu_5}$$

$$L_5 = h_{chamber} - (h_{canopy} + d_{PPF_{ref}}) - d_{pf}$$

Equation of state of the air in the shoot lower chamber

$P_5 V_5 = N_5 R T_5$

with linearization:

$\delta P_5 V_5 + P_5 \delta V_5 = \delta N_5 R T_5 + N_5 R \delta T_5$

Airflow total pressure loss: flow from lower chamber into discharge duct (path 5).

$P_5 - P_6 = K_5 \frac{MW_6 R T_5}{2000 P_5} \frac{1}{A_5^2} n_6^2$

with linearization:

$\delta P_5 - \delta P_6 = K_5 \frac{MW_6 R T_5}{1000 P_5} \frac{1}{A_5^2} n_6 \delta n_6$ (the incompressible flow model of this process is employed)

$MW_6 = MW_5$

$\rho_6 = \rho_5$

Airflow total pressure loss: flow duct (path 5 between points 6 and 8); both direction change ("bend") and duct length. Both Ignored: $P_8 = P_6$

Airflow total pressure loss: in expansion between points 8 and 9 (path 5)

Ignored: $(P_9 = P_8)$

Airflow total pressure loss: HEPA filter (path 6)

$P_9 - P_{10} = K_6 n_5^2$

K_6 is essentially a porous plug characteristic. Linearization gives

$\delta P_9 - \delta P_{10} = 2 K_6 n_5 \delta n_5$

Airflow total pressure loss: from HEPA filter discharge through control valve 12 (path 7). Includes contraction loss in reentering duct upon exiting HEPA filter, the fixed (wide open) loss of the valve, and the loss due to the valve element being partially closed. A_v is the control variable.

$P_{11} - P_{12} = K_7 n_5^2$

$$K_7 = K_7^o + K_7^1$$

$$K_7^o = \frac{K_7^o \, MW_7 \, RT_{11}}{2P_{11} g_c A_7^2}$$

$$K_7^1 = \frac{K_7^1 \, MW_7 \, RT_{11}}{2P_{11} g_c A_v^2} \left(1 - \frac{A_v^2}{A_7^2}\right)$$

linearization gives:

$$\delta P_{11} - \delta P_{12} = \delta K_7^1 \, n_5^2 + 2K_7^1 \, n_5 \delta n_5$$

$$MW_7 = MW_5$$

All the pressure loss from point 5 to point 12 can be combined:

$$P_5 - P_{12} = (K_5 + K_6 + K_7^o + K_7^1) \, n_5^2$$

linearization gives:

$$\delta P_5 - \delta P_{12} = 2 \, (K_5 + K_6 + K_7)(n_9 + n_{10,2})(\delta n_9 + \delta n_{10,2}) + (n_9 + n_{10,2})^2 \, \delta K_7$$

Oxygen extraction: at point 12.

$$n_8 = n_5 - n_{10,2}$$

Airflow total pressure loss: due to extraction of oxygen at point 12.

Ignored.

Airflow total pressure loss due to flow shear at duct wall: all the lower duct system friction-induced pressure loss is lumped into one single section in this model (path 13 between points 12 and 13).

$$P_{12} - P_{13} = K_8 \, n_8^2$$

$$K_8 \doteq (.0735)\left(\frac{\pi \, D_8 \, L_8}{A_8}\right)(Re_{L_8})^{-\frac{1}{5}}\left(\frac{MW_8}{2000 \, \rho_8 A_8^2}\right)$$

$$n_5 = n_6 = n_7 = n_8 + n_{10,2}$$

$$Re_{L_8} = \frac{\rho_8 \, MW_8 \, V_8 \, L_8}{1000 \, \mu_8}$$

$$V_8 = \frac{n_8}{\rho_8 A_8}$$

$$\rho_8 = \rho_6$$

$$MW_8 = \sum_{k=1}^{4} MW_{7,k} \frac{N_{5,k}}{N_5} - MW_{7,2} \frac{n_{10,2}}{n_8}$$

$$n_9 = n_8$$

$$MW_8 = MW_9$$

linearization gives:

$$\delta P_{12} - \delta P_{13} = 2 K_8 n_9 \delta n_9$$

Fluid inertance in the lower duct:

$$\dot{n}_9 = \frac{1000 g_c A_9}{MW_9 L_9} (P_{13} - P_{14})$$

$$A_9 = A_8$$

$$L_9 = L_8$$

$$MW_9 = MW_8$$

linearization gives:

$$\delta \dot{n}_9 = \frac{1000 g_c A_9}{MW_9 L_9} (\delta P_{13} - \delta P_{14})$$

Air Mover and Drive Motor Subsystem (AM&DMS).

It was concluded that it was desirable for the model of the AM&DMS to reflect the addition of power to the fluid-thermodynamic systems and the rotational dynamics of the rotor components. To accomplish this, the relations among pressure rise, torque, rotational speed, molar flow rate, power transfer, and the rotational dynamics equations must be generated.

The Fan Equations.

An option to using First Principles in the modeling of the air mover characteristics is the use of the empirical fan equations which are implicit in the

conventional fan curves so common in industry;

$P_{16} - P_{15} = f_{fan}(\omega_{37}, n_{12})$

linearization gives:

$$\delta P_{16} - \delta P_{15} = \frac{\partial f_{fan}(\omega_{37}, n_{12})}{\partial \omega_{37}} \delta\omega_{37} + \frac{\partial f_{fan}(\omega_{37}, n_{12})}{\partial n_{12}} \delta n_{12}$$

this is a steady flow relation, and approximations of the partial derivatives can be taken directly from fan curves.

Power Conversion (mechanical rotational power to fluid power):

With perfect power conversion, the mechanical rotational power supplied to the fluid via the air mover impeller would be converted to fluid power. Since the process is not perfect, the overall efficiency is used to describe the actual situation:

Mechanical power in (delivered to blower rotor) × efficiency = increase in fluid power out

$$\omega_{37}\, \tau_{36}\, \eta_o = (P_{16} - P_{15}) \frac{n_{12}}{\rho_{14}}$$

assuming constant density, linearization gives:

$$\omega_{37}\, \delta\tau_{36}\, \eta_o + \delta\omega_{37}\, \tau_{36}\, \eta_o = (P_{16} - P_{15}) \frac{\delta n_{12}}{\rho} + (\delta P_{16} - \delta P_{15}) \frac{n_{12}}{\rho}$$

Air Temperature Rise Due to Air Mover.

The temperature rise associated with the passage of the air through the air mover is the sum of that due to the isentropic pressure rise:

$$n_{12}\, c_{p12}\, T_{16} - n_{12}\, c_{p12}\, T_{15} = (P_{16} - P_{15}) \frac{n_{12}}{\rho_{14}}$$

and that due to the overall inefficiency of the air mover:

$$n_{12}\, c_{p12}\, T_{16} - n_{12}\, c_{p12}\, T_{15} = (1 - \eta_o)\omega_{37}\, \tau_{36}$$

Linearization of each (assuming constant density) gives:

$$c_{p12}\, \delta T_{16} - c_p\, \delta T_{15} = (\delta P_{16} - \delta P_{15}) \frac{1}{\rho_{14}}$$

and

$$c_{p12}\, \delta T_{16} - c_p\, \delta T_{15} = (1 - \eta_o)\delta\omega_{37}\, \tau_{36} + (1 - \eta_o)\omega_{37}\, \delta\tau_{36}$$

$n_{12} = n_9$

Combined pump and motor rotor dynamics.

Drive motor rotor and pump rotor:

$(J_{impeller} + J_{motor})\ \dot{\omega}_{37} + b_1\omega_{37} + b_2\omega_{37}^2 = \tau_c - \tau_{36}$

linearization gives:

$(J_{impeller} + J_{motor})\ \delta\dot{\omega}_{37} + (b_1 + 2\ b_2\omega_{37})\delta\omega_{37} = \delta\tau_c - \delta\tau_{36}$

The Gas Injection and Mixing Chamber

The gas injection and mixing chamber is modeled to serve two purposes: account for the injection of carbon dioxide, oxygen, water vapor, and nitrogen content into the flowstream, and to reflect the effects of the volume of the ducting and fittings in that area on the overall system dynamics.

Airflow total pressure loss: into gas injection and mixing chamber.

$$P_{16} - P_{36} = \frac{K_{13} MW_{13} R T_{16}}{2\ P_{16}\ g_c A_{13}^2}\left(1 - \frac{A_{13}^2}{A_{14}^2}\right) n_{13}^2$$

$MW_{13} = MW_9$

this pressure loss is ignored

Rate of accumulation of the air constituents in the gas injection and mixing chamber (point 36):

In the following, the equations of like level are grouped. Previously all equations addressing the same constituent were grouped.

$\dot{N}_{36,1} = n_{13,1} + n_{17,1} - n_{14,1}$

$\dot{N}_{36,2} = n_{13,2} + n_{17,2} - n_{14,2}$

$\dot{N}_{36,3} = n_{13,3} + n_{17,3} - n_{14,3}$

$\dot{N}_{36,4} = n_{13,4} + n_{17,4} - n_{14,4}$

$$n_{13,k} = \frac{N_{5,k}}{N_5}\ (n_9 + n_{10,2}),\ k = 1,3,4;\ n_{13,k} = \frac{N_{5,k}}{N_5}\ (n_9 + n_{10,2}) - n_{10,2},\ k = 2$$

$$n_{14,k} = \frac{N_{36,k}}{N_{36}}\ (n_{14}) = \frac{N_{36,k}}{N_{36}}\ (n_1 + n_{18}),\ k = 1,2,3,4$$

$$\dot{N}_{36,1} = (n_9 + n_{10,2})\ \frac{N_{5,1}}{N_5} + n_{17,1} - (n_1 + n_{18})\ \frac{N_{36,1}}{N_{36}}$$

$$\dot{N}_{36,2} = (n_9 + n_{10,2})\ \frac{N_{5,2}}{N_5} - n_{10,2} + n_{17,2} - (n_1 + n_{18})\ \frac{N_{36,2}}{N_{36}}$$

$$\dot{N}_{36,3} = (n_9 + n_{10,2})\ \frac{N_{5,3}}{N_5} + n_{17,3} - (n_1 + n_{18})\ \frac{N_{36,3}}{N_{36}}$$

$$\dot{N}_{36,4} = (n_9 + n_{10,2})\ \frac{N_{5,4}}{N_5} + n_{17,4} - (n_1 + n_{18})\ \frac{N_{36,4}}{N_{36}}$$

linearization gives:

$$\delta\dot{N}_{36,1} = (\delta n_9 + \delta n_{10,2})\ \frac{N_{5,1}}{N_5} + (n_9 + n_{10,2})\ \frac{\delta N_{5,1}}{N_5} - (n_9 + n_{10,2})\ \frac{N_{5,1}}{N_5^2} \sum_{k=1}^{4} \delta N_{5,k}$$

$$+ \delta n_{17,1} - (\delta n_1 + \delta n_{18})\ \frac{N_{36,1}}{N_{36}} - (n_1 + n_{18})\ \frac{\delta N_{36,1}}{N_{36}} + (n_1 + n_{18})\ \frac{N_{36,1}}{N_{36}^2} \sum_{k=1}^{4} \delta N_{36,k}$$

$$\delta\dot{N}_{36,2} = (\delta n_9 + \delta n_{10,2})\ \frac{N_{5,2}}{N_5} + (n_9 + n_{10,2})\ \frac{\delta N_{5,2}}{N_5} - (n_9 + n_{10,2})\ \frac{N_{5,2}}{N_5^2} \sum_{k=1}^{4} \delta N_{5,k}$$

$$- \delta n_{10,2} + \delta n_{17,2} - (\delta n_1 + \delta n_{18})\ \frac{N_{36,2}}{N_{36}} - (n_1 + n_{18})\ \frac{\delta N_{36,2}}{N_{36}} + (n_1 + n_{18})\ \frac{N_{36,2}}{N_{36}^2} \sum_{k=1}^{4} \delta N_{36,k}$$

$$\delta\dot{N}_{36,3} = (\delta n_9 + \delta n_{10,2})\ \frac{N_{5,3}}{N_5} + (n_9 + n_{10,2})\ \frac{\delta N_{5,3}}{N_5} - (n_9 + n_{10,2})\ \frac{N_{5,3}}{N_5^2} \sum_{k=1}^{4} \delta N_{5,k}$$

$$+ \delta n_{17,3} - (\delta n_1 + \delta n_{18})\ \frac{N_{36,3}}{N_{36}} - (n_1 + n_{18})\ \frac{\delta N_{36,3}}{N_{36}} + (n_1 + n_{18})\ \frac{N_{36,3}}{N_{36}^2} \sum_{k=1}^{4} \delta N_{36,k}$$

$$\delta\dot{N}_{36,4} = (\delta n_9 + \delta n_{10,2})\ \frac{N_{5,4}}{N_5} + (n_9 + n_{10,2})\ \frac{\delta N_{5,4}}{N_5} - (n_9 + n_{10,2})\ \frac{N_{5,4}}{N_5^2} \sum_{k=1}^{4} \delta N_{5,k}$$

$$+ \delta n_{17,4} - (\delta n_1 + \delta n_{18})\ \frac{N_{36,4}}{N_{36}} - (n_1 + n_{18})\ \frac{\delta N_{36,4}}{N_{36}} + (n_1 + n_{18})\ \frac{N_{36,4}}{N_{36}^2} \sum_{k=1}^{4} \delta N_{36,k}$$

Energy balance in the gas injection and mixing chamber

$$\dot{E}_{36} = \sum_{k=1}^{4} h^{o}_{13,k} + \sum_{k=1}^{4} h^{o}_{17,k} - \sum_{k=1}^{4} h^{o}_{14,k}$$

$$\downarrow$$

$$(N_{36,1}\, c_{v_{36,1}} + N_{36,2}\, c_{v_{36,2}} + N_{36,3}\, c_{v_{36,3}} + N_{36,4}\, c_{v_{36,4}})\, \dot{T}_{36} =$$

$$(n_{9,1}\, c_{p_{16,1}} + n_{9,2}\, c_{p_{16,2}} + n_{9,3}\, c_{p_{16,3}} + n_{9,4}\, c_{p_{16,4}})\, (T_{16} - 273.15)$$

$$+ (n_{17,1}\, c_{p_{17,1}} + n_{17,2}\, c_{p_{17,2}} + n_{17,3}\, c_{p_{17,3}} + n_{17,4}\, c_{p_{17,4}})\, (T_{17} - 273.15)$$

$$- (n_{14,1}\, c_{p_{36,1}} + n_{14,2}\, c_{p_{36,2}} + n_{14,3}\, c_{p_{36,3}} + n_{14,4}\, c_{p_{36,4}})\, (T_{36} - 273.15)$$

$$n_9\, c_{p_{16}} \doteq n_{9,1}\, c_{p_{16,1}} + n_{9,2}\, c_{p_{16,2}} + n_{9,3}\, c_{p_{16,3}} + n_{9,4}\, c_{p_{16,4}}$$

$$n_{14}\, c_{p_{36}} \doteq n_{14,1}\, c_{p_{36,1}} + n_{14,2}\, c_{p_{36,2}} + n_{14,3}\, c_{p_{36,3}} + n_{14,4}\, c_{p_{36,4}}$$

linearization gives:

$$(N_{36,1}\, c_{v_{36,1}} + N_{36,2}\, c_{v_{36,2}} + N_{36,3}\, c_{v_{36,3}} + N_{36,4}\, c_{v_{36,4}})\, \delta\dot{T}_{36} =$$

$$\delta n_9\, c_{p_{16}}\, (T_{16} - 273.15) + n_9\, c_{p_{16}}\, \delta T_{16}$$

$$+ (\delta n_{17,1}\, c_{p_{17,1}} + \delta n_{17,2}\, c_{p_{17,2}} + \delta n_{17,3}\, c_{p_{17,3}} + \delta n_{17,4}\, c_{p_{17,4}})\, (T_{17} - 273.15)$$

$$+ (n_{17,1}\, c_{p_{17,1}} + n_{17,2}\, c_{p_{17,2}} + n_{17,3}\, c_{p_{17,3}} + n_{17,4}\, c_{p_{17,4}})\, \delta T_{17}$$

$$- (\delta n_1 + \delta n_{18})\, c_{p_{36}} (T_{36} - 273.15) - (n_1 + n_{18})\, c_{p_{36}} \delta T_{36}$$

Equation of state for the gas injection and mixing chamber.

$$P_{36}\, V_{36} = N_{36}\, R\, T_{36}$$

$$\delta P_{36}\, V_{36} = (\sum_{k=1}^{4} \delta N_{36,k})\, R\, T_{36} + N_{36}\, R\, \delta T_{36}$$

Airflow total pressure loss: exiting from the gas injection and mixing chamber. (GIMC).

$$P_{36} - P_{17} = K_{14}\, \frac{MW_{36} R T_{36}}{2000\ P_{36}}\, \frac{1}{A_{14u}{}^2}\, \left(\frac{A_{14u}{}^2}{A_{14d}{}^2} - 1 \right)\, n_{14}{}^2$$

where

A_{14u} is the flow area at the upstream end of flow path 14

A_{14d} is the flow area at the downstream end of flow path 14

$MW_{36} = \sum \rho_{36,i}\, c_{p,i}$; the molecular weight of the gas in the GIMC

this pressure loss is ignored

Water Vapor Removal System

The water removal system must route the necessary fraction of the total flow through the condensing heat exchanger so that the evapo-transpiration water is removed. It is presumed that the temperature of the air exiting the condensing heat exchanger is fixed (e.g., by the use of feedback control) at a prescribed level, and is saturated at that temperature.

By-Pass Fraction Determination

The by-pass fraction is the fraction of the total flow through the water vapor removal system which is diverted around the heat exchanger

$$\chi_{14} \triangleq \frac{n_{16}}{n_{14}} = \frac{n_{14} - n_{15}}{n_{14}}$$

There are three equivalent, relevant, and related relationships among specific humidity, concentration, and partial pressure,

(1) $SH_{14} = N_{36,4} / \sum_{i=1}^{3} N_{36,i}$, (2) $SH_{14} = Cc_{14,4}/(1 - Cc_{14,4})$, and

(3) $Cc_{14,4}$ = (partial pressure of the water vapor at 36)/P_{36}

The water removed by the heat exchanger can be expressed in terms of the total air side flow by

$$n_{18} = (SH_{36} - SH_{21})(1 - SH_{36})\, n_{15}$$

and linearization gives:

$$\delta n_{18} = (\delta SH_{36} - \delta SH_{21})(1 - SH_{36})\, n_{15} - (SH_{36} - SH_{21})\delta SH_{36}\, n_{15} + (SH_{36} - SH_{21})(1 - SH_{36})\, \delta n_{15}$$

$$n_{15} = (1 - \chi_{14})\, n_{14}$$

linearization gives

$$\delta n_{15} = -\delta\chi_{14}\, n_{14} + (1-\chi_{14})\, \delta n_{14}$$

The nominal value of χ_{14} is established by setting n_{18} to equal $n_{2,4}$ to determine the nominal value of n_{15}, and then solving for χ_{14}. The requirement of matter conservation in the flow split establishes that

$$n_{15} + n_{16} = n_{14} = n_1 + n_{18}$$

which with linearization gives:

$$\delta n_{15} + \delta n_{16} = \delta n_1 + \delta n_{18}$$

Airflow total pressure loss: through control valve 21 (heat exchanger by-pass)

$$P_{18} = P_{17}$$

$$P_{19} = P_{17}$$

as is pressure loss in the by-pass up to the control valve.

$$P_{20} = P_{18}$$

$$P_{20} - P_{23} = \frac{K_{20} MW_{36} RT_{36}}{2\, P_{20}\, g_c A_{v20}^2}\left(1 - \frac{A_{v20}^2}{A_{20}^2}\right) n_{20}^{\,2}$$

$$P_{20} - P_{23} = K_{20}\, n_{20}^{\,2}$$

$$K_{20} \doteq \frac{K_{20} MW_{36} RT_{36}}{2\, P_{20}\, g_c A_{v20}^2}\left(1 - \frac{A_{v20}^2}{A_{20}^2}\right)$$

$$MW_{20} = MW_{36}$$

linearization gives:

$$\delta P_{20} - \delta P_{23} = 2\, n_{20}\, K_{20}\, \delta n_{20} + n_{20}^{\,2}\, \delta K_{20}$$

$$n_{21} = n_{20}$$

Airflow total pressure loss: through control valve 22 and dehumidifying heat exchanger.

Control valve in water removal system heat exchanger path duct:

$$P_{21} - P_{22} = K_{19}\, n_{21}^{\,2}$$

$$K_{19} \doteq \frac{K_{19} MW_{36} R T_{36}}{2\, P_{21}\, g_c A_{v19}^2}\left(1 - \frac{A_{v19}^2}{A_{19}^2}\right)$$

linearization gives:

$$\delta P_{21} - \delta P_{22} = \delta K_{19}\, n_{21}{}^2 + 2 K_{19}\, n_{21} \delta n_{21}$$

For the heat exchanger:

$$P_{19} - P_{21} = K_{15}\, n_{19}{}^2$$

For preliminary work, one can estimate K_{15} via Reynolds' analogy or simply budget a reasonable pressure loss. Linearization gives:

$$\delta P_{19} - \delta P_{21} = 2 K_{15}\, n_{19} \delta n_{19}$$

These two pressure loss expressions can be combined:

$$\delta P_{19} - \delta P_{22} = n_{19}{}^2 \delta K_{19} + 2(K_{15} + K_{19})\, n_{19}\, \delta n_{19}$$

$$MW_{22} = MW_{21} = MW_{14}$$

$$MW_{22} = \sum_{k=1}^{4} MW_{36,k} \frac{N_{36,k}}{N_{36}} - MW_{,4} \frac{n_{18}}{n_{15}}$$

$$n_{22} = n_{15} - n_{18}$$

Energy balance: condensing heat exchanger. (reference is liquid water at triple point)

$$n_{15}\, c_{p,36} T_{36} - n_{22}\, c_{p,21} T_{21} - n_{18} h_{38} = 0$$

linearization gives:

$$\delta n_{15}\, c_{p,36} T_{36} + n_{15}\, c_{p,36} \delta T_{36} - \delta n_{22}\, c_{p,21} T_{21} - n_{22}\, c_{p,21} \delta T_{21} - \delta n_{18}\, h_{38} + n_{18}\, \delta h_{38} = 0$$

Energy balance: recombination of flow streams of the water vapor removal system.

$$n_1\, c_{p_{24}} (T_{24} - 273.15) = n_{21}\, c_{p_{23}} (T_{23} - 273.15) + n_{22}\, c_{p_{22}} (T_{22} - 273.15)$$

$$n_1\, c_{p_{24}} \doteq \sum_{k=1}^{4} n_{1,k}\, c_{p_{24,k}}$$

$$n_{21}\, c_{p_{23}} \doteq \sum_{k=1}^{4} n_{21,k}\, c_{p_{23,k}}$$

$$n_{22}\, c_{p_{22}} \doteq \sum_{k=1}^{4} n_{22,k}\, c_{p_{22,k}}$$

$$n_{21} = n_{20} = n_1 - n_{10,2} - n_{15}$$

$$c_{p_{23}} = c_{p_{36}}$$

$c_{p_{22}} = c_{p_{21}}$

$c_{p_{24}} = c_{p_{36}} = c_{p_{21}}$

$T_{23} = T_{36}$

$T_{22} = T_{21}$

linearization gives:

$$n_1 c_{p_{24}} \delta T_{24} + \delta n_1 c_{p_{24}} (T_{24} - 273.15) = (n_1 - n_{10,2} - n_{15}) c_{p_{36}} \delta T_{36}$$
$$+ (\delta n_1 - \delta n_{10,2} - \delta n_{15}) c_{p_{36}} (T_{36} - 273.15) + (\delta n_{15} - \delta n_{18}) c_{p_{21}} (T_{21} - 273.15)$$
$$n_1 \delta T_{24} + \delta n_1 (T_{24} - 273.15) = (n_1 - n_{10,2} - n_{15}) \delta T_{36}$$
$$+ (\delta n_1 - \delta n_{10,2} - \delta n_{15}) (T_{36} - 273.15) + (\delta n_{15} - \delta n_{18}) (T_{21} - 273.15)$$

Airflow total pressure loss: combining flows of water removal system paths

(1) heat exchanger bypass path (path 16)

$$P_{24} - P_{23} = \frac{K_{21-23}\, MW_{21}^2 RT_{25}}{P_{24}} \left[a_1 \left(\frac{n_{23}}{A_{23}}\right)^2 - a_2 \left(\frac{n_{21}}{A_{21}}\right)^2 - a_3 \left(\frac{n_{21}^2}{A_{23}\, A_{21}}\right) - a_3 \left(\frac{n_{22}^2}{A_{22}\, A_{23}}\right)\right]$$

This pressure loss is ignored.

(2) heat exchanger path (path 15)

$$P_{24} - P_{22} = \frac{K_{22-23}\, MW_{22}^2 RT_{21}}{P_{22}} \left[a_1 \left(\frac{n_{23}}{A_{23}}\right)^2 - a_2 \left(\frac{n_{22}}{A_{22}}\right)^2 - a_3 \left(\frac{n_{22}^2}{A_{23}\, A_{22}}\right) - a_3 \left(\frac{n_{22}^2}{A_{22}\, A_{23}}\right)\right]$$

This pressure loss is ignored.

Airflow total pressure loss: duct between water removal subsystem and air temperature manipulation subsystem (path 23).

$$P_{24} - P_{25} = K_{23}\, n_{23}^2$$

$$K_{23} \doteq (.0735)\left(\frac{\pi\, D_{23}\, L_{23}}{A_{23}}\right)\left(Re_{L_{23}}\right)^{-\frac{1}{5}}\left(\frac{MW_{23}}{2000\, \rho_{23} A_{23}^2}\right)$$

$$Re_{L_{23}} = \frac{\rho_{23}\, MW_{23}\, V_{23}\, L_{23}}{1000\, \mu_{23}},\ v_{23} = \frac{n_{23}}{\rho_{23}\, A_{23}}$$

$MW_{23} = MW_1$

$n_{23} = n_1$

linearization gives

$$\delta P_{24} - \delta P_{25} = 2\, K_{23}\, n_1\, \delta n_1$$

The Airflow Cooling/Heating System

The airflow cooling/heating system (AC/HS) must route the necessary fraction of the total flow through either the cooling heat exchanger or the heating heat exchanger so that the temperature of the flowstream exiting the AC/HS is at the required level. It is presumed that the temperature of the air exiting the active heat exchanger is fixed (e.g., by the use of feedback control) at a prescribed level, and no condensation occurs.

By-Pass Fraction Determination

For the present demonstration, the by-pass fraction is the fraction of the total flow which is diverted around the cooling heat exchanger

$$\chi_{23} \triangleq \frac{n_{25}}{n_{23}} = \frac{n_{23} - n_{26}}{n_{23}}$$

$$n_{25} = \chi_{23}\, n_{23}$$

linearization gives:

$$\delta n_{25} = \delta\chi_{23}\, n_{23} + \chi_{23}\, \delta n_{23}$$

The nominal value of χ_{23} is established by performing a thermal energy balance analysis so that the required nominal discharge temperature at 35 is achieved, as is explained in the following.

Matter conservation across the flow split requires that

$$n_{25} + n_{26} = n_{23}$$

and linearization (in this case, a redundant operation) gives:

$$\delta n_{25} + \delta n_{26} = \delta n_{23}$$

$$n_1 = n_{23}$$

Energy balance at recombination of airflow streams from airflow cooling system.

$$n_1\, c_{p_{35}}\, (T_{35} - 273.15) = n_{31}\, c_{p_{33}}\, (T_{33} - 273.15) + n_{32}\, c_{p_{34}}\, (T_{34} - 273.15)$$
$$+ n_{30}\, c_{p_{30}}\, (T_{32} - 273.15)$$

where

$$n_1 \, c_{p_{35}} \doteq \sum_{k=1}^{4} n_{1,k} \, c_{p_{35,k}}$$

$$n_{31} \, c_{p_{33}} \doteq \sum_{k=1}^{4} n_{31,k} \, c_{p_{33,k}}$$

$$n_{32} \, c_{p_{34}} \doteq \sum_{k=1}^{4} n_{32,k} \, c_{p_{34,k}}$$

$$n_{31} = n_{28}$$

$$n_{32} = n_{27}$$

$$c_{p_{33}} = c_{p_{24}}$$

$$c_{p_{34}} = c_{p_{29}}$$

$$T_{33} = T_{24}$$

$$T_{34} = T_{29}$$

along with linearization, gives:

$$n_1 \, c_{p_{35}} \, \delta T_{35} + \delta n_1 \, c_{p_{35}} \, (T_{35} - 273.15) = n_{28} \, c_{p_{24}} \, \delta T_{24} + \delta n_{28} \, c_{p_{24}} \, (T_{24} - 273.15)$$
$$+ (\delta n_1 - \delta n_{28}) \, c_{p_{29}} \, (T_{29} - 273.15)$$

or, since

$$c_{p_{35}} = c_{p_{24}} = c_{p_{29}}$$

$$n_1 \, \delta T_{35} + \delta n_1 \, (T_{35} - 273.15) = n_{28} \, \delta T_{24} + \delta n_{28} \, (T_{24} - 273.15)$$
$$+ (\delta n_1 - \delta n_{28}) \, (T_{29} - 273.15)$$

$$MW_{26} = MW_{27} = MW_1$$

$$P_{28} = P_{25}$$

$$P_{34} = P_{35}$$

One may establish the nominal value of χ_{23} for the scenario demonstrated in this study through simultaneous solution of the two equations

$$n_{23} \, c_{p_{35}} \, (T_{35} - 273.15) = n_{25} \, c_{p_{33}} \, (T_{33} - 273.15) + n_{25} \, c_{p_{34}} \, (T_{34} - 273.15)$$

and

$$n_{25} = \chi_{23}\, n_{23}$$

to satisfy the requirement for T_{35}

Airflow total pressure loss: air entering each of the three airflow temperature manipulation subsystem ducts;

(1) heating heat exchanger path (path 24).

$$P_{25} - P_{26} = \frac{K_{23-24}\, MW_{23}^2\, RT_{25}}{P_{25}} \left[a_1 \left(\frac{n_{24}}{A_{24}}\right)^2 - a_2 \left(\frac{n_{23}}{A_{23}}\right)^2 - a_3 \left(\frac{n_{24} n_{23}}{A_{24}\, A_{23}}\right)\right]$$

This pressure loss is ignored .

(2) bypass path (path 25)

$$P_{25} - P_{27} = \frac{K_{23-25}\, MW_{23}^2\, RT_{25}}{P_{25}} \left[a_1 \left(\frac{n_{25}}{A_{25}}\right)^2 - a_2 \left(\frac{n_{23}}{A_{23}}\right)^2 - a_3 \left(\frac{n_{25} n_{23}}{A_{25}\, A_{23}}\right)\right]$$

This pressure loss is ignored.

(3) cooling heat exchanger path (path 26)

$$P_{25} - P_{28} = \frac{K_{23-26}\, MW_{23}^2\, RT_{25}}{P_{25}} \left[a_1 \left(\frac{n_{26}}{A_{26}}\right)^2 - a_2 \left(\frac{n_{23}}{A_{23}}\right)^2 - a_3 \left(\frac{n_{26} n_{23}}{A_{26}\, A_{23}}\right)\right]$$

Airflow total pressure loss: air flowing in each of the three airflow temperature manipulation subsystem ducts;

(1) heating heat exchanger path (path 24).

$$P_{26} - P_{31} = \frac{K_{24}\, MW_{23}^2\, RT_{25}}{P_{26}} \left(\frac{n_{24}}{A_{24}}\right)^2$$

This pressure loss is ignored.

(2) bypass path (path 25)

$$P_{27} - P_{30} = \frac{4\, f_{25}\, L_{25}}{D_{25}} \frac{MW_{25}^2 RT_{25}}{2\, P_{27}\, A_{25}^2}\; n_{25}^2$$

This pressure loss is ignored.

(3) cooling heat exchanger path (path 26).

$$P_{28} - P_{29} = \frac{K_{26}\, MW_{23}^2\, RT_{25}}{P_{28}} \left(\frac{n_{26}}{A_{26}}\right)^2$$

linearization gives

$$\delta P_{28} - \delta P_{29} = K_{26}\, \delta n_{26}$$

this pressure loss is combined with the fixed part of the control valve pressure loss.

Airflow total pressure loss: control valves in the air temperature manipulation system

(1) heating heat exchanger path and control valve (path 29).

heat exchanger; use Reynolds' analogy or budget a reasonable pressure loss

$$P_{26} - P_{31} = \frac{K_{24}\, MW_{24}\, RT_{26}}{2\, P_{26}\, g_c A_{24}^2}\, n_{29}^2 = K_{29}\, n_{29}^2$$

linearization gives:

$$\delta P_{26} - \delta P_{31} = 2K_{29}\, n_{29} \delta n_{29}$$

control valve:

$$P_{31} - P_{32} = \frac{K_{29}\, MW_{23}\, RT_{31}}{2\, P_{31}\, g_c A_{v29}^2} \left(1 - \frac{A_{v29}^2}{A_{29}^2}\right) n_{29}^2 = K_{29}\, n_{29}^2$$

linearization gives:

$$\delta P_{31} - \delta P_{32} = \delta K_{29}\, n_{29}^2 + 2K_{29}\, n_{29}\, \delta n_{29}$$

This pressure loss was not relevant to the scenario demonstrated in this study.

(2) bypass path (path 28).

control valve:

$$P_{30} - P_{33} = \frac{K_{28}\, MW_{23}\, RT_{31}}{2\, P_{30}\, g_c A_{v28}^2} \left(1 - \frac{A_{v28}^2}{A_{28}^2}\right) n_{28}^2$$

$$P_{30} - P_{33} = K_{28}\, n_{28}^2$$

linearization gives

$$\delta P_{30} - \delta P_{33} = \delta K_{28}\, n_{28}^2 + 2K_{28}\, n_{28}\, \delta n_{28}$$

(3) cooling heat exchanger and control valve (path 27).

heat exchanger: use Reynolds' analogy or budget a reasonable pressure loss,

$$P_{28} - P_{29} = K_{26}\, n_{26}^2$$

linearization gives

$$\delta P_{28} - \delta P_{29} = 2K_{26}\, n_{26}\, \delta n_{26}$$

control valve:

$$P_{29} - P_{34} = \frac{K_{27}\, MW_{23}\, RT_{31}}{2\, P_{29}\, g_c A_{v27}^2} \left(1 - \frac{A_{v27}^2}{A_{27}^2}\right) n_{27}^2$$

$$P_{29} - P_{34} = K_{27} \; n_{27}^2$$

linearization gives:

$$\delta P_{29} - \delta P_{34} = \delta K_{27} \; n_{27}^2 + 2 \, K_{27} \; n_{27} \delta n_{27}$$

$$n_{27} = n_{26}$$

Airflow total pressure loss: recombination of air temperature manipulation subsystem flow (into path 1).

(1) heating heat exchanger path (path 30)

$$P_{32} - P_{35} = \frac{K_{25-33} \, MW_1^2 RT_{35}}{P_{35}} \left[a_1 \left(\frac{n_{28}}{A_{28}}\right)^2 - a_2 \left(\frac{n_{21}}{A_{21}}\right)^2 - a_3 \left(\frac{n_{21}^2}{A_{23} \, A_{21}}\right) - a_3 \left(\frac{n_{22}^2}{A_{22} \, A_{23}}\right)\right]$$

This pressure loss is ignored.

(2) bypass path (path 31)

$$P_{33} - P_{35} = \frac{K_{22-23} \, MW_{22}^2 RT_{21}}{P_{22}} \left[a_1 \left(\frac{n_{23}}{A_{23}}\right)^2 - a_2 \left(\frac{n_{22}}{A_{22}}\right)^2 - a_3 \left(\frac{n_{22}^2}{A_{23} \, A_{22}}\right) - a_3 \left(\frac{n_{22}^2}{A_{22} \, A_{23}}\right)\right]$$

This pressure loss is ignored.

(3) cooling heat exchanger path (path 32)

$$P_{34} - P_{35} = \frac{K_{23-25} \, MW_{23}^2 \, RT_{25}}{P_{25}} \left[a_1 \left(\frac{n_{25}}{A_{25}}\right)^2 - a_2 \left(\frac{n_{23}}{A_{23}}\right)^2 - a_3 \left(\frac{n_{25} n_{23}}{A_{25} \, A_{23}}\right)\right]$$

This pressure loss is ignored.

$$MW_{28} = MW_1$$

$$n_1 = n_{27} + n_{28}$$

$$P_{30} = P_{25}$$

$$P_{33} = P_{35}$$

The heating heat exchanger control valve is fully closed in the scenario for which this study is done. The overall pressure loss for the airflow heating/cooling subsystem can be expressed in terms of either of the two active paths (25-28-31 or 26-27-32):

$$\delta P_{25} - \delta P_{35} = 2 \, (n_1 - n_{27}) \, K_{28} \, (\delta n_1 - \delta n_{27}) + (n_1 - n_{27})^2 \, \delta K_{28}$$

$$\delta P_{25} - \delta P_{35} = 2 \, (K_{26} + K_{27}) \, n_{27} \, \delta n_{27} + \delta K_{27} \, n_{27}^2$$

Airflow total pressure loss from inside the discharge end of the flow duct (path 1) into the shoot upper chamber:

$$P_3 - P_1 = K_1 \frac{MW_1^2 RT_3}{P_3 A_3^2} [\, 1 - \frac{A_3^2}{A_1^2}] \, n_1^2$$

linearization gives:

$$\delta P_3 - \delta P_1 = 2 K_1 \frac{MW_1^2 RT_3}{P_3 A_3^2} [\, 1 - \frac{A_3^2}{A_1^2}] \, n_1 \delta n_1 - K_1 \frac{MW_1^2 RT_3}{P_3^2 A_3^2} [\, 1 - \frac{A_3^2}{A_1^2}] \, n_1^2 \delta P_3$$

This pressure loss is ignored.

Recognizing the effect of glove port activity on upper chamber volume completes the inventory of relevant processes:

$$\dot{V}_1 = \dot{V}_g$$

$$\delta \dot{V}_1 = \dot{V}_g$$

5.5 - THE MODELED SCENARIO

The control study is directed to a plausible research experimental condition. The defining parameters of this experiment are:

(1). Temperature of the air exiting the upper chamber, T_1: 20 C.

(2). Relative humidity of the air exiting the upper chamber, RH_1: 70%.

(3). Absolute pressure of the air in the upper chamber, P_1: 101,458 Pa.

(4). Temperature of the upper chamber wall, T_4: 22 C.

(5). Source of PAR: on.

(6). Leaf area index: 30.

(7). Energy radiated from lamps which enters the CGC: 6000 Watts.

(8). Canopy absorbs all incident radiation.

(9). One-sixth of the absorbed energy evaporates transpiration water

(10). Five-sixths of the absorbed energy heats the air flowing through the CGC.

The system performance and physical configuration requirements, the

parameters of the prescribed experiment, along with enough bridging assumptions, when substituted into the modeling equations, generate the nominal values of each of the flow variables and point variables of the CSSEDS model.

Solving the above nonlinear equations for the equilibrium values of the system variables provides one with the values of all the variables which can be used in the linearized equations to determine the dynamical properties of the system for values of the system variables in the neighborhood of those of the experimental scenario.

5.6 - NOMINAL VALUES OF THE POINT VARIABLES AND THE FLOW VARIABLES

A_{pf} = 2.0 m^2, A_1= 0.1297 m^2, A_3 = 0.64 m^2, A_4 = 7.791 m^2, A_5= 0.1297 m^2, A_7 = 6.2402 m^2

b1 = 0.0 Newton-meters/radian per second,
b_2= 0.0013 Newton-meters/(radian per second)^2,

$(cp_{1,1})_{nom}$ = 29.1531 Joules mol^{-1} K^{-1}, $(cp_{1,2})_{nom}$ = 29.4908 Joules mol^{-1} K^{-1}
$(cp_{1,3})_{nom}$ = 37.0476 Joules mol^{-1} K^{-1}, $(cp_{1,4})_{nom}$ = 33.7301 Joules mol^{-1} K^{-1}
The above values are also used for these properties at points 2, 17, and 36.

$(cp_1)_{nom}$ = 29.14 Joules mol^{-1} K^{-1}
The above value is used for this property at points 5, 12, 16, 17, 21, 24, 35, and 36.

$(cv_{1,1})_{nom}$ = 20.8387 Joules mol^{-1} K^{-1}, $(cv_{1,2})_{nom}$ = 21.2055 Joules mol^{-1} K^{-1}
$(cv_{1,3})_{nom}$ = 28.7333 Joules mol^{-1} K^{-1}, $(cv_{1,4})_{nom}$ = 25.4158 Joules mol^{-1} K^{-1}
The above values are also used for these properties at points 5 and 36.
d_{pf} = 0.12439 m

D_8 = 0.4064 m

$\frac{\partial f(\omega_{37},\, n_9)}{\partial \omega_{37}}$ = 40.6 Pa/(radian per second), $\frac{\partial f(\omega_{37},\, n_9)}{\partial n_9}$ = 1.792 Pa/(mole per second),

$h_{chamber}$ = 0.7576 m

$h_{canopy} + d_{PPF_{ref}} = h_{chamber}$

$(h_{c_2})_{nom}$ = 34.577 watts m^{-2} K^{-1}, $(h_{c_4})_{nom}$ = 4.239 watts m^{-2} K^{-1}

$(h_{c_7})_{nom}$ = 7.3196 watts m^{-2} K^{-1}

$J_{impeller}$ = 4.468 kg m^2, J_{motor} = 1.328 kg m^2

$(k_1)_{nom}$ = 0.0263 watts m^{-1} K^{-1}

K_{filter} = .09555 n $m^{-2}mole^{-2}sec^2$, K_3 = 1.0 n $m^{-2}mole^{-2}sec^2$,

K_5 = 1.0 n $m^{-2}mole^{-2}sec^2$, $K_6 = K_{filter}$ = .09555 n $m^{-2}mole^{-2}sec^2$

K_7^0 = 0.00016 n $m^{-2}mole^{-2}sec^2$, K_7^1 = 0.055332 n $m^{-2}mole^{-2}sec^2$

K_8 = 0.002031 n $m^{-2}mole^{-2}sec^2$

K_{15} = 68.4 n $m^{-2}mole^{-2}sec^2$ $K_{21} = K_{20}$ = 158.8 n $m^{-2}mole^{-2}sec^2$

K_{22} = 114.0 n $m^{-2}mole^{-2}sec^2$ K_{23} = 158.8 n $m^{-2}mole^{-2}sec^2$

K_{26} = 0.0 n $m^{-2}mole^{-2}sec^2$ K_{27} = 0.1362 n $m^{-2}mole^{-2}sec^2$

K_{28} = 1.215 n $m^{-2}mole^{-2}sec^2$ K_{28} = 1.215 n $m^{-2}mole^{-2}sec^2$

LAI = 30 (unitless)

L_1 = 3.85 m L_5 = .2544 m L_8 = 3.85 m L_{23} = 3.85 m

$(MW_1)_{nom} = (MW_{35})_{nom}$ = 28.9700 g/mol, $(MW_3)_{nom}$ = 28.8277 g/mol,

$(MW_8)_{nom}$ = 28.8277 gm $mole^{-1}$ $(MW_9)_{nom} = (MW_8)_{nom}$ = 28.8277 gm $mole^{-1}$

$(MW_1)_{nom}$ = 28.8277 gm $mole^{-1}$ $(MW_5)_{nom}$ = 28.8277 gm $mole^{-1}$

$(n_1\, c_{p_{35}})_{nom} = (n_3\, c_{p_1})_{nom} = (102.26)(29.67) = 3034.448$ Watts K^{-1}

$(n_1)_{nom}$ = 102.2369 moles sec^{-1}, $(n_{1,1})_{nom}$ = 75.944 moles sec^{-1}

$(n_{1,2})_{nom}$ = 24.54225 moles sec^{-1}, $(n_{1,3})_{nom}$ = 0.122844 moles sec^{-1}

$(n_{1,4})_{nom}$ = 1.6278 moles sec^{-1},

$(n_{2,2}[resp])_{nom}$ = 0.0 moles sec^{-1},

$(n_{2,2})_{nom} = (n_{2,2}[\hbar\nu])_{nom} = -0.00014699$ moles sec^{-1},

$(n_{2,3}[\hbar\nu])_{nom} = 0.0$ moles sec^{-1},

$(n_{2,3}[resp])_{nom} = (n_{2,3})_{nom} = 0.00013542$ moles sec^{-1},

$(n_{2,4})_{nom} = -0.022236$ moles sec^{-1}

$(n_3)_{nom} = 102.1592$ moles sec^{-1}

$(n_3\ c_{p_1})_{nom} = (102.26)(29.67) = 3034.448$ Watts K^{-1}

$(n_{3,1})_{nom} = (n_{1,1})_{nom} = 75.944$ moles sec^{-1}, $(n_{3,2})_{nom} = 24.5420$ moles sec^{-1},

$(n_{3,3})_{nom} = 0.122712$ moles sec^{-1}, $(n_{3,4})_{nom} = 1.6505$ moles sec^{-1}

$(n_5)_{nom} = (n_3)_{nom} = 102.1592$ moles sec^{-1}, $(n_6)_{nom} = (n_3)_{nom} = 102.1592$ moles sec^{-1}

$(n_8)_{nom} = 102.1591$ moles sec^{-1} $(n_9)_{nom} = 102.1591$ moles sec^{-1}

$(n_{10,2})_{nom} = 0.00014699$ moles sec^{-1}

$(n_{14})_{nom} = (n_1 + n_{18})_{nom} = 102.2595$ moles sec^{-1} $(n_{15})_{nom} = 2.0861$ moles sec^{-1}

$(n_{16})_{nom} = (n_{20})_{nom} = (n_{21})_{nom} = 100.195636$ moles sec^{-1}

$(n_{17,1})_{nom} = 0.0$ moles sec^{-1} $(n_{17,2})_{nom} = 0.0$ moles sec^{-1}

$(n_{17,3})_{nom} = 0.00013542$ moles sec^{-1} $(n_{17,4})_{nom} = 0.0$ moles sec^{-1}

$(n_{19})_{nom} = (n_{15})_{nom} = 2.0861$ moles sec^{-1}

$(n_{18})_{nom} = -(n_{2,4})_{nom} = 0.022236$ moles sec^{-1}

$(n_{21})_{nom} = (n_{14})_{nom} - (n_{22})_{nom} = 100.195636$ moles sec^{-1}

$(n_{22})_{nom} = (n_{15})_{nom} - (n_{18})_{nom} = 2.063864$ moles sec^{-1}

$(n_{26})_{nom} = (n_{27})_{nom} = 76.64$ moles sec^{-1} $(n_{28})_{nom} = 25.5969$ moles sec^{-1}

$(n_{22})_{nom} = (n_{15})_{nom} - (n_{18})_{nom} = 2.063864$ moles sec^{-1}

$$(N_{1,1}\ c_{v_{1,1}} + N_{1,2}\ c_{v_{1,2}} + N_{1,3}\ c_{v_{1,3}} + N_{1,4}\ c_{v_{1,4}})_{nom} = 1778.2525 \text{ Joules } sec^{-1}$$

$(N_1)_{nom} = 83.2528$ moles,

$(\frac{N_{1,1}}{N_1})_{nom} = .74266$ unitless, $(\frac{N_{1,2}}{N_1})_{nom} = .24$ unitless,

$(\frac{N_{1,3}}{N_1})_{nom} = .001200$ unitless, $(\frac{N_{1,4}}{N_1})_{nom} = .01614$ unitless,

$(N_5)_{nom} = 28.3055$ moles,

$(\frac{N_{5,1}}{N_5})_{nom} = (\frac{n_{5,1}}{n_5})_{nom} = (\frac{n_{3,1}}{n_3})_{nom} = 0.74266$ unitless,

$(\frac{N_{5,2}}{N_5})_{nom} = (\frac{n_{5,2}}{n_5})_{nom} = (\frac{n_{3,2}}{n_3})_{nom} = 0.239936$ unitless,

$(\frac{N_{5,3}}{N_5})_{nom} = (\frac{n_{5,3}}{n_5})_{nom} = (\frac{n_{3,3}}{n_3})_{nom} = 0.0012$ unitless,

$(\frac{N_{5,4}}{N_5})_{nom} = (\frac{n_{5,4}}{n_5})_{nom} = (\frac{n_{3,4}}{n_3})_{nom} = 0.01614$ unitless,

$(N_{36})_{nom} = 41.622$ moles,

$(\frac{N_{36,1}}{N_{36}})_{nom} = .742663$ unitless,

$(\frac{N_{36,2}}{N_{36}})_{nom} = .239987$ unitless,

$(\frac{N_{36,3}}{N_{36}})_{nom} = .0012013$ unitless,

$(\frac{N_{36,4}}{N_{36}})_{nom} = .0161401$ unitless,

$Nu_{x=L_5} = 35.4046$ unitless,

$(P_1)_{nom} = 101{,}458$ Pa,

$(P_3)_{nom} = 101{,}458$ Pa

$(P_1 - P_5)_{nom} = 8.84$ Pa,

$(P_5)_{nom} = 101{,}449$ Pa

$(P_5 - P_6)_{nom} = 214.765$ Pa

$(P_6)_{nom} = 101{,}234$ Pa

$(P_9)_{nom} = 101{,}234$ Pa,

$(P_9 - P_{10})_{nom} = 999.2$ Pa

$(P_{10})_{nom} = 100{,}235$ Pa,

$(P_{11})_{nom} = 100{,}235$ Pa

$(P_{11} - P_{12})_{nom} = 599.5$ Pa,

$(P_{12})_{nom} = 99635$ Pa

$(P_{12} - P_{13})_{nom} = 212$ Pa

$(P_{13})_{nom} = 99{,}423$ Pa

$(P_{13} - P_{14})_{nom} = 0$

$(P_{14})_{nom} = 99{,}423$ Pa

$(P_{14} - P_{16})_{nom} = -3850$ Pa

$(P_{36})_{nom} = 103{,}272$ Pa

$(P_{17})_{nom} = 103{,}272$ Pa

$(P_{24})_{nom} = 102{,}472$ Pa

$(P_{25})_{nom} = 102{,}260$ Pa

$(P_{35})_{nom} = 101{,}458$ Pa

$(P_{36})_{nom} = (P_{17})_{nom} = 103{,}272.1$ Pa

$(Pr_1)_{nom} = 0.707$ unitless,

$(Pr_5)_{nom} = 0.707$ unitless

$R = 8.31441$ Joules $mole^{-1} K^{-1}$

$(Re_{L_1})_{nom} = 42{,}600$ unitless

$(Re_{L_5})_{nom} = 14{,}329$ unitless

$(Re_{L_8})_{nom} = 4.413 \times 10^6$ unitless

$SH_{21} = 0.008595$,

$SH_{36} = 0.016405$

$(T_1)_{nom} = 293.15$ K

$(T_2)_{nom} = 295.15$ K

$(T_3)_{nom} = 291.4179$ K

$(T_5)_{nom} = 293.173$ K

$(T_{17})_{nom} = (T_{36})_{nom} = (T_{16})_{nom} = 298.1$ K
$(T_{24})_{nom} = 294.8$ K
$(T_{27})_{nom} = (T_{28})_{nom} = 294.8$ K
$(T_{30})_{nom} = 294.9$ K
$(T_{36})_{nom} = 298.1$ K

$(T_{21})_{nom} = 278.2$ K
$(T_{25})_{nom} = (T_{24})_{nom} = 294.8$ K
$(T_{29})_{nom} = 288.85$ K
$(T_{35})_{nom} = 291.4179$ K

$(UA)_{4\ nom} = 33.03$ watts K^{-1}
$(UA)_{7\ nom} = 45.676$ watts K^{-1}

$(UA)_{2\ nom} = 4149.24$ watts K^{-1}

$V_1 = 2.0\ m^3$ $V_5 = 0.68\ m^3$ $V_{36} = 2\ A_1\ L_{23} = .99869\ m^3$

$(\mu_1)_{nom} = 0.00001983$ kg m^{-1} sec^{-1}
$\eta_p = .6$
$(\rho_5)_{nom} = 41.62$ moles m^{-3}
$(\chi_{14})_{nom} = 0.0204$ (unitless)

$(\mu_5)_{nom} = 0.00001983$ kg m^{-1} sec^{-1}
$(\rho_1)_{nom} = 41.63$ mol m^{-3}
$(\omega_{37})_{nom} = 189$ rad sec^{-1}
$(\chi_{23})_{nom} = .6134$ (unitless)

5.7 - THE CONDENSED PRIMITIVE EQUATIONS

To express the system of equations in the format of Equations (1) and (2), we assign $\eta, \sigma, u,\ d$ elements to the perturbed variables, $\delta(\cdot)$ as is shown in Table 1;

As an aid to the reader, the inverse assignments are listed in Table 2.

The result of using these assignments and inserting the nominal numerical values into the linearized equations is:

$$\dot{\eta}_1 = 1.279\ \sigma_1 - 1.279\ \sigma_2 \tag{5.7.1}$$

$$\dot{\eta}_2 = 0.7427\eta_1 - 0.3163\eta_2 + 0.9127\eta_3 + 0.9127\eta_4 + 0.9127\eta_5 + 0.6330\eta_{13} - 1.826\eta_{14} - 1.826\eta_{15} - 1.826\eta_{16} - 0.7427\sigma_3 + 0.7427\sigma_4 \tag{5.7.2}$$

$$\dot{\eta}_3 = 0.24\eta_1 + 0.2949\eta_2 - 0.9341\eta_3 + 0.2949\eta_4 + 0.2949\eta_5 - 0.5901\eta_{13} + 1.896\eta_{14} - 0.5901\eta_{15} - 0.5901\eta_{16} - 0.24\sigma_3 + 0.24\sigma_4 - d_1 \tag{5.7.3}$$

$$\dot{\eta}_4 = 0.001201\eta_1 + 0.001475\eta_2 + 0.001475\eta_3 - 1.228\eta_4 + 0.001475\eta_5 - 0.002953\eta_{13} + 0.002953\eta_{14} + 2.456\eta_{15} - 0.5901\eta_{16} - 0.0012\sigma_3 + 0.0012\sigma_4 + d_2 \tag{5.7.4}$$

Table 1. Assignment of the Primitive (Perturbation) Variables to the Fundamental Variables

$\delta K_7 \doteq u_1$,	$\delta K_{21} \doteq u_8$,	$\delta K_{22} \doteq u_9$,	$\delta K_{27} \doteq u_{10}$,	$\delta K_{28} \doteq u_{11}$,	$\delta n_1 \doteq \eta_1$,
$\delta n_{2,2} \doteq d_1$,	$\delta n_{2,3} \doteq d_2$,	$\delta n_{2,4} \doteq d_3$,	$\delta n_3 \doteq \sigma_3$,	$\delta n_9 \doteq \eta_{12}$,	$\delta n_{10,2} \doteq u_2$,
$\delta n_{15} \doteq \sigma_{13}$,	$\delta n_{17,1} \doteq u_4$,	$\delta n_{17,2} \doteq u_5$,	$\delta n_{17,3} \doteq u_6$,	$\delta n_{17,4} \doteq u_7$,	$\delta n_{18} \doteq \sigma_4$,
$\delta n_{27} \doteq \sigma_{17}$,	$\delta N_{1,1} \doteq \eta_2$,	$\delta N_{1,2} \doteq \eta_3$,	$\delta N_{1,3} \doteq \eta_4$,	$\delta N_{1,4} \doteq \eta_5$,	$\delta N_{5,1} \doteq \eta_7$,
$\delta N_{5,2} \doteq \eta_8$,	$\delta N_{5,3} \doteq \eta_9$,	$\delta N_{5,4} \doteq \eta_{10}$,	$\delta N_{36,1} \doteq \eta_{13}$,	$\delta N_{36,2} \doteq \eta_{14}$,	$\delta N_{36,3} \doteq \eta_{15}$,
$\delta N_{36,4} \doteq \eta_{16}$,	$\delta P_1 \doteq \sigma_2$,	$\delta P_5 \doteq \sigma_5$,	$\delta P_{12} \doteq \sigma_7$,	$\delta P_{13} \doteq \sigma_8$,	$\delta P_{14} \doteq \sigma_9$,
$\delta P_{24} \doteq \sigma_{14}$,	$\delta P_{25} \doteq \sigma_{16}$,	$\delta P_{35} \doteq \sigma_1$,	$\delta P_{36} \doteq \sigma_{11}$,	$\delta T_1 \doteq \eta_6$,	$\delta T_2 \doteq d_4$,
$\delta T_4 \doteq d_5$,	$\delta T_5 \doteq \eta_{11}$,	$\delta T_7 \doteq d_6$,	$\delta T_{16} \doteq \sigma_{10}$,	$\delta T_{24} \doteq \sigma_{15}$,	$\delta T_{35} \doteq \sigma_6$,
$\delta T_{36} \doteq \eta_{17}$,	$\delta T_{38} \doteq d_8$,	$\delta\tau_{36} \doteq \sigma_{12}$,	$\delta\tau_{37} \doteq u_3$,	$\dot{V}_g \doteq d_7$,	$\delta V_1 \doteq \eta_{19}$,
$\delta\omega_{37} \doteq \eta_{18}$,					

$$\dot{\eta}_5 = 0.0161\eta_1 + 0.01978\eta_2 + 0.01978\eta_3 + 0.1978\eta_4 - 1.209\eta_5 - 0.03958\eta_{13} - 0.03958\eta_{14} - 0.03958\eta_{15} + 2.509\eta_{16} - 0.0161\sigma_3 - 0.9839\sigma_4 + d_3 \tag{5.7.5}$$

$$1731.0\dot{\eta}_6 = 540.12\eta_1 - 7121.0\eta_6 - 583.4\sigma_3 + 2981\sigma_6 - 648.8d_1 - 741d_2 - 742.4d_3 + 4080.0d_4 + 60.0d_5 - 133.3d_6 \tag{5.7.6}$$

$$2.0\sigma_2 = 2437.0\eta_2 + 2437.0\eta_3 + 2437.0\eta_4 + 2437.0\eta_5 + 692.1.0\eta_6 - 101{,}460.08\eta_{19} \tag{5.7.7}$$

$$\sigma_2 - .08688\sigma_3 - \sigma_5 = 0 \tag{5.7.8}$$

$$\dot{\eta}_7 = 0.3163\eta_2 - 0.9127\eta_3 - 0.9127\eta_4 - 0.9127\eta_5 - 0.93\eta_7 + 2.684\eta_8 + 2.684\eta_9 + 2.684\eta_{10} - 0.7427\eta_{12} + 0.7427\sigma_3 - 0.7427u_2 \tag{5.7.9}$$

$$\dot{\eta}_8 = -0.2949\eta_2 + 0.9341\eta_3 - 0.2949\eta_4 - 0.2949\eta_5 + 0.8673\eta_7 - 2.747\eta_8 + 0.8673\eta_9 + 0.8673\eta_{10} - 0.24\eta_{12} + 0.24\sigma_3 - 0.24u_2 \tag{5.7.10}$$

$$\dot{\eta}_9 = -0.001475\eta_2 - 0.001475\eta_3 + 1.228\eta_4 - 0.001475\eta_5 + 0.004324\eta_7 + 0.004324\eta_8 - 3.610\eta_9 + 0.004324\eta_{10} - 0.0012\eta_{12} + 0.0012\sigma_3 - 0.0012u_2 \tag{5.7.11}$$

$$\dot{\eta}_{10} = -0.01978\eta_2 - 0.01978\eta_3 - 0.01978\eta_4 + 3.556\eta_5 + 0.05818\eta_7 + 0.05818\eta_8 + 0.05818\eta_9 - 3.556\eta_{10} - 0.0161\eta_{12} + 0.0161\sigma_3 - 0.0161u_2 \quad (5.7.12)$$

Table 2. Assignment of the Fundamental Variables to the Primitive (Perturbation) Variables.

$d_1 \doteq \delta n_{2,2}$,	$d_2 \doteq \delta n_{2,3}$,	$d_3 \doteq \delta n_{2,4}$,	$d_4 \doteq \delta T_2$,	$d_5 \doteq \delta T_4$,	$d_6 \doteq \delta T_7$,
$d_7 \doteq \dot{V}_g$,	$d_8 \doteq \delta T_{38}$,	$\eta_1 \doteq \delta n_1$,	$\eta_2 \doteq \delta N_{1,1}$,	$\eta_3 \doteq \delta N_{1,2}$,	$\eta_4 \doteq \delta N_{1,3}$,
$\eta_5 \doteq \delta N_{1,4}$,	$\eta_6 \doteq \delta T_1$,	$\eta_7 \doteq \delta N_{5,1}$,	$\eta_8 \doteq \delta N_{5,2}$,	$\eta_9 \doteq \delta N_{5,3}$,	$\eta_{10} \doteq \delta N_{5,4}$,
$\eta_{11} \doteq \delta T_5$,	$\eta_{12} \doteq \delta n_9$,	$\eta_{13} \doteq \delta N_{36,1}$,	$\eta_{14} \doteq \delta N_{36,2}$,	$\eta_{15} \doteq \delta N_{36,3}$,	$\eta_{16} \doteq \delta N_{36,4}$,
$\eta_{17} \doteq \delta T_{36}$,	$\eta_{18} \doteq \delta \omega_{37}$,	$\eta_{19} \doteq \delta V_1$,	$\sigma_1 \doteq \delta P_{35}$,	$\sigma_2 \doteq \delta P_1$,	$\sigma_3 \doteq \delta n_3$,
$\sigma_{16} \doteq \delta P_{25}$,	$\sigma_4 \doteq \delta n_{18}$,	$\sigma_5 \doteq \delta P_5$,	$\sigma_6 \doteq \delta T_{35}$,	$\sigma_7 \doteq \delta P_{12}$,	$\sigma_8 \doteq \delta P_{13}$,
$\sigma_9 \doteq \delta P_{14}$,	$\sigma_{10} \doteq \delta T_{16}$,	$\sigma_{11} \doteq \delta P_{36}$,	$\sigma_{12} \doteq \delta T_{36}$,	$\sigma_{13} \doteq \delta n_{15}$,	$\sigma_{14} \doteq \delta P_{24}$,
$\sigma_{15} \doteq \delta T_{24}$,	$\sigma_{17} \doteq \delta n_{27}$,	$u_1 \doteq \delta K_7$,	$u_2 \doteq \delta n_{10,2}$,	$u_3 \doteq \delta \tau_{37}$,	$u_4 \doteq \delta n_{17,1}$,
$u_5 \doteq \delta n_{17,2}$,	$u_6 \doteq \delta n_{17,3}$,	$u_7 \doteq \delta n_{17,4}$,	$u_8 \doteq \delta K_{21}$,	$u_9 \doteq \delta K_{22}$,	$u_{10} \doteq \delta K_{27}$,
$u_{11} \doteq \delta K_{28}$,					

$$588.6\dot{\eta}_{11} = -2981\eta_6 - 3041.0\eta_{11} - 582.4\eta_{12} + 583.4\sigma_3 - 582.4u_2 + 60.0d_7 \quad (5.7.13)$$

$$\dot{\eta}_{12} = 1.279\ \sigma_8 - 1.279\ \sigma_9 \quad (5.7.14)$$

$$\sigma_5 - \sigma_7 = 35.9\eta_{12} + 10{,}470u_1 + 35.9u_2 \quad (5.7.15)$$

$$\sigma_7 - \sigma_8 = 4.145\eta_{12} \quad (5.7.16)$$

$$0.68\sigma_5 = 2437.0\eta_7 + 2437.0\eta_8 + 2437.0\eta_9 + 2437.0\eta_{10} + 235.4\eta_{11} \quad (5.7.17)$$

$$0.02402\sigma_9 + 29.14\sigma_{10} - 0.02402\sigma_{11} = 29.14\eta_{11} + 92.48\eta_{12} \quad (5.7.18)$$

$$2.457\sigma_9 - 2.457\sigma_{11} + 54.19\sigma_{12} = 92.48\eta_{12} - 62.82\eta_{18} \quad (5.7.19)$$

$$\dot{\eta}_{18} = -0.4051\eta_{18} - 0.1725\ \sigma_{12} + 0.1725u_3 \quad (5.7.20)$$

$$-20.29\sigma_4 + 20.29\sigma_{13} + 102.3\sigma_{15} = 0.42\eta_1 + 100.2\eta_{17} \quad (5.7.21)$$

$$\sigma_{14} - \sigma_{16} = 158.8\eta_1 \tag{5.7.22}$$

$$-\sigma_1 + \sigma_{16} + 51.31\sigma_{17} = 51.31\eta_1 + 658.3u_{11} \tag{5.7.23}$$

$$-\sigma_1 + \sigma_{16} - 20.88\sigma_{17} = 5874.0u_{10} \tag{5.7.24}$$

$$102.3\sigma_6 - 25.66\sigma_{15} + 9.15\sigma_{17} = 6.87\eta_1 \tag{5.7.25}$$

$$-16.26\sigma_4 + \sigma_{11} + 16.26\sigma_{13} - \sigma_{14} = 16.26\eta_1 + 839.4u_8 \tag{5.7.26}$$

$$\sigma_{11} - 763.9\sigma_{13} - \sigma_{14} = 4.385u_9 \tag{5.7.27}$$

$$\sigma_4 = 0.01064\sigma_{13} \tag{5.7.28}$$

$$0.9987\sigma_{11} = 2481.0\eta_{13} + 2481.0\eta_{13} + 2481.0\eta_{14} + 2481.0\eta_{15} + 2481.0\eta_{16} + 345.9\eta_{17} \tag{5.7.29}$$

$$\begin{aligned}\dot{\eta}_{13} = {} & -0.7472\eta_1 + 0.93\eta_7 - 2.684\eta_8 - 2.684\eta_9 - 2.684\eta_{10} + 0.7427\eta_{12} - 0.622\eta_{13} + 1.837\eta_{14} \\ & + 1.837\eta_{15} + 1.837\eta_{16} - 0.7472\sigma_4 + 0.7427u_2 + u_4\end{aligned} \tag{5.7.30}$$

$$\begin{aligned}\dot{\eta}_{14} = {} & -0.24\eta_1 - 0.8673\eta_7 + 2.747\eta_8 - 0.8673\eta_9 - 0.8673\eta_{10} + 0.24\eta_{12} + 0.5901\eta_{13} - 1.869\eta_{14} \\ & + 0.5901\eta_{15} + 0.5901\eta_{16} + 0.24\sigma_4 - 0.76u_2 + u_4\end{aligned} \tag{5.7.31}$$

$$\begin{aligned}\dot{\eta}_{15} = {} & -0.0012\eta_1 - 0.004336\eta_7 - 0.004336\eta_8 + 3.61\eta_9 - 0.004336\eta_{10} + 0.0012\eta_{12} + 0.002951\eta_{13} \\ & + 0.002951\eta_{14} - 2.455\eta_{15} + 0.002951\eta_{16} - 0.0012\sigma_4 + 0.0012u_2 + u_6\end{aligned} \tag{5.7.32}$$

$$\begin{aligned}\dot{\eta}_{16} = {} & -0.0161\eta_1 - 0.05818\eta_7 - 0.05818\eta_8 - 0.05818\eta_9 + 3.556\eta_{10} + 0.0161\eta_{12} + 0.03958\eta_{13} \\ & + 0.03958\eta_{14} + 0.03958\eta_{15} - 2.418\eta_{16} - 0.0161\sigma_4 + 0.0161u_2 + u_7\end{aligned} \tag{5.7.33}$$

$$\begin{aligned}1213.0\dot{\eta}_{17} = {} & -8696.0\eta_1 + 8696.0\eta_{12} - 2981.0\eta_{17} - 8696.0\sigma_4 + 2981.0\sigma_{10} + 8708.0u_4 + 8800.0u_5 \\ & + 11{,}060.0u_6 + 11{,}070.0u_7 + 0.08597d_8\end{aligned} \tag{5.7.34}$$

$$\sigma_{11} - \sigma_9 = 40.6\eta_{18} + 1.792\eta_{12} \tag{5.7.35}$$

$$\dot{\eta}_{19} = d_7 \tag{5.7.36}$$

5.7 - THE STATE VARIABLE FORM OF THE LINEARIZED MATHEMATICAL MODEL

The equations are arranged compatibly with the symbolic form of the primitive equations from section 5.1. To obtain the state variable representation of the model (Equations 5.1.5 and 5.1.6), one can load the coefficients in the 36 equations from Section 5.7, (which are in the form of Equations 5.1.1 and 5.1.2) into arrays A1, A2, A3, A4, A5, B1, B2, B3, and B4 in a MATLAB compatible format for reduction to state space format. A compact MATLAB input form for each of the matrices follows:

```
A1
//coefficient of d(eta)/dt for study condition 1.;
//25Jl89;
a1=eye(19);
a1(6,6)=1731;
a1(11,11)=588.6;
a1(17,17)=1213.;

A2
//A2 for study condition 1.;
//24Jl89;
a2(19,19)=0.;
a2(2,1:5)=<.7427,-.3163,.9127,.9127,.9127>;
a2(2,13:16)=<.633,-1.826,-1.826,-1.826>;
a2(3,1:5)=<.24,.2949,-.9341,.2949,.2949>;
a2(3,13:16)=<-.5901,1.869,-.5901,-.5901>;
a2(4,1:5)=<.001201,.001475,.001475,-1.228,.001475>;
a2(4,13:16)=<-.002953,-.002953,2.456,-.002953>;
a2(5,1:5)=<.0161,.01978,.01978,.01978,-1.209>;
a2(5,13:16)=<-.03958,-.03958,-.03958,2.509>;
a2(6,1)=540.1;a2(6,6)=-7121.;
a2(7,2:12)=<.3163,-.9127,-.9127,-.9127,0.,-.93,2.684,2.684,2.684,...
  0,-.7427>;
a2(8,2:12)=<-.2949,.9341,-.2949,-.2949,0.,.8673,-2.747,...
  .8673,.8693,0.,-.24>;
a2(9,2:12)=<-.001475,-.001475,1.228,-.001475,0.,.004324,.004324,...
  -3.61,.004324,0.,-.0012>;
a2(10,2:12)=<-.01978,-.01978,-.01978,1.209,0.,.05818,.05818,.05818,...
  -3.556,0.,-.0161>;
```

```
a2(11,6)=2981.;a2(11,11)=-3041.;a2(11,12)=-582.4;
a2(13,1)=-.7472;a2(13,7:16)=<.93,-2.68,-2.684,-2.684,0.,...
   .7427,-.622,1.837,1.837,1.837>;
a2(14,1)=-.24;a2(14,7:16)=<-.8673,2.747,-.8673,-.8673,0.,...
   .24,.5901,-1.869,.5901,.5901>;
a2(15,1)=-.0012;a2(15,7:16)=<-.004336,-.004336,3.61,-.004336,0.,...
   .0012,.002951,.002951,-2.455,.002951>;
a2(16,1)=-.0161;a2(16,7:16)=<-.05818,-.05818,-.05818,3.556,...
   0.,.0161,.03958,.03958,.03958,-2.418>;
a2(17,1)=-8696.;a2(17,12)=8676.;a2(17,17)=-2981.;
a2(18,18)=-.04051;

A3
//This is A3 for control study model 1.
a3(19,17)=0.,
a3(1,1:2)=<1.279,-1.279>;
a3(2,3:4)=<-.7427,.7427>;
a3(3,3:4)=<-.24,.24>;
a3(4,3:4)=<-.0012,.0012>;
a3(5,3:4)=<-.0161,-.9839>;
a3(6,3)=-583.4;a3(6,6)=2981.;
a3(7,3)=.7427;
a3(8,3)=.24;
a3(9,3)=.0012;
a3(10,3)=.0161;
a3(11,3)=-583.4;
a3(12,8:9)=<1.279,-1.279>;
a3(13,4)=-.7424;
a3(14,4)=.24;
a3(15,4)=-.0012;
a3(16,4)=-.0161;
a3(17,4)=-8696.;a3(17,10)=2981.;
a3(18,12)=-.1725;

A4
//This is A4 for control study case 1;
//24J189;
a4(19,11)=0.;
a4(7,2)=-.7427;
a4(8,2)=-.24;
a4(9,2)=-.0012;
a4(10,2)=-.0161;
a4(11,2)=-582.4;
a4(13,2:4)=<.7427,0.,1.>;
a4(14,2)=-.76;a4(14,5)=1.;
a4(15,2)=.0012;a4(15,6)=1.;
a4(16,2)=.0161;a4(16,7)=1.;
a4(17,4:7)=<8708.,8800.,11060.,10070.>;
a4(18,3)=.1725;

A5
//This is A5 for control study system 1.;
```

```
//24Jl89;
a5(19,8)=0.;
a5(3,1)=-1;
a5(4,2)=-1.;
a5(5,3)=1.;
a5(6,1:6)=<-648.8,-741,-742.1,4080.,60.,-133.3>;
a5(11,7)=60.;
a5(17,8)=.08597;
a5(19,6)=1.;

B1
//this is the B1 matrix for the first control study model;
//24Jl89;
b1(17,17)=0.;
b1(1,2)=2.;
b1(2,2)=1.;b1(2,3)=-8.688e-2;b1(2,5)=-1;
b1(3,5)=1.;b1(3,7)=-1;
b1(4,7)=1;b1(4,8)=-1;
b1(5,5)=.68;
b1(6,9)=.02402;b1(6,10)=29.14;b1(6,11)=-.02402;
b1(7,9)=2.457;b1(7,11)=-2.457;b1(7,12)=54.19;
b1(8,11)=.9987;
b1(9,4)=-16.26;b1(9,11)=1.;b1(9,13)=16.26;b1(9,14)=-1.;
b1(10,11)=1.;b1(10,13)=-763.9;b1(10,14)=-1.;
b1(11,4)=-20.29;b1(11,13)=20.29;b1(11,15)=102.3;
b1(12,14)=1.;b1(12,16)=-1.;
b1(13,1)=-1.;b1(13,16)=1.;b1(13,17)=51.31;
b1(14,6)=102.3;b1(14,15)=-76.64;b1(14,17)=9.;
b1(15,4)=1.;b1(15,13)=-.01064;
b1(16,9)=-1.;b1(16,11)=1.;
b1(17,1)=-1.;b1(17,16)=1.;b1(17,17)=-20.88;

B2
//this is b2 for the first control studies model.;
//24Jl89;
b2(17,19)=0.;
b2(1,2:6)=<2437.,2437.,2437.,2437.,692.1>;b2(1,19)=-101460.;
b2(3,12)=35.9;
b2(4,12)=4.145;
b2(5,7:11)=<2437,2437,2437,2437,235.4>;
b2(6,11)=29.14,
b2(7,12)=92.48;b2(7,18)=-62.82;
b2(8,13:17)=<2481,2481,2481,2481,345.9>;
b2(9,1)=16.26;
b2(11,1)=.42;b2(11,17)=100.2;
b2(12,1)=158.8;
b2(13,1)=51.31;
b2(14,1)=-6.87;
b2(16,12)=1.792;b2(16,18)=40.60;

B3
//this is b3 for control studies model 1;
```

```
//24J189;
b3(17,11)=0.;
b3(3,1:2)=<10470,35.9>;
b3(9,8)=839.4;
b3(10,9)=4.385;
b3(13,11)=658.3;
b3(17,10)=5874.;

B4
//B4 is empty
```

6 - SOME PROPERTIES OF THE LINEARIZED STATE VARIABLE MODEL

With the primitive form matrices available for manipulation via MATLAB, the determination of the linear state variable representation coefficient matrices is quite straightforward. SVD analysis shows both A_1 and B_1 to be maximum rank, and the resulting $\mathcal{A}$, $\mathcal{B}$, $\mathcal{C}$, $\mathcal{D}$, $\mathcal{E}$, and $\mathcal{F}$ matrices in Equations 5.1.5 and 5.1.6 are quickly generated. For a system of this size, the specific numerical values of any element is of tertiary significance, and thus the presentation of these matrices is relegated to Appendix 3. However, an item of great interest is the eigenvalues of the state coefficient matrix, $\mathcal{A}$:

```
EVV  =
  1.0D+04 *
-5.266821895634872      0.000000000000000i
-0. 021360198075745     0.000000000000000i
-0. 003977263492918     0.009552095834877i
-0. 003977263492918    -0.009552095834877i
-0. 000459990795721     0.000120566056909i
-0. 000459990795721    -0.000120566056909i
-0. 000093892720314    -0.000000000000000i
-0. 000021248217594    -0.000000000000000i
-0. 000366233205798     0.000176262166536i
-0. 000365106096282     0.000173786717458i
-0. 000365101237584     0.000173829082129i
-0. 000366233205798    -0.000176262166536i
-0. 000365106096282    -0.000173786717458i
-0. 000365101237584    -0.000173829082129i
 0.000002445599342      0.000000000000000i
 0.000000294968294      0.000000000000000i
-0. 000000000002605     0.000000000000000i
 0.000000027480837      0.000000000000000i
```

EVV(continued)
0.000000000000000 0.000000000000000i

It is seen that the four left-most eigenvalues are greater than 39.0 in magnitude, suggesting that a representation of 15th order (a reduced order representation) should be acceptable for control studies. The remainder reflect dynamics which will require at least 2 seconds to play out, and which may be very important to the determination of the feedback control structure. One should be mindful that the very small (but non-zero) eigenvalues might be due to numerical error in the computational finite arithmetic, but a singular value analysis indicates that in this case the small but non-zero eigenvalues are in fact just that, and the plant is very mildly (slow dynamics) unstable about the prescribed experimental operating condition. This conclusion is consistent with the physical nature of the system. To further understand the dynamic behavior of the model, it is important to reformulate the model into smaller individual subsystems, the canonical basis. We employ the Real Jordan canonical decomposition.

6.1 - A REAL JORDAN CANONICAL FORM OF THE LINEAR STATE VARIABLE REPRESENTATION

For systems of this dimension, the Jordan canonical decomposition is of great value to gain insights into the system behavior (see Brogan, 1985). In the classical Complex Jordan canonical transformation (JCT), one can investigate the system in the *canonical state*, which is characterized by

$$\boldsymbol{x}(t) = \boldsymbol{M}\boldsymbol{J}\boldsymbol{q}(t)$$
$$\dot{\boldsymbol{q}}_{CJ}(t) = \boldsymbol{\Lambda}\boldsymbol{q}_{CJ}(t) + \boldsymbol{B}\boldsymbol{J}\boldsymbol{u}(t) + \boldsymbol{C}\boldsymbol{J}\boldsymbol{d}(t)$$

where

$\boldsymbol{MJ}$ is the Complex Jordan modal matrix (CJMM) (generally complex)

$q_{CJ}(t)$ is the Complex Jordan state vector (generally complex)

Λ is the Complex Jordan eigenvalue matrix (CJEM) (generally complex and sometimes

diagonal but often having some ones in the first superdiagonal)

$\boldsymbol{BJ} = \boldsymbol{MJ}^{-1}\mathfrak{B}$ (generally complex), and

$\boldsymbol{CJ} = \boldsymbol{MJ}^{-1}\mathfrak{C}$ (generally complex).

Often the JCT is satisfactory, but in the present case the JCT produces a CJMM requiring thirty-eight (38) columns to present, half of them imaginary. By employing a real Jordan Canonical transformation (RJCT) (see Takahashi, Rabins, and Auslander, 1970), one can obtain a nineteen column Real Jordan Modal Matrix (RJMM) $\boldsymbol{MR}$ and a Real Jordan Eigenvalue Matrix (RJEM) $\boldsymbol{ER}$. If any entry in Λ is complex, then the Real Jordan canonical state vector differs from the Complex Jordan state vector, although they are related. In the sequel we employ the asymmetric Real Jordan Eigenvalue Matrix (RJEM) form (Takahashi, et al, 1970). To denote this case,

$$\boldsymbol{x}(t) = \boldsymbol{MR}\boldsymbol{q}(t)$$

$$\dot{\boldsymbol{q}}(t) = \boldsymbol{ER}\boldsymbol{q}(t) + \boldsymbol{BR}\boldsymbol{u}(t) + \boldsymbol{CR}\boldsymbol{d}(t)$$

where

$\boldsymbol{MR}$ is the Real Jordan modal matrix (real)

$\boldsymbol{ER}$ is the eigenvalue matrix (real and tri-diagonal possibly with block asymmetry; in some cases having some ones on the superdiagonal just above the diagonal)

$\boldsymbol{BR} = \boldsymbol{MR}^{-1}\mathfrak{B}$ (real), and

$\boldsymbol{CR} = \boldsymbol{MR}^{-1}\mathfrak{C}$ (real).

Four forms of the Real Jordan Transformation are available (Takahashi, *et al*, 1970, and Šiljak, 1986. In the version we use here Takahashi, *et al*, 1970), the resulting Real Jordan Eigenvalue Matrix is tri-diagonal and block asymmetric. The real part of each of the complex Jordan eigenvalues appears on the diagonal, and

the negative imaginary part appears above the diagonal while its negative appears below the diagonal. Here, to save space, we present the blocks concatenated in a two-row, nineteen column matrix;

```
DBER =
  1.0D+04 *
   Columns 1 thru 4
-5.266821895634871   0.000000000000000  -0.003977263492919   0.009552095834876
 0.000000000000000  -0.021360198075745  -0.009552095834876  -0.003977263492918
   Columns 5 thru 8
-0.000459990795721  -0.000120566056908  -0.000093892720314   0.000000000000000
 0.000120566056908  -0.000459990795721   0.000000000000000  -0.000021248217594
   Columns 9 thru 12
-0.000366233205798   0.000176262166536  -0.000365106096282   0.000173786717458
-0.000176262166536  -0.000366233205798  -0.000173786717458  -0.000365106096282
   Columns 13 thru 16
-0.000365101237584   0.000173829082129   0.000002445599342   0.000000000000000
-0.000173829082129  -0.000365101237584   0.000000000000000   0.000000294968294
   Columns 17 thru 19
-0.000000000002605   0.000000000000000   0.000000000000000
 0.000000000000000   0.000000027480838   0.000000000000000
```

The associated Real Jordan modal matrix is

```
MR   =
   Columns 1 thru 4
 0.021374485835695   0.984576311054076  -0.222861859233880   0.322197951244839
 0.487360549065908  -0.001955648123576   0.005816754894363  -0.003751480241953
 0.157488261878300  -0.000631875128675   0.001879634406395  -0.001212404055158
 0.000787441309857  -0.000003163992840   0.000009401663918  -0.000006061316275
 0.010564837649393  -0.000041386247457   0.000125394594452  -0.000081420370778
 0.221177235667850   0.000096446984620   0.002584220507461  -0.001201962066472
-0.487360123124829  -0.000868067795239   0.001402104579983  -0.000485856568940
-0.157488125006523  -0.000280512407754   0.000453080327699  -0.000157002400103
-0.000787440784020  -0.000001402604758   0.000002265548592  -0.000000784867518
-0.010564828397520  -0.000018823588278   0.000030396185574  -0.000010523959557
 0.650447775541264   0.002825999155352   0.010702876866564  -0.012052105651288
 0.051688720402714   0.172709078715878  -0.381326891771549  -0.833086493557783
-0.000000412153971   0.002844266330721  -0.007234575766325   0.004234483907949
-0.000000136513800   0.000911896962854  -0.002332320942123   0.001369490254180
-0.000000000675574   0.000004561937004  -0.000011663425357   0.000006847095427
-0.000000009161841   0.000061206155787  -0.000156484554555   0.000091864777795
-0.000034465044499   0.027550330062014  -0.071485556002443   0.039486759722147
 0.000000302667457   0.000249544898103   0.001859344897543  -0.002002273880364
 0.000000000000000   0.000000000000000   0.000000000000000   0.000000000000000
   Columns 5 thru 8
 0.023978462944404   0.029493847479883  -0.002568503774483  -0.170333623713372
-0.007084457634296   0.025311329129724   0.016182368235621   0.009271856159084
-0.002320135705025   0.008169161137254   0.005169242141229   0.003569791470073
```

MR(continued)

-0.000012098438914	0.000040819503345	0.000025905961077	0.000017923850718
-0.000164258756038	0.000533867262298	0.000362212241106	0.000196493162171
0.202604293203552	-0.038048117289116	0.171601361074757	0.040494054146723
-0.025478334763020	-0.049290720473403	0.003741219057719	-0.001732833228306
-0.008215011499415	-0.015943111731417	0.001181558255228	-0.000352542308634
-0.000041406652986	-0.000080134199729	0.000005911968398	-0.000001727130129
-0.000538211083104	-0.001067719061769	0.000086347194217	-0.000039178193928
0.523635785674718	0.769014585609127	0.196136838947666	0.108489631181109
-0.138683675631643	-0.172002174168538	0.022504076070899	-0.168037356184343
0.032485032408920	0.023965232663896	-0.019631368541019	-0.010424941737283
0.010534793286127	0.007773824942749	-0.006350693074713	-0.003131532280652
0.000053380935448	0.000039173375510	-0.000031773551538	-0.000015571595920
0.000688589834673	0.000528457533651	-0.000409479782940	-0.000234635785042
-0.132208556882285	-0.134156712888075	0.436058794716317	0.092275627607291
-0.011987363542998	-0.008688571309677	0.008888177603467	-0.952601895329476
0.000000000000000	0.000000000000000	0.000000000000000	0.000000000000000

Columns 9 thru 12

-0.000434549338021	-0.002365889272441	-0.000168637166761	-0.000007487154907
-0.333604970041021	0.083748057550945	-0.324410007385080	0.252277615693271
-0.110676221670387	0.011827578249793	0.323082733665237	-0.252065311662433
-0.000539486289905	0.000137051277497	0.001166063755237	0.000071652116033
0.450460633757361	-0.098016095540404	0.000216340950950	-0.000110198673781
0.004695728699299	-0.012815136031644	-0.000845902687344	-0.000564650385160
0.069447849286962	0.234874927207185	0.183247014243786	0.225511990573353
0.011517247536669	0.078290731338212	-0.182999358919719	-0.224609147353368
0.000113388994367	0.000379988557379	0.000033286646231	-0.000825646783815
-0.076749231164386	-0.311843457165495	-0.000080476569712	-0.000151242264971
-0.020268951933378	-0.038544150768501	-0.002726952896061	0.000813576716260
0.002413053767813	0.013556551929108	0.000966820438091	0.000050523205025
0.264173290919339	-0.318691699740971	0.141231439230398	-0.477511486074352
0.099126440708361	-0.089963600874162	-0.140083367030527	0.476674545754798
0.000425958175786	-0.000516962540559	-0.001199002422559	0.000753955953713
-0.362464456254652	0.405204053935332	-0.000130725847818	0.000257469144136
0.015262522898163	0.006277594254333	0.000560853205478	-0.001209068228379
-0.000309454575899	0.001037430467572	0.000066645761575	0.000037619146834
0.000000000000000	0.000000000000000	0.000000000000000	0.000000000000000

Columns 13 thru 16

-0.000078989144497	-0.000001534446000	0.002127499073159	-0.001249937877648
0.009929433211928	-0.373765232568121	-0.118764556142297	-0.857448582488209
0.014324858119588	-0.064326976103987	-0.013039260699884	-0.001038607482383
-0.024252456132820	0.438160068345558	0.000108773981237	0.000877705234494
0.000038235837291	0.000031136207611	-0.850335665841901	-0.000277775049492
-0.000397613710317	-0.000268080980026	-0.004624688434761	0.003685286338719
-0.264356820743857	-0.001438689585612	-0.041878623768547	-0.291430937702131
-0.045696087138582	-0.009178093458171	-0.005138670800554	-0.000385007648221
0.310129833762039	0.010607832143095	0.000035151784017	0.000299289112009
0.000019931422614	-0.000028474169719	-0.287200647192445	-0.000097086177615
-0.001259213077060	0.000467889438399	-0.001593536101620	0.002980417496428
0.000452642963183	0.000012798653809	-0.003764851461600	0.002041513814356
0.254464536530617	0.375231370860600	-0.056307401242189	-0.423848960773323
0.031371215925709	0.073505078970693	-0.005299944868085	0.001312670859152

MR(continued)

-0.285862028060663	-0.448637501247626	0.000061912601134	0.000448816238949
-0.000057032339740	-0.000002070183515	-0.418055811773158	-0.000015706546943
0.000298663976310	-0.000615576198059	-0.018368371512324	0.012426412413986
0.000031581325941	0.000016846781909	0.006360851231764	-0.003909868113154
0.000000000000000	0.000000000000000	0.000000000000000	0.000000000000000

Columns 17 thru 19

0.000016412362758	0.000023656694458	0.000000051400872
-0.668318523019703	-0.634070002293218	0.950909182004328
0.534857523446167	-0.000070529334320	0.307243950675371
-0.001354064207911	0.574758903861677	0.001536156292617
-0.000041012067976	-0.000014753075049	0.020611724800414
-0.000059372032713	-0.000023887458395	0.000036634532086
-0.227253876620181	-0.215654455358315	0.000000533624518
0.181877033253038	-0.000038953357662	-0.000000411699438
-0.000460405901928	0.195499349292086	0.000000001131302
-0.000013694027642	-0.000006059271029	0.000000000197389
-0.000060628271828	0.000031561837089	0.000070776809305
-0.000026516334553	-0.000038039401422	0.000000051505625
-0.333067189232513	-0.316633187948755	0.000000776667388
0.267615210333714	0.000074545807038	-0.000000607552454
-0.000675540588126	0.287443866902551	0.000000001651331
0.000000040019953	-0.000000005204576	0.000000000125281
-0.000183998003297	-0.000145735125755	0.000070773448986
0.000051731173235	0.000074082924124	-0.000000100483148
0.000000000000000	0.000000000000000	0.030751715660749

The rows of MR show how the Jordan canonical state variables contribute to the descriptive state variables. As an example, it is clear that Jordan state 19 solely determines descriptive state 19 (the volume of the upper chamber). All the others are not so clear-cut, and this is generally the case. Another item of interest is the influence the individual processes of the primitive form have on the Jordan elements, and how the descriptive state variables contribute to the Jordan canonical states.

The first question is not so easily answered, and strictly involves (1) perturbing the coefficients of the individual process equations one at a time, (2) constructing the A_1, A_2, $\cdots$ *and* B_1, B_2, $\cdots$, (3) constructing $\mathcal{A}$, and (4) obtaining the Jordan elements, *for each perturbation*; a very large task which in some cases may be well worth the effort.

The second question is much more easily addressed; one needs the effective inverse of MR, MRNV.

```
MRNV =
  1.0D+02 *
   Columns 1 thru 4
-0.000000079360991   0.004058094461690   0.004058094461691   0.004058094605937
 0.011027036117855   0.046300274368076   0.046300258010397   0.046300248492862
 0.004303637906307   0.133032132081097   0.133032326987938   0.133032162106799
 0.000330492422439  -0.047947626278134  -0.047947545627571  -0.047947473501417
-0.000028472726969  -0.021029860724648  -0.020986976831392  -0.021038110671024
-0.000064132701893   0.003434273108404   0.003446348835286   0.003424352323812
-0.000051803236422   0.017930573774850   0.017974005745429   0.017960546499401
 0.000011053728587   0.000799112951901   0.000806778357354   0.000803074701879
-0.000000014223569  -0.000174749685292  -0.000181435760722  -0.000176206203828
-0.000000001495674  -0.000051705146068  -0.000052420806710  -0.000052802519075
-0.000000029038514  -0.003065888425097   0.009491348409376  -0.001254296004910
 0.000000062645297   0.000496610685218  -0.001505837137098  -0.000107602331880
-0.000000000083374   0.000009059687593   0.000003534084696  -0.006296304394037
-0.000000000178431  -0.000004170475201  -0.000037576131655   0.010064370948144
 0.000000003635636   0.000001036616354   0.000001080948813   0.000001074283795
 0.000000069891068  -0.006362957631631  -0.007960180072798  -0.007016244971145
 0.000000002864779  -0.000000794483606   0.010158017373222  -0.000000532029538
-0.000000000084737   0.000009776455899   0.000036147127610   0.009464088565077
 0.000000000000000   0.000000000000000   0.000000000000000   0.000000000000000
   Columns 5 thru 8
 0.004058094394871   0.001152686400887  -0.011935557140388  -0.011935557208376
 0.046300285905894   0.013265246187142   0.057116207072712   0.057119033703496
 0.133032135860233   0.037911355587235   0.160928666851032   0.160928822588576
-0.047947738407967  -0.014374467244194  -0.061640535666758  -0.061658213660490
-0.020691099176059   0.034921422890468  -0.011098488099617  -0.011227956679605
 0.003803974812573  -0.027779428033610   0.007250430113147   0.007259378246052
 0.017254737184331   0.008719287158453   0.027215376969202   0.027225627932003
 0.000712572446781   0.000002971673030   0.000813120253453   0.000819460384678
 0.010710862653134   0.000000005468609   0.000270145171574   0.000282356727909
 0.003122887569759   0.000001590921333   0.000349617405094   0.000360623476204
-0.000063017657065   0.000003234124340   0.006737159169779  -0.020841670347579
-0.000314719087115   0.000000103145409   0.003360182233558  -0.010450036641585
-0.000001308118171  -0.000000011508949  -0.000023667284594  -0.000060026655955
-0.000000122913299   0.000000038795494  -0.000004712455155   0.000068936054341
-0.006360029205293  -0.000000008741358   0.000003202670888   0.000003247885522
 0.000998588949181  -0.000000040047863  -0.006361272919333  -0.007962328802177
-0.000151815240640   0.000000000005285  -0.000000794104094   0.010158017537432
-0.000000656698796   0.000000000012694   0.000009772131394   0.000036148699686
 0.000000000000000   0.000000000000000   0.000000000000000   0.000000000000000
   Columns 9 thru 12
-0.011935557213817  -0.011935556727441  -0.001153018373085  -0.000000248506030
 0.057116497941355   0.057116149439601   0.005877579478471   0.002019520710580
 0.160928817515437   0.160924826314253   0.015481543135955  -0.004711091034897
-0.061642367708082  -0.061639763771372  -0.008191542717668  -0.009418427332986
-0.011069980331601  -0.012388839824255  -0.001926214702688   0.000040158286908
```

MRNV(continued)

0.007268062053405	0.006569233515909	0.013288497480227	-0.000100749151063
0.027218872955276	0.027057618485695	0.006410068997662	-0.000068165259628
0.000816391908286	0.000741546948676	0.000011816052571	0.000010907601423
0.000271282179571	-0.016734526561433	0.000000402932000	-0.000000012114450
0.000353721933110	-0.021552321505284	-0.000000127640973	0.000000002118973
0.002311184512667	-0.000328079037130	-0.000000279987031	-0.000000021340049
0.001988447601716	0.000713091713345	-0.000000818879114	0.000000058911711
0.026630590408530	0.000002490265615	0.000000016567716	-0.000000000077779
-0.010920585174335	0.000001975484830	-0.000000000840476	-0.000000000095633
0.000003240250745	-0.006484464908057	0.000000131861654	0.000000001504711
-0.007016128237641	0.001017945335061	0.000001063842386	0.000000054453148
-0.000000531650199	-0.000151814857910	0.000000000007851	0.000000002793429
0.009466197440280	-0.000000663357369	-0.000000000410084	-0.000000000055846
0.000000000000000	0.000000000000000	0.000000000000000	0.000000000000000

Columns 13 thru 16

-0.000000010232328	-0.000000010240033	-0.000000010228713	-0.000000017134799
-0.133980202090320	-0.133980287282974	-0.133979525845905	-0.133998944505850
-0.382771126779035	-0.382771142181409	-0.382771042151076	-0.382774278702508
0.140439624292678	0.140440163283337	0.140435389120294	0.140557461037831
0.050451431376845	0.050422807895227	0.050432091026318	0.051033750070013
-0.012030447082541	-0.012061160764686	-0.012023977207041	-0.012278165752610
-0.054798544384965	-0.054723502606230	-0.054788422679860	-0.054926300217334
-0.002087890892367	-0.002079371998441	-0.002084544597349	-0.002155565300914
0.000165692758078	0.000170723208760	0.000167688144985	-0.010289394705628
-0.000133847727189	-0.000139761062429	-0.000134412953131	0.008450891278060
0.001550864973431	-0.004810297437559	0.000936745540861	0.000361908678533
-0.003270455776704	0.010134931293734	-0.001127783648698	0.000159967277918
-0.000001985481366	0.000033805350703	-0.005522465530611	0.000000996741591
0.000011478775925	0.000028203612623	-0.012696905624139	-0.000001209177829
0.000001608382963	0.000001652255851	0.000001646354553	-0.006529960873376
-0.006372995381737	-0.007968303847082	-0.007028360747631	0.001016652104691
-0.000000373998128	0.010158437949212	-0.000000111581489	-0.000157015973551
0.000009801360430	0.000036169084491	0.009466914237013	-0.000000654927085
0.000000000000000	0.000000000000000	0.000000000000000	0.000000000000000

Columns 17 thru 19

-0.000000029080641	0.000000000245057	-0.168951276001464
-0.018977198942561	-0.000484003880011	-1.927626665785087
-0.053399192557579	0.005275456198033	-5.538549285503272
0.021447381911251	-0.000419192722920	1.996212015962940
-0.008633654390757	-0.000567608615953	0.874873693278677
0.003955724022687	0.000950500410444	-0.143355254541355
0.012028361877980	0.003266159255409	-0.746547286512787
0.000030505602496	-0.010457639483299	-0.033288760591338
0.000000086887107	0.000000133434329	0.000046090546549
-0.000000466753684	-0.000000087561853	0.000032058549404
-0.000000879334351	-0.000000076367255	0.000079066352446
-0.000000214565499	-0.000000832746981	-0.000094870844419
-0.000000000258151	0.000000001592361	-0.000000055535734
-0.000000009969529	0.000000000864010	0.000001721555178
0.000000375872476	0.000000597411480	0.004219980627829
0.000002758842500	0.000018968559298	0.275968582994403

MRNV(continued)

0.000000012863846	0.000000924297613	-0.101363240880237
-0.000000005200491	-0.000000021013929	-0.001135783570108
0.000000000000000	0.000000000000000	0.325185108704812

The rows of MRNV show how the descriptive states map into the canonical states, e.g., a zero element shows that the corresponding descriptive state does not influence the canonical state. Again the graphic example of the present MRNV is that only descriptive state 19 influences canonical state 19.

To a large degree, one can anticipate control problems by surveying the rows of BR.

BR =

1.0D+04 *

Columns 1 thru 4

0.000033277765579	0.000130878405621	0.000000000000423	-0.000000002189992
-0.270436643730725	-0.001556613041551	-0.000000834906693	-0.002702155264034
0.630868324901464	0.000400677767752	0.000009100161942	-0.007661183393029
1.261233848115660	0.005022089592311	-0.000000723107447	0.002944081335121
-0.005377648405604	0.000112434200427	-0.000000979124863	-0.000115286695586
0.013491449792794	-0.000157447850720	0.000001639613208	0.000163672815156
0.009128098531653	-0.000304870438139	0.000005634124716	0.000315518061785
-0.001460651086450	-0.000013335794888	-0.000018039428109	-0.000018688943660
0.000001622261810	-0.000001712921902	0.000000000230174	0.000001663165115
-0.000000283754463	0.000001430941848	-0.000000000151044	-0.000001371985030
0.000002857673731	0.000048166826014	-0.000000000131734	0.000015445523242
-0.000007888943861	-0.000101336533629	-0.000000001436489	-0.000032719961200
0.000000010415520	-0.000000338031286	0.000000000002747	-0.000000019873346
0.000000012806328	-0.000000281318062	0.000000000001490	0.000000114072057
-0.000000201497800	-0.000000041532455	0.000000001030535	0.000000043067321
-0.000007291891854	0.000079545751508	0.000000032720765	-0.000063531899403
-0.000000374071657	-0.000101582365427	0.000000001594413	-0.000000002816499
0.000000007478451	-0.000000361385178	-0.000000000036249	0.000000097640266
0.000000000000000	0.000000000000000	0.000000000000000	0.000000000000000

Columns 5 thru 8

-0.000000002212125	-0.000000002753828	-0.000000002585545	-0.000002306030737
-0.002716549374846	-0.003070115293947	-0.002915425499070	-0.115956370297978
-0.007701684171251	-0.008696589808871	-0.008260800240074	-0.045287281245884
0.002960353494491	0.003359902480967	0.003186078615706	-0.003461762875487
-0.000122121126643	-0.000282886159496	-0.000206405283429	0.000208279141379
0.000166365897709	0.000240438774433	0.000205611919625	0.000747435461862
0.000325391392126	0.000548848521515	0.000449299274094	0.000514396152568
-0.000018580617742	-0.000018063978837	-0.000019023159875	-0.000116123010280
0.000001713535522	0.000001684803720	-0.000102886733922	-0.000001067549952
-0.000001431472392	-0.000001386687617	0.000084470164144	-0.000000353921731
-0.000048166767799	0.000009287278674	0.000003546086811	0.000000039440308
0.000101333746768	-0.000011297400332	0.000001581860128	-0.000000066100955

BR(continued)

0.000000338034779	-0.000055224678844	0.000000009945985	0.000000002912779
0.000000281312863	-0.000126969965252	-0.000000012919422	0.000000003334174
0.000000043791131	0.000000050735183	-0.000065268404811	0.000000690081205
-0.000079482891612	-0.000070032059265	0.000010395552737	-0.000001288497919
0.000101585312731	0.000000000057096	-0.000001569091814	0.000000545544026
0.000000361313563	0.000094668668195	-0.000000006981002	0.000000002955551
0.000000000000000	0.000000000000000	0.000000000000000	0.000000000000000

Columns 9 thru 11

0.000000016497528	0.000146339651628	-0.000015732112866
-0.000012689405687	-0.587192408382382	-0.027037126660512
-0.000004786497825	-0.225134351923371	-0.011004316774894
-0.000000451242909	-0.019419884191736	-0.000606243705685
0.000000508824808	0.005825476261093	-0.000413131342874
-0.000000307751985	-0.000000023556181	0.000539977992367
0.000000218150669	0.003841121645717	0.000005690443116
-0.000000013315908	-0.000589886727719	-0.000026959915354
0.000000006374565	0.000000760192096	0.000000034562735
0.000000001932760	0.000000275993849	-0.000000018337603
0.000000001422565	0.000001949313747	0.000000026034463
-0.000000003168099	-0.000003332452360	-0.000000153983516
-0.000000000010540	0.000000003033222	0.000000000362044
-0.000000000007410	0.000000014310614	-0.000000000101466
-0.000000003808865	-0.000000195215325	-0.000000008733001
0.000000002811293	-0.000003737018697	-0.000000169650612
-0.000000003010574	-0.000000152974373	-0.000000006976594
-0.000000000010687	0.000000004526379	0.000000000206182
0.000000000000000	0.000000000000000	0.000000000000000

If the entries corresponding to a canonical block are all zero, then that canonical state cannot be influenced by any of the control variables and it is said to be *uncontrollable.* If, in addition, the uncontrollable block is not stable, then all descriptive states which are influenced by the unstable canonical block cannot be controlled. If all entries in the set are not zero, but all have very small values, then one is faced with a condition of poor control authority, and the hardware realization of an effective controller system is likely to be difficult.

CR =

1.0D+02 *

Columns 1 thru 4

-0.004490135441989	-0.004551532285346	0.003563924216883	0.002716903821848
-0.051272234744203	-0.051978785422193	0.040613319299609	0.031266438153402
-0.147241967372107	-0.149261113285390	0.116779093121188	0.089357787865926

CR (continued)

0.053335271998474	0.054100841628481	-0.041785235726328	-0.033880893331203
0.007897999840441	0.006089078688449	-0.035662322704087	0.082310459499198
0.006965721013476	0.008467361236503	0.015713341388969	-0.065476641465701
-0.021242101359759	-0.021693066305532	0.013516676525586	0.020551526058053
-0.000807892176801	-0.000804346804545	0.000711298455703	0.000007004289984
0.000181433711021	0.000176203862846	0.010710860308677	0.000000012889615
0.000051824509910	0.000052121483427	0.003122205523126	0.000003749831911
-0.009492560598788	0.001252911553069	-0.000064404164098	0.000007622892726
0.001505798476935	0.000107558177780	-0.000314763306762	0.000000243115696
-0.000003529771001	0.006296309320745	-0.000001303184149	-0.000000027126812
0.000037561590629	-0.010064387555574	-0.000000139545383	0.000000091441720
-0.000001077672445	-0.000001070541827	-0.006360025457770	-0.000000020603548
0.007960195083228	0.007016262114685	0.000998606118169	-0.000000094393576
-0.010158017375203	0.000000532027276	-0.000151815242906	0.000000000012456
-0.000036147132368	-0.009464088570511	-0.000000656704239	0.000000000029921
0.000000000000000	0.000000000000000	0.000000000000000	0.000000000000000
0.000039954467968	-0.169040041511134	-0.000117535002353	-0.000000000002061
0.000459800561079	-1.928648189364952	0.000599141638988	-0.000001344987463
0.001314085115675	-5.541468744601931	0.001578138953716	-0.000003784607242
-0.000498248431341	1.997318957894570	-0.000835019645022	0.000001520058881
0.001210447933812	0.872184481452392	-0.000196352161334	-0.000000611900468
-0.000962891786260	-0.141216029956213	0.001354586899106	0.000000280357456
0.000302228324383	-0.747218737106791	0.000653421916173	0.000000852496513
0.000000103004264	-0.033288989432478	0.000001204490578	0.000000002162050
0.000000000189553	0.000046090125425	0.000000041073598	0.000000000006158
0.000000055144587	0.000031936036514	-0.000000013011312	-0.000000000033081
0.000000112101364	0.000078817300583	-0.000000028540982	-0.000000000062322
0.000000003575231	-0.000094878787391	-0.000000083473916	-0.000000000015207
-0.000000000398924	-0.000000054649459	0.000000001688860	-0.000000000000018
0.000000001344731	0.000001718567633	-0.000000000085675	-0.000000000000707
-0.000000000302993	0.004219981300979	0.000000013441555	0.000000000026640
-0.000000001388141	0.275968586078390	0.000000108444688	0.000000000195530
0.000000000000183	-0.101363240880644	0.000000000000800	0.000000000000912
0.000000000000440	-0.001135783571085	-0.000000000041803	-0.000000000000369
0.000000000000000	0.325185108704812	0.000000000000000	0.000000000000000

7 - AN ELEMENTARY CONTROL STUDY

The purpose of this report is to present the details of generating the mathematical model to be used in investigating the control problem of a CGRC. A commensurate presentation of the full investigation of the control problem will require a report of similar magnitude. However, it is desirable to present a sufficiently detailed control study to illustrate the use of the model.

STATEMENT OF THE CONTROL PROBLEM TO BE INVESTIGATED

The positive eigenvalues of the matrix $\mathcal{A}$ reflect a clearly defined problem with the model behavior. If intervention via the control variables is not invoked, the eigenstates will tend to go to infinity with time, and thus all descriptive states which are related to the canonical states (via the mapping MR) will tend to go to infinity with time. Thus, it is necessary to manipulate the control variables in such a way that the resulting controlled system will have no eigenvalues with positive real parts. In the following, we demonstrate a procedure for choosing feedback control so that the canonical state having the most positive eigenvalue (eigenstate 15). Left to itself, this eigenstate ($q_{15}(t)$) will tend to infinity according to $e^{0.0245t}$ (coefficient of t is rounded). The Science Advisory Working Group did not address the question of dynamic properties requirements, so we have no guidance from that source to help with the choice of parametrization of the dynamic properties of the controlled system. Arbitrarily, we select the criterion that the dynamics of eigenstate 15 should decay according to e^{-1t} and ask what feedback control $\mathbf{u} = K\mathbf{x}$ will provide the desired behavior. The first question is "does a K exist such that we can obtain this behavior?" If the answer to the first question is "yes," then the second question is "will the gain matrix K have impractically large elements?" (as a rough rule of thumb large gains are difficult to attain and are thus undesirable).

The procedure we will demonstrate is due to C. Blackwell (1991) and distributes the burden of assigning the new eigenvalue among the control variables according to the control authority of each individual control variable. In this way, the wasteful assignment of load to a control variable with little authority is avoided, advantage of a control variable with high authority will be taken, and

those control variables having equal authority will be weighted equally. The fundamentals are relatively straightforward.

For the case when all disturbances are zero, the dynamic equation of canonical state 15 is

$$\dot{q}_{15} = \lambda_{15}\, q_{15} + \boldsymbol{br}_{15}\mathbf{u}$$

where $\boldsymbol{br}_{15}$ is the fifteenth row of $\boldsymbol{BR}$. By using a control law which relates $\mathbf{u}$ to q_{15},

$$\mathbf{u} = \boldsymbol{k}_{15}\, q_{15}$$

we make the dynamics of q_{15} dependent on q_{15} only

$$\dot{q}_{15} = \lambda_{15}\, q_{15} + \boldsymbol{br}_{15}\boldsymbol{k}_{15}\, q_{15}$$

or

$$\dot{q}_{15} = (\lambda_{15} + \boldsymbol{br}_{15}\boldsymbol{k}_{15})\, q_{15}$$

We now select $\boldsymbol{k}_{15}$ to be related to $\boldsymbol{br}_{15}$ in a very useful way:

$$\boldsymbol{k}_{15} = \alpha\, \boldsymbol{br}_{15}' / \| \boldsymbol{br}_{15} \|^2$$

and this choice gives us a very simple expression for the dynamics of q_{15}

$$\dot{q}_{15} = (\lambda_{15} + \alpha)\, q_{15}$$

Now suppose we would like the controlled system to exhibit dynamics

$$\dot{q}_{15} = \bar{\lambda}_{15}\, q_{15}$$

then we must have

$$(\lambda_{15} + \alpha) = \bar{\lambda}_{15}$$

which tells us that

$$\alpha = \bar{\lambda}_{15} - \lambda_{15}$$

Now we know $\boldsymbol{k}_{15}$. In terms of the entire canonical state, what we have done is represented by

$$\dot{\boldsymbol{q}} = (\boldsymbol{ER} + \boldsymbol{BRK}_q)\boldsymbol{q} + \boldsymbol{CRd}$$

where

$$K_q = [0 \mid k_{15} \mid 0]$$

($\mathbf{k}_{15}$ is in the fifteenth column). K_q is the canonical state gain matrix. To find the gains on the descriptive states, one uses the fact that $q = MR^{-1}x$. Thus

$$K = K_q MR^{-1}$$

NUMERICAL DETAILS

The following is an edited MATLAB dialog transcript of the process of finding K. The sequence of MATLAB transactions follows the sequence which was followed in the preceding explanation. The object is to change an eigenvalue so that it has a desirable value.

```
<>
lm15=er(15,15)//It is also equal to DBER(1,15).
 LM15  =
  0.024455993417775
 <>
L15=-1.0//We want to replace LM15 with this value.
 L15   =
    -1
 <>
alph=l15-lm15
 ALPH  =
 -1.024455993417775
 <>
BR15=BR(15,1:11);K15=ALPH*BR15'/(NORM(BR15)**2)
 K15   =
  0.004845071804937
  0.000998659667081
 -0.000024779501890
 -0.001035565963037
 -0.001052970165541
 -0.001219941869759
  1.569397322971582
 -0.016593198483799
  0.000091585233884
  0.004694007912200
  0.000209987492911
 <>
KQ(11,19)=0;KQ(1:11,15)=K15
```

KQ =

Columns 1 thru 4

0.000000000000000	0.000000000000000	0.000000000000000	0.000000000000000
0.000000000000000	0.000000000000000	0.000000000000000	0.000000000000000
0.000000000000000	0.000000000000000	0.000000000000000	0.000000000000000
0.000000000000000	0.000000000000000	0.000000000000000	0.000000000000000
0.000000000000000	0.000000000000000	0.000000000000000	0.000000000000000
0.000000000000000	0.000000000000000	0.000000000000000	0.000000000000000
0.000000000000000	0.000000000000000	0.000000000000000	0.000000000000000
0.000000000000000	0.000000000000000	0.000000000000000	0.000000000000000
0.000000000000000	0.000000000000000	0.000000000000000	0.000000000000000
0.000000000000000	0.000000000000000	0.000000000000000	0.000000000000000
0.000000000000000	0.000000000000000	0.000000000000000	0.000000000000000

Columns 5 thru 8

0.000000000000000	0.000000000000000	0.000000000000000	0.000000000000000
0.000000000000000	0.000000000000000	0.000000000000000	0.000000000000000
0.000000000000000	0.000000000000000	0.000000000000000	0.000000000000000
0.000000000000000	0.000000000000000	0.000000000000000	0.000000000000000
0.000000000000000	0.000000000000000	0.000000000000000	0.000000000000000
0.000000000000000	0.000000000000000	0.000000000000000	0.000000000000000
0.000000000000000	0.000000000000000	0.000000000000000	0.000000000000000
0.000000000000000	0.000000000000000	0.000000000000000	0.000000000000000
0.000000000000000	0.000000000000000	0.000000000000000	0.000000000000000
0.000000000000000	0.000000000000000	0.000000000000000	0.000000000000000
0.000000000000000	0.000000000000000	0.000000000000000	0.000000000000000

Columns 9 thru 12

0.000000000000000	0.000000000000000	0.000000000000000	0.000000000000000
0.000000000000000	0.000000000000000	0.000000000000000	0.000000000000000
0.000000000000000	0.000000000000000	0.000000000000000	0.000000000000000
0.000000000000000	0.000000000000000	0.000000000000000	0.000000000000000
0.000000000000000	0.000000000000000	0.000000000000000	0.000000000000000
0.000000000000000	0.000000000000000	0.000000000000000	0.000000000000000
0.000000000000000	0.000000000000000	0.000000000000000	0.000000000000000
0.000000000000000	0.000000000000000	0.000000000000000	0.000000000000000
0.000000000000000	0.000000000000000	0.000000000000000	0.000000000000000
0.000000000000000	0.000000000000000	0.000000000000000	0.000000000000000
0.000000000000000	0.000000000000000	0.000000000000000	0.000000000000000

Columns 13 thru 16

0.000000000000000	0.000000000000000	0.004845071804937	0.000000000000000
0.000000000000000	0.000000000000000	0.000998659667081	0.000000000000000
0.000000000000000	0.000000000000000	-0.000024779501890	0.000000000000000
0.000000000000000	0.000000000000000	-0.001035565963037	0.000000000000000
0.000000000000000	0.000000000000000	-0.001052970165541	0.000000000000000
0.000000000000000	0.000000000000000	-0.001219941869759	0.000000000000000
0.000000000000000	0.000000000000000	1.569397322971582	0.000000000000000
0.000000000000000	0.000000000000000	-0.016593198483799	0.000000000000000
0.000000000000000	0.000000000000000	0.000091585233884	0.000000000000000
0.000000000000000	0.000000000000000	0.004694007912200	0.000000000000000
0.000000000000000	0.000000000000000	0.000209987492911	0.000000000000000

Columns 17 thru 19

0.000000000000000	0.000000000000000	0.000000000000000
0.000000000000000	0.000000000000000	0.000000000000000

KQ(continued)

0.000000000000000	0.000000000000000	0.000000000000000
0.000000000000000	0.000000000000000	0.000000000000000
0.000000000000000	0.000000000000000	0.000000000000000
0.000000000000000	0.000000000000000	0.000000000000000
0.000000000000000	0.000000000000000	0.000000000000000
0.000000000000000	0.000000000000000	0.000000000000000
0.000000000000000	0.000000000000000	0.000000000000000
0.000000000000000	0.000000000000000	0.000000000000000
0.000000000000000	0.000000000000000	0.000000000000000

<>

K=KQ*MRNV

K =

Columns 1 thru 4

0.000000001761492	0.000000502248067	0.000000523727462	0.000000520498212
0.000000000363076	0.000000103522694	0.000000107949998	0.000000107284390
-0.000000000009009	-0.000000002568684	-0.000000002678537	-0.000000002662022
-0.000000000376494	-0.000000107348461	-0.000000111939380	-0.000000111249173
-0.000000000382822	-0.000000109152609	-0.000000113820685	-0.000000113118879
-0.000000000443526	-0.000000126461169	-0.000000131869472	-0.000000131056378
0.000000570575775	0.000162686293142	0.000169643817340	0.000168597811167
-0.000000006032683	-0.000001720078092	-0.000001793639821	-0.000001782580424
0.000000000033297	0.000000009493875	0.000000009899895	0.000000009838853
0.000000001706571	0.000000486588537	0.000000507398228	0.000000504269663
0.000000000076344	0.000000021767647	0.000000022698573	0.000000022558616

Columns 5 thru 8

-0.003081479818114	-0.000000004235251	0.000001551717042	0.000001573623857
-0.000635150464878	-0.000000000872964	0.000000319837824	0.000000324353227
0.000015759835571	0.000000000021661	-0.000000007936059	-0.000000008048099
0.000658622976893	0.000000000905225	-0.000000331657696	-0.000000336339970
0.000669692100514	0.000000000920439	-0.000000337231689	-0.000000341992656
0.000775886592043	0.000000001066395	-0.000000390707231	-0.000000396223154
-0.998141280880727	-0.000001371866426	0.000502626311729	0.000509722284378
0.010553322696618	0.000000014504709	-0.000005314255372	-0.000005389280912
-0.000058248476228	-0.000000000080058	0.000000029331736	0.000000029745836
-0.002985402741147	-0.000000004103200	0.000001503336249	0.000001524560034
-0.000133552658766	-0.000000000183558	0.000000067252083	0.000000068201534

Columns 9 thru 12

0.000001569924753	-0.003141769809613	0.000000063887918	0.000000000729043
0.000000323590773	-0.000647577356628	0.000000013168492	0.000000000150269
-0.000000008029180	0.000016068181044	-0.000000000326747	-0.000000000003729
-0.000000335549338	0.000671509114729	-0.000000013655144	-0.000000000155823
-0.000000341188736	0.000682794808768	-0.000000013884639	-0.000000000158442
-0.000000395291755	0.000791067024432	-0.000000016086355	-0.000000000183566
0.000508524084486	-1.017670186760809	0.000020694332727	0.000000236148934
-0.000005376612375	0.010759801328062	-0.000000218800660	-0.000000002496797
0.000000029675912	-0.000059388123522	0.000000001207658	0.000000000013781
0.000001520976263	-0.003043812958480	0.000000061895965	0.000000000706313
0.000000068041213	-0.000136165652891	0.000000002768930	0.000000000031597

Columns 13 thru 16

0.000000779273095	0.000000800529824	0.000000797670602	-0.003163812931494
0.000000160622719	0.000000165004128	0.000000164414789	-0.000652120855186

```
  K(continued)
 -0.000000003985493  -0.000000004094208  -0.000000004079585   0.000016180917780
 -0.000000166558665  -0.000000171101992  -0.000000170490874   0.000676220522043
 -0.000000169357928  -0.000000173977612  -0.000000173356223   0.000687585398181
 -0.000000196213372  -0.000000201565609  -0.000000200845685   0.000796617267732
  0.000252419191705   0.000259304590911   0.000258378442745  -1.024810311378582
 -0.000002668821775  -0.000002741620928  -0.000002731828787   0.010835293686337
  0.000000014730413   0.000000015132224   0.000000015078177  -0.000059804799384
  0.000000754976236   0.000000775570204   0.000000772800130  -0.003065168800599
  0.000000033774031   0.000000034695306   0.000000034571386  -0.000137121011261
    Columns 17 thru 19
  0.000000182112913   0.000000289450152   0.002044610915727
  0.000000037536868   0.000000059661075   0.000421432444888
 -0.000000000931393  -0.000000001480356  -0.000010456901794
 -0.000000038924074  -0.000000061865899  -0.000437006830286
 -0.000000039578250  -0.000000062905646  -0.000444351370026
 -0.000000045854257  -0.000000072880728  -0.000514813105746
  0.000058989325709   0.000093757597701   0.662282630030616
 -0.000000623692659  -0.000000991296726  -0.007002297615535
  0.000000003442437   0.000000005471407   0.000038648791279
  0.000000176434837   0.000000280425421   0.001980862245636
  0.000000007892852   0.000000012544894   0.000088614315217
<>
//Check to see that the K just computed does generate the desired eigenvalue
AC=A+B*K;EIG(AC)//AC is the state coefficient matrix of the controlled system
ANS  =
   1.0D+04 *
 -5.266821895634869        0.000000000000000i
 -0.021360198075745        0.000000000000000i
 -0.003977263492918        0.009552095834876i
 -0.003977263492918      - 0.009552095834876i
 -0.000459990795721      - 0.000120566056908i
 -0.000459990795721        0.000120566056908i
 -0.000021248217594        0.000000000000000i
 -0.000093892720314        0.000000000000000i
 -0.000100000000000      - 0.000000000000000i
 -0.000366233205798        0.000176262166536i
 -0.000365106096282        0.000173786717458i
 -0.000365101237584        0.000173829082129i
 -0.000366233205798      - 0.000176262166536i
 -0.000365106096282      - 0.000173786717458i
 -0.000365101237584      - 0.000173829082129i
  0.000000294968295        0.000000000000000i
 -0.000000000002605        0.000000000000000i
  0.000000027480838        0.000000000000000i
  0.000000000000000        0.000000000000000i
<>
//The result confirms the correct execution of the procedure.
<>
exit
(END OF MATLAB SESSION)
```

One can easily confirm that the eigenvalue .000002445599342 does not appear in the list of eigenvalues of the controlled system, and that an eigenvalue with value -1.0, the value which was desired, has appeared. All the other eigenvalues are unchanged. No element of the gain matrix is appreciably greater than 1.0 which implies, as a course rule of thumb, that one may expect to encounter no difficulty in accomplishing the eigenvalue change. The basic procedure is seen to be simple, but a negative side is that to change other eigenvalues by this method will require successively obtaining the RJCT after each reassignment and repeating the process we have demonstrated.

Several matters of interest are spawned by this demonstration. One is that literally all 19 states must be known and 165 gain elements are required to set this eigenvalue. However, good results can often be obtained by setting relatively small gains to zero, thus not requiring full state feedback. In the present example, it was found that setting all gains to zero except those having order of magnitude one reassigned the target eigenvalue to a stable value, but it was not -1.0. Also, many other eigenvalues were changed, but none changed to unstable values (compare to root locus principles). Another matter of interest is the behavior of the volume change descriptive state (the nineteenth state). This state is not controllable since its only influence is the glove manipulation disturbance (note that this state is connected only to the nineteenth canonical state and that the last row of BR is zero). This might appear to be a problem for system control, but it is not in fact. If, for example we replace V with P as a state, we find that all nineteen states are controllable.

8 - CONCLUDING REMARKS

The principal thrust of this study was to begin familiarization with the control problem specific to a CGRC system. It was brought to the point of displaying the system characteristics which are relevant to the control problem. A number of processes to make the control problem study meaningful are illustrated, but not all the actions which should be taken were done in this study. An important example is that the system linearized state variable format model matrices should be balanced to maximize numerical effectiveness and to make physical judgment as effective as possible. The modal matrix is normalized, however. A serious study should include both these important enhancements in preparation for the control law synthesis.

The control synthesis demonstration is very elementary, but it suffices to demonstrate that the local stability problem is resolvable via straightforward multivariate means. Although canonical space eigenvalue placement was used in the demonstration, alternate choices such as linear quadratic regulator synthesis or minimum norm gain matrix synthesis could have been used. To describe the full control study will require an additional report which is based on the contents of this report but which is dedicated to the synthesis activity. The uncertainties in the model are yet to be characterized, and as a consequence, robustness considerations cannot be brought into the control design process at this stage. Because of the dynamic dimensionality and the hypothetical nature of the object of the study, it is not certain that any significant constructive purpose can be served by further addressing the control problem via this model. Stated differently, the resource might be better expended in the design of the control system for a model which is generated from a more completely defined physical system.

ACKNOWLEDGEMENTS

This work was partially supported by NASA - ASEE (Stanford University - NASA Ames Research Center) Summer Faculty Fellowships awarded to A. L. Blackwell (1988-1989) and C. C. Blackwell (1989-1990), and by NASA Ames Research Center - University of Texas at Arlington Joint Research Interchange No. NCA 2-484: "Development of a Plan for Conducting the Activities Required in Modeling, Analysis, and Control Synthesis for the CELSS Program."

REFERENCES

Blackwell, A. L., and C. C. Blackwell. 1990. A modeling system for control of the thermal and fluid dynamics of the NASA CELSS crop growth research chamber. *Proc. 1990 American Control Conference*, San Diego, California, May 23 - 25, 1:2113-2114.

Blackwell, A. L., and C. C. Blackwell. 1989. A modeling system for control of the thermal and fluid dynamics of the NASA CELSS crop growth research chamber. *Trans. SAE, J. Aerospace*, 98(1):1079-1089.

Blackwell, C. C. 1991. Eigenvalue assignment in canonical state space according to control authority. (in preparation)

Brogan, W. R. 1985. *Modern Control Theory.* Prentice-Hall Publishing Company, New York.

MacElroy, R. D., and D. T. Smernoff, eds. 1987. Controlled ecological life support system: regenerative life support systems in space. NASA CP 2480.

MacElroy, R. D., D. T. Smernoff, and J. D. Rummel, eds. 1987. Controlled ecological life support system: design, development, and use of a ground-based plant growth module. NASA CP 2479.

Šiljak, D. D., 1986. Stability of reduced-order models via vector Liapunov functions. *Proc.* 1987*American Control Conference*, Minneapolis, Minnesota. June 10-12, vol. 1, 428-489.

Takahashi, Y., M. J. Rabins, D. M. Auslander. 1970. *Control and dynamic systems.* Addison-Wesley, Reading, MA.

APPENDICES

Appendix A1. A formal symbology and structure for generating the mathematical model of mixed energy systems; A. L. Blackwell and C. C. Blackwell. 1989. A modeling system for control of the thermal and fluid dynamics of the NASA CELSS Crop Growth Research Chamber, *SAE Transactions: J. Aerospace*, 90(1):1073-1089.

891570

A Modeling System for Control of the Thermal and Fluid Dynamics of the NASA CELSS Crop Growth Research Chamber

Ann L. Blackwell and C. C. Blackwell

Department of Mechanical Engineering

The University of Texas at Arlington

ABSTRACT

The Crop Growth Research Chamber (CGRC), which is being developed under the Controlled Ecological Life Support System program at NASA Ames Research Center, will be operated to support research on the growth dynamics of crops of higher plants within a closed, precisely controlled environment. The CGRC is the first in a series of instruments which will be incorporated into bioregenerative life support systems for space habitats. The dynamic processes of the thermal and fluid portions of the CGRC are profoundly coupled with those of the plants and there is strong reason to believe that consideration of these interactions is necessary in order to design a CGRC which will support sound research.

In this paper we describe the modeling system which we have developed for the thermal and fluid dynamics of the CGRC. The bases of the modeling system are symbolic representations of the individual processes which are included in the representation. The system includes the plant growth chamber, the associated control system components and the control devices. An example of the derivation of the dynamic equations of the system from the symbolic modeling system is presented.

AN IMPORTANT ELEMENT of the Controlled Ecological Life Support System (CELSS) Program at NASA Ames Research Center is the development of a crop growth research chamber (CGRC). This CGRC contains a plant growth chamber (PGC) requiring a precisely controlled internal environment. The CELSS program and its recent status are described in [1].

The CGRC is one of a sequence of physical devices which are to be developed under the CELSS program, leading eventually to fully cycling bioregenerative life support systems for space or planetary habitats [2]. It will be used to conduct research on the growth of crops of higher plants from seed to maturation employing stringent control of all environmental parameters (e.g., lighting, temperature, atmospheric oxygen, carbon dioxide concentrations, humidity, and pressure, nutrient solution temperature, ion and dissolved oxygen concentrations, and pressure) which affect the production of biomass, oxygen, and transpired water vapor, and the consumption of carbon dioxide, liquid water, and nutrients by the plants. Knowledge of the autecology of the crop plant populations to be used in a CELSS will permit utilization of the CELSS plant growth unit as a multiple input-multiple output (MIMO) life support system component whose function and performance can be varied as needed by application of the appropriate control strategy.

The prototype chamber unit currently under development is a precursor to a space-based unit (CROP) that will be capable of conducting experiments on the effect of the space environment on the growth of plant crops. It is desirable to regulate environmental conditions within the space-based unit to the same degree of accuracy as those within the ground-based unit in order to separate the effects of flight mission variables, principally gravity, from the effects of controllable environmental parameters on plant growth response. Suggested ancillary uses of the chambers are to "develop' control systems, to validate models of plant growth and system operation, to explore the development of expert systems for operation of plant growth devices, and to explore the use of automation and robotics and other devices to save human labor" [3].

Both the ground-based and the space-based units will be designed to provide environmental conditions that are independent of those of the ambient environment. While the space-based unit and follow-on versions of the prototype ground-based unit will be closed with respect to the exchange of materials, the initial ground based unit will emulate closure by including sufficiently large storages and sinks of materials which require removal or replenishment during particular phases of plant growth.

Tolerance specifications for environmental variables for the ground-based and space-based units were developed and modified at workshops held in September 1984, April 1986 and June 1988 [4, 5]. The tolerances on environmental variables are described in [6] and are given in Table 1. The CGRC differs from other plant growth chambers described in the literature [7 - 12] in size, degree of material closure, tightness of control, and number of controlled environmental variables.

PRECEDING PAGE BLANK NOT FILMED

TABLE 1. Tolerance requirements for the atmospheric variables in the shoot zone of the plant growth chamber of the NASA CELSS Crop Growth Research Chamber.

Air temperature	5-40° C ± 1° C
Relative humidity	35-90% ± 2%
Carbon dioxide	25-5000 ppm ± 0.2%
Oxygen	5-25% ± 5%
Nitrogen	75-95% ± 5%
Gage pressure	0.5" H_2O ± 0.25"
Air velocity	0.5 m sec^{-1} ± (•)
Photosynthetic photon flux	0-3000 μmoles m^{-2} s^{-1} ± 10 μmoles m^{-2} s^{-1}
Surface temperatures	Air temperature + 2° C

• not established

The dynamic processes of the thermal and fluid aspects of the CGRC are profoundly coupled with those of the plants and there is strong reason to believe that consideration of these interactions is necessary in order to design a CGRC which will support sound research. For the case of complex systems, practical necessity predicates the systematic examination of control issues on the use of adequately accurate mathematical models of the system being examined.

Many very important questions related to the acceptability of performance of a passively controlled system with closure can be evaluated by analyzing a mathematical model of the dynamic behavior of the system. Due to disturbances, uncertainties, or variations in physical or biological characteristics of the system components, passive control may fail to provide acceptable performance. In that case, recourse to the use of active control is a compelling alternative since active control is well established to have highly reduced sensitivity to uncertainty. The same mathematical models used to determine the adequacy of passive control can and should be used to study the requirements for active control laws which will provide stable, desirable system performance in which compensation is provided for disturbances and for uncertain or variable characteristics of elements of the controlled system.

Uncertainties in the CGRC system are most manifest in the living component. The inherent variability of biological systems [13] makes the task of precise mathematical description of their behavior difficult.

The term "stable" is used here in the sense of stability to a region, i.e. the states of the system remain within an acceptable tolerance of the desired system state. The region of tolerance is described by the specifications on the environmental variables given in Table 1.

For a plant growth unit operating as a regulating system, this implies prescribed bounds on the deviation of the actual system variables from desired fixed values. For a plant growth unit operating as the MIMO tracking system described earlier, i.e., one which is transitioning from an initial to a final state along a prescribed performance path, this implies prescribed bounds on the deviation of the actual system variables from the desired trajectory between initial and final states. A control which provides stability as defined is said to be a robust control for the system subject to the specified uncertainties.

Control strategies, proposed or implemented, have been reported for growth chambers, greenhouses, and livestock buildings [9, 11, 12, 14 - 23]. These control strategies have been developed using *ad hoc* methods or, to varying degrees, utilizing control theory formalism. Most depend upon some form of episodic manual tuning to retain desirable performance. It is possible that a robust control may achieved by manual tuning, but it is difficult to know whether robustness has been achieved or whether future system perturbations will require retuning. If it desirable to develop a control system that requires little or no human intervention, as will be the case for the space borne system, a formal procedure for the synthesis of a control strategy is required.

The robustness objectives are most readily achieved through the development and utilization of mathematical models of the components of the CGRC, i.e. the PGC and the associated elements of the control system. The mathematical model which will be developed for the CGRC is based upon the philosophy that a model which is developed for control system design is one in which biophysical and physical phenomena are represented in the most parsimonious format which is adequate for the analytical and computational needs of control design in contrast to the representation of microscopic detail. The issue of control modeling and scientific research modeling is discussed in [2].

Approaches to robust control theory under current development fall in five major categories which can be briefly described as: (1) H_∞ methods [24], (2) linear optimal quadratic Gaussian with loop transfer recovery (LQG/LTR) [25], (3) quantitative feedback theory (QFT) [26], (4) variable structure with sliding modes (VS/SM) [27], and (5) Lyapunov theory based methods [28]. The mathematical modeling structure developed in this paper is oriented toward the utilization of (5), a methodology which appears to be most promising for the types of systems, uncertainties, and performance measures encountered in CGRC research and CELSS applications. Illustrations of CELSS related applications of Lyapunov theory based methods of robust control design can be found in [29] and [30].

The purpose of this paper is to illustrate the approach to the derivation of a continuous time state variable format mathematical model for use in developing a robust control law for the CGRC.

SYSTEM DESCRIPTION

The development of a system to control the environmental conditions within the PGC of the CGRC involves (1) the selection of component devices (i.e.

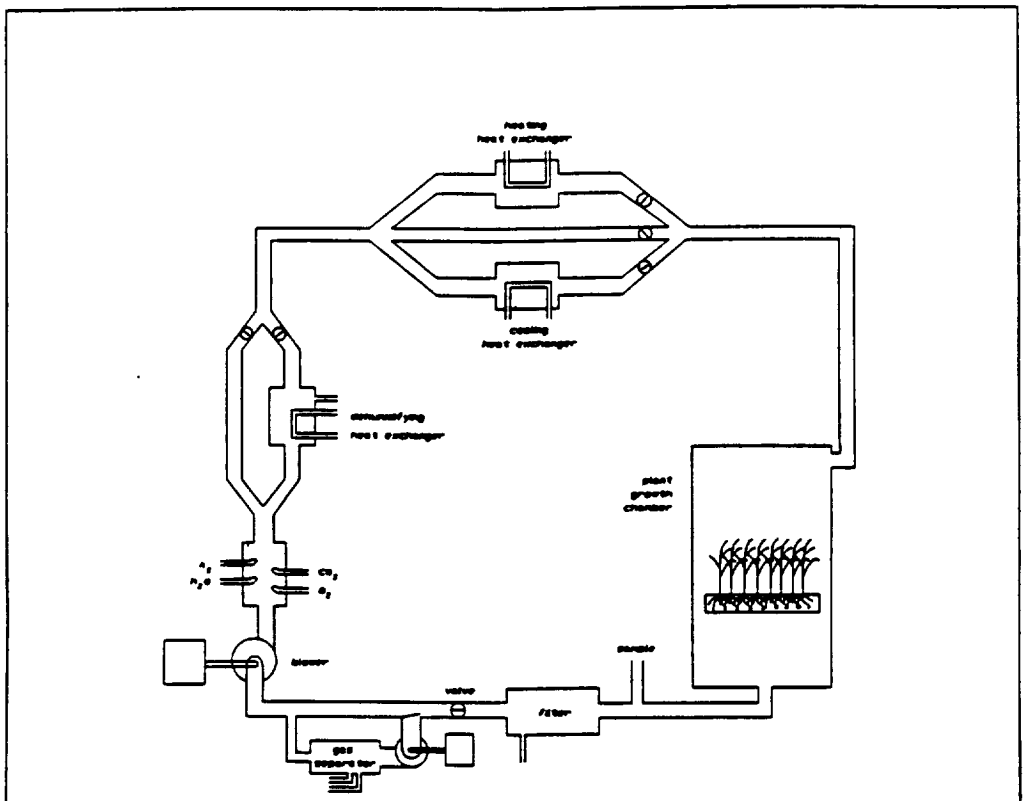

Fig. 1. Conceptual model of the Plant Growth Chamber and atmospheric control system of the NASA CELSS Crop Growth Research Chamber.

actuators) which will affect the environmental variables that are to be controlled, (2) the selection of component devices which will provide suitable measures of the environmental variables (i.e. measurement instruments), and (3) the development of control algorithms which utilize the outputs of the measurement instruments to provide the necessary combinations and time sequencing of inputs to the actuators so that the required performance characteristics of the environmental variables within the CGRC are met.

Fig. 1 is a representation of the arrangement of the components hypothesized for control of the atmosphere of the plant growth chamber. The plants receive radiant energy from a light source above the chamber (not shown). Water and nutrients are supplied to the roots by means of a nutrient delivery system that is materially isolated from the chamber atmosphere. Air flow into the chamber is assumed to be sufficient to assure that uniform conditions exist in the atmospheric control volume within the chamber and surrounding the plant canopy control volume. Gaseous exchange of carbon dioxide, water vapor and oxygen occurs between the canopy and the atmosphere.

Air enters near the top of the upper chamber and is thoroughly mixed with the air in the upper portion of the chamber. The resulting mixture flows between the walls and the baffle formed by the plant support surface into the lower portion of the chamber and then into the ducting located near the bottom. A HEPA filter is provided to remove particulates from the air as it leaves the chamber. Air flow out of the filter is affected by the controllable orifice flow area of a valve. A portion of the air flow is diverted, by means of a controllable flapper valve and fan, into a gas separator which removes excess oxygen or carbon dioxide. A centrifugal pump (blower) serves to compensate for pressure losses within the system and provide the required air movement within the system. Makeup gases are injected into the flow stream to

maintain the required atmospheric composition. A portion of the flow is diverted through a dehumidifying heat exchanger, where the condensate is removed from the system. Two variable flow area orifices are present, one each in the flow path through the dehumidifier and in the parallel bypass. The orifice flow areas are variable in order to regulate the mass flow ratio of the paths. The air in the two flow paths is mixed and flows through a section of ducting. A portion of the flow is diverted through either a heater or a cooling heat exchanger. Three variable flow area orifices are present one each in the flow path through the cooling heat exchanger, the heater and the parallel bypass. The orifice flow areas are variable in order to regulate the mass flow ratio of the paths. Since meeting performance specification is considered paramount to economic constraints in this design concept, two independently controlled heat exchangers are utilized in humidity control and temperature regulation. The flows are mixed and flow through the ducting to the chamber inlet.

The task of modeling the processes which affect the dynamics of the thermal environment of greenhouses, plant growth chambers, livestock houses and confined spaces has been addressed [9, 11, 12, 14, 18, 19, 31 - 37]. The processes included in the model depend upon the assumptions of importance of each process in determining the dynamics of interest for the particular system being modeled. While the physics of the processes which have been included in these models are applicable to the dynamics of the CGRC, they do not include all the processes necessary to account for the dynamics of the variables of interest in the CGRC.

In the following sections, we describe the assumptions which we have made concerning the function of each component of the CGRC and the physical and biophysical processes which we hypothesize to contribute significantly to the thermal and fluid dynamics within them. In this formulation, we consider the scenario in which the PGC contains a crop of plants forming a closed canopy and the system goal is to maintain temperature, relative humidity, pressure, carbon dioxide concentration, oxygen concentration, and mean air velocity in the chamber within set tolerances about constant operating points.

MODELING PROCEDURE

The process of mathematical model development is enhanced by the preliminary formulation of a symbolic model of the system. The symbolic model is a schematic representation of each of the generic elemental physical and biological processes which are to be included in the mathematical model and the manner in which these processes interact in the particular system being analyzed. The mathematical equations describing these elemental processes and the structure of their interactions combine to become the mathematical model of the dynamic behavior of the system. Other symbologies have been used for developing models of engineering systems for control system studies. These include linear graphs and circuit diagrams [38, 39] and bond graphs [40, 41]. In this paper we present the symbology of the modeling system which we have developed for the thermal and fluid dynamics of the atmospheric control system of the CGRC.

ASSUMPTIONS – Some assumptions are made in order to achieve the minimum complexity model for the current analysis. These assumptions may be modified as more specific details of the system become available.

(1) Leakage from the system is negligible.

(2) The air in the system consists solely of nitrogen, oxygen, water vapor and carbon dioxide and behaves as an ideal gas.

(3) The boundary of the system includes the PGC and the elements of the environmental control system.

(4) The air ducts of the system are perfectly insulated. Thermal capacitance of the air duct walls is negligible.

(5) Distributed phenomena are adequately represented by lumped models.

(6) The radiant energy source consists of lamps (and their associated reflectors) which produce photosynthetically active radiation (PAR) as well as long wave radiant energy. Control of the radiant energy intensity at the canopy level, frequency content, and sequencing (i.e. effective photoperiod) is unaffected by PGC processes. A substantial portion of the long wave radiant energy produced by the radiant energy source in the 2800 nm to 100,000 nm range is absorbed by a liquid water/glass filter [42]. The water in the filter is cooled by a separate control system which maintains the water at a prescribed temperature.

(7) The control system for the nitrogen gas blanket which separates the inner walls from the exterior walls of the PGC is able to maintain the temperature of the inner walls at a prescribed temperature above the dewpoint of the chamber air.

(8) The canopy processes of transpiration, photosynthesis, photorespiration and maintenance respiration are the only canopy processes of significance for the time scale considered in this model. (See Fig. 3.3 in [43].) Growth is negligible, i.e. the leaf carbohydrate pool as defined in [44] is an infinite source/sink. Similarly, there is an infinite water source for internal water associated with the plant.

(9) The plant population can be modeled by aggregating the sum of individual plant processes and their interactions into a single canopy process. The canopy biomass is sufficiently large to affect the fluid and thermal dynamics of chamber. The conditions within the chamber affect the physiological dynamics of the canopy.

(10) A nutrient delivery system in the lower chamber is maintained at fixed temperature above the dew point of the chamber air. There is no material interchange between the nutrient delivery system and the chamber air. Water and nutrients are delivered to the plants at the ideal concentration, pH and pressure. Dynamics of nutrient delivery and plant uptake and translocation are negligible.

(11) The flow rates and entrance temperatures of the working fluid in the heat exchangers are maintained by separate control systems whose dynamics are negligible.

(12) An infinite sink exists for the removal of gases and condensate.

(13) An infinite source exists for the addition of gases and water vapor.

(14) The dynamics of air diversion from the main flow

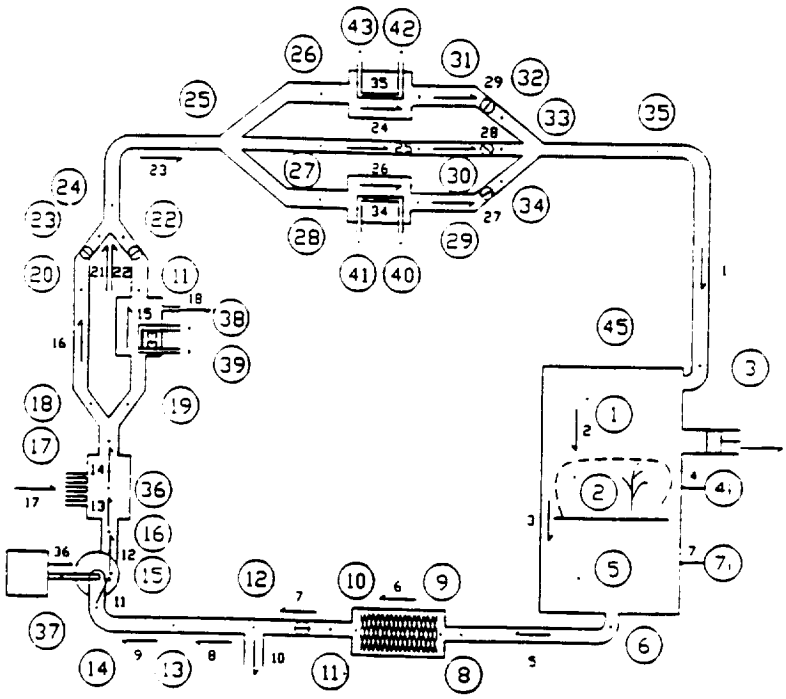

Fig. 2. Conceptual model of the Plant Growth Chamber and atmospheric control system of the Crop Growth Research Chamber indicating points and flow path designations for symbolic modeling. Points are indicated as encircled numbers. Flow paths are shown as numbered arrows. Arrows indicate the direction of assigned positive flow.

path, gas separation, component gas removal, and reintroduction of the diverted gas into the main flow path can be neglected. The process can be represented by instantaneous removal of the gas component from the main flow stream.

(15) The dynamics of source gas or water vapor injection are negligible. The process can be represented by instantaneous addition of the gas or vapor to the main flow stream at a prescribed temperature.

(16) Flows are turbulent but fully developed.

(17) Other than in the blower, incompressible flow relationships are adequate to describe system processes.

ASSIGNMENT OF POINTS AND FLOW PATHS – Fig. 2 represents the conceptual model of the CGRC with the points and flow paths needed for the modeling symbology assigned to the system. A point is the location at which all the variables representing potentials with respect to a fixed reference within a designated volume may be assumed to be concentrated. Point numbers are shown encircled. Flow paths represent the constitutive relationships (processes) which occur between points. Flow paths are shown which arrows indicating the flow direction which is assigned a positive value. Path numbers are not circled.

CONSTITUTIVE RELATIONSHIPS – The symbology for the constitutive relationships is representative of processes between and at points. In many cases, the symbol represents aggregated phenomena, i.e. total molar flow rates.

Storages – We account for molar storages and energy storages in the system. Fig. 3 illustrates the molar storage at point 1. The symbol illustrates the rate of change of upper chamber atmospheric mass as a function of molar flow rate into the chamber through flow path 1 (from the atmospheric control system) (n_1) and flow path 2 (from the plant canopy, through gaseous exchange of the products of transpiration, photosynthesis, photorespiration and maintenance respiration) (n_2) and molar flow rate out

of the upper chamber through flow path 3 (to the atmospheric control system) (n_3) and flow path 2 (to the plant canopy, through gaseous exchange of the reactants for photosynthesis, photorespiration and maintenance respiration) (n_2). Significant molar storages in the system are located at points 1 (upper chamber atmosphere), 2 (plant canopy), 5 (lower chamber atmosphere), 15 (blower entrance), and 36 (gas resupply chamber). Within the plant canopy, molar storage is composed of three substorages: substomatal cavity (gaseous products) (point 2), leaf carbohydrate pool (point 46), and internal plant water pool (point 44). (Points 46 and 44 are not shown on Fig. 2.) The remaining small amounts of molar storage in the system are lumped into these storages.

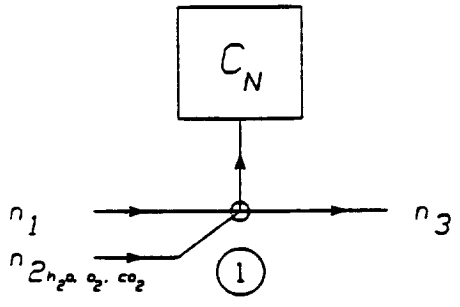

$$\dot{n}_1 = n_1 + n_{2\ h_2o,\ o_2,\ co_2} - n_3$$

Fig. 3. Symbology and sample equation for molar storage processes. The process is illustrated for the molar storage at point 1 on Fig. 2. Molar flow rate n_i represents the sum of all atmospheric species in that flow. Flow path arrows indicate the direction of assigned positive flow.

Fig. 4 illustrates the energy storage at point 1. The symbol illustrates the rate of change of upper chamber atmosphere energy as a function of enthalpy flow rate into the upper chamber atmosphere through flow path 1 (from the atmospheric control system) ($\dot{H}_1^\circ$) and flow path 2 (from the plant canopy, through gaseous exchange of the products of transpiration, photosynthesis, photorespiration and maintenance respiration) ($\dot{H}_2^\circ$), enthalpy flow rate out of the upper chamber atmosphere through flow path 3 (to the atmospheric control system) ($\dot{H}_3^\circ$) and flow path 2 (to the plant canopy, through gaseous exchange of the reactants for photosynthesis, photorespiration and maintenance respiration) ($\dot{H}_2^\circ$), heat transfer into the upper chamber atmosphere from the plant canopy ($\dot{Q}_2$) and from the walls and lights ($\dot{Q}_{4i}$), and work ($P_1\dot{V}_1$) done at the moving boundary (glove ports). These storages are located at points 1 (upper chamber atmosphere), 2 (plant canopy), 5 (lower chamber atmosphere), 15 (blower entrance), and 36 (gas resupply chamber). An additional energy storage within the plant canopy represents energy storage associated with the chemical bonds in the leaf carbohydrate (point 46). Mechanical energy storage occurs at point 37, is illustrated in Fig. 14, and is discussed in conjunction with blower processes.

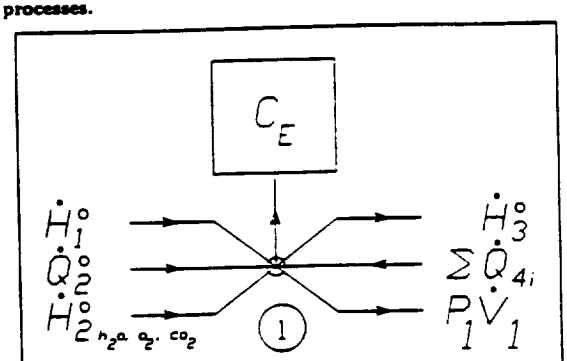

$$\dot{E}_1 = \dot{H}_1^\circ + \dot{H}_{2\ h_2o,\ o_2,\ co_2}^\circ - \dot{H}_3^\circ + \dot{Q}_2 + \sum_i \dot{Q}_{4i} - P_1\dot{V}_1$$

Fig. 4. Symbology and sample equation for energy storage processes. The process is illustrated for the energy storage at point 1 on Fig. 2. Flow path arrows indicate the direction of assigned positive flow.

Inertance – We account for total fluid inertia within the system by lumping all inertance effects into two fluid inertances, one in each section of the control system between the blower and the PGC. Fig. 5 illustrates fluid inertance located between points 13 and 14. The rate of change of the molar flow rate between points 13 and 14 (n_9) is proportional to the total pressure difference between points 13 and 14. A similar process is located between points 35 and 3.

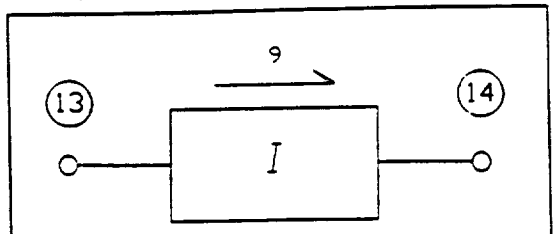

$$\dot{n}_9 = \frac{A_c}{L\,MW_d}(P_{13} - P_{14})$$

Fig. 5. Symbology and sample equation for fluid inertance processes. The process is illustrated for fluid inertance between points 13 and 14 on Fig. 2. Arrows indicate the direction of assigned positive flow.

Pipe Friction – We account for total pressure losses due to friction in the ductwork (constant area) within the system by lumping all constant area friction effects into two friction loss processes, one in each section of the control system between the blower and the PGC. Fig. 6 illustrates pipe friction located between points 12 and 13. The total pressure difference between points 13 and 14 is proportional to the square of the molar flow rate between points 13 and 14 (n_8). The friction factor is determined by the duct surface and the Reynolds number. Effects of fittings and bends are included in equivalent length. A similar process is located between points 24 and 25.

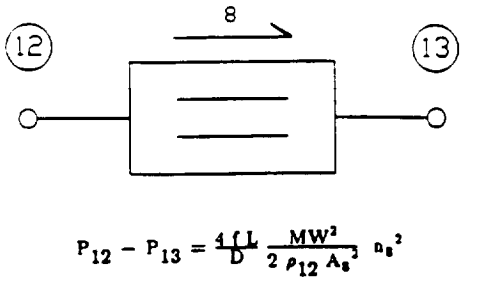

$$P_{12} - P_{13} = \frac{4 f L}{D} \frac{MW^2}{2 \rho_{12} A_8^2} n_8^2$$

Fig. 6. Symbology and sample equation for pressure changes due to pipe friction for constant area, single phase flow. The process is illustrated for friction between point 12 and 13 on Fig. 2. Arrows indicate the direction of assigned positive flow.

Flow Splitting and Joining – We account for total pressure changes due to flow division and flow merging. These processes occur in the section of the control system involving dehumidification and temperature balancing. Fig. 7 illustrates flow division between points 17 and points 18 and 19. The total pressure difference between point 17 and point 18 (or between point 17 and point 19) is a bilinear function of the molar flow rates (n_{14}) and (n_{16}) (or (n_{14}) and (n_{15})). The weighting of each term ($a_{1,2,3}$) is a function of the splitter geometry. A similar process is located between points 25 and points 26, 27, and 28.

Fig. 8 illustrates flow merging among from points 22 and 23 to point 24. The total pressure difference between point 22 and 24 (or 23 and 24) is a bilinear function of the molar flow rates (n_{21}), (n_{22}), and (n_{23}). A corresponding process relates the flows through points 32, 33, 34, and 35.

Sudden Expansion – We account for total pressure changes due to sudden increases in cross sectional flow area. Fig. 9 illustrates sudden expansion from point 3 to point 1. Pressure change varies as a function of the square of the molar flow rate between points 3 and 1 (n_1). Similar processes are located between points 8 and 9, 14 and 13, and 16 and 36.

Sudden Contraction – We account for total pressure changes due to sudden decreases in cross sectional flow area. Fig. 10 illustrates sudden contraction from point 5 to point 6. Pressure change varies as a function of the square of the molar flow rate between points 5 and 6 (n_5) and as a function of the upstream and downstream duct diameters. Similar processes are located between points 10 and 11, and 13 and 17.

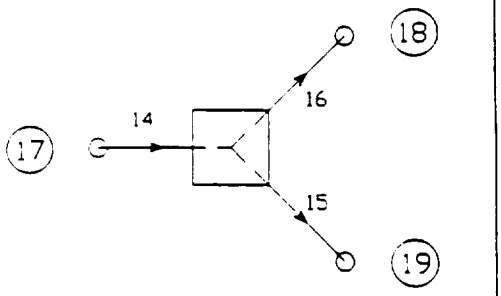

$$P_{17} - P_{18} = \frac{K\,MW^2}{\rho_{17}}\left[a_1 \left(\frac{n_{16}}{A_{16}}\right)^2 - a_2 \left(\frac{n_{14}}{A_{14}}\right)^2 - a_3 \left(\frac{n_{16} n_{14}}{A_{16} A_{14}}\right)\right]$$

$$n_{14} = n_{15} + n_{16}$$

$$\dot{H}_{14}^{\circ} = \dot{H}_{15}^{\circ} + \dot{H}_{16}^{\circ}$$

Fig. 7. Symbology and sample equations for flow splitting process. The process is illustrated for flow splitting between point 17 and points 18 and 19 on Fig. 2. Pressure relationship from [45]. Arrows indicate the direction of assigned positive flow.

Flow through an Orifice – We account for total pressure changes due to flows through orifices. Fig. 11 illustrates flow through an orifice between points 11 and 12. Pressure drop across the orifice varies as a function of the square of molar flow rate between points 11 and 12 (n_7). For a circular variable diameter thin plate orifice K_i can be approximated as a quadratic function of the orifice to duct diameter. Similar processes are located between points 21 and 22, 20 and 23, 31 and 32, 30 and 33, and 29 and 34. All of these orifice areas are shown as variable. These orifice areas are available as system control inputs. A similar process occurs between points 1 and 5 around the plant growth platform which forms a baffle between the upper and lower regions of the PGC. In that case, the orifice area is fixed.

Flow through a Porous Media – We account for total pressure changes through the particulate filter. Fig. 12 illustrates flow through a filter between points 9 and 10. The pressure difference between points 9 and 10 is proportional to the square of the molar flow rate between points 9 and 10 (n_6). Filter porosity may decrease as material accumulates within the filter.

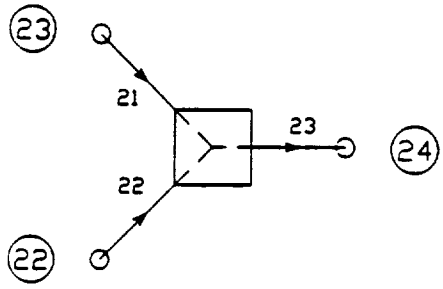

$$P_{24} - P_{23} = \frac{K\,MW^2}{\rho_{24}}\left[a_1 \left(\frac{n_{23}}{A_{23}}\right)^2 - a_2 \left(\frac{n_{21}}{A_{21}}\right)^2 - a_3 \left(\frac{n_{21}}{A_{23}\,A_{21}}\right) - a_3 \left(\frac{n_{22}^2}{A_{22}\,A_{23}}\right)\right]$$

$$n_{23} = n_{22} + n_{21}$$

$$\dot{H}_{23}^{\circ} = \dot{H}_{22}^{\circ} + \dot{H}_{21}^{\circ}$$

Fig. 8. Symbology and sample equations for flow merging process. The process is illustrated for flow merging from points 22 and 23 to point 24 on Fig. 2. Pressure relationship from [45]. Arrows indicate the direction of assigned positive flow.

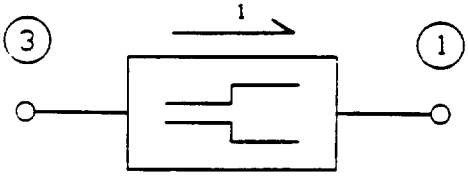

$$P_3 - P_1 = MW^2 \left[\frac{1}{\rho_1 A_e^2} - \frac{1}{\rho_3 A_1 A_e}\right] n_1^2$$

Fig. 9. Symbology and sample equation for sudden expansion process. The process is illustrated for sudden cross sectional flow area expansion from point 3 to point 1 on Fig. 2. Arrows indicate the direction of assigned positive flow.

Gas Removal – We account for the removal of excess atmospheric gases from the system. Fig. 13 illustrates selective removal of gases from the system at point 12. The molar and entropy flow rates downstream of the extraction point are equal to the upstream rates less the rate of gas removal.

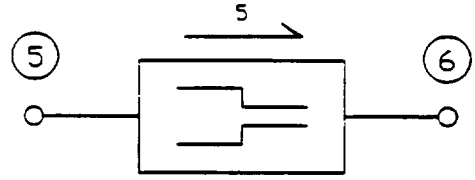

$$P_5 - P_6 = \frac{MW^2(1 + K_t)}{2\,\rho_6\,A_5^2}\, n_5^2$$

Fig. 10. Symbology and sample equation for sudden contraction process. The process is illustrated for sudden cross sectional flow area contraction from point 5 to point 6 on Fig. 2. The formulation of K_t is specific to the sudden contraction flow process and may be approximated as proportional to the ratio of downstream to upstream duct diameters. Arrows indicate the direction of assigned positive flow.

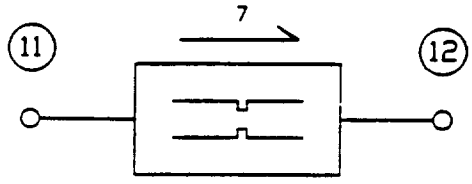

$$P_{11} - P_{12} = \frac{K_7}{A_7^2}\left(\frac{R\,T_{11}}{P_{11}}\right) MW\; n_7^2$$

Fig. 11. Symbology and sample equation for flow through an orifice. The process is illustrated for flow through the orifice from point 11 to point 12 on Fig. 2. The formulation of K_i is specific to the orifice flow process and may be approximated as a quadratic function of the duct to orifice diameter. Arrows indicate the direction of assigned positive flow.

Gas Injection – We account for the addition of atmospheric gases. This process is illustrated in Figs. 3 and 4. In that case, the gases which are added to molar storage originate from another system component (the plant canopy). A molar flow rate of additional gases (n_{17}) from an external source is indicated at point 13. Molar and energy influx rates from the external sources are modeled in a fashion similar to that shown in Figs. 3 and 4, respectively.

Blower – We account for thermal, mechanical and fluid processes associated with the blower. The processes involved with the blower are illustrated in Fig. 14. These

processes occur between points 15, 37 and 16. Motor torque is available as a control input. A mechanical energy storage (due to the rotational inertia of the motor and impeller) occurs at point 37. Mechanical power is added to the system by the pump motor. Pump efficiency is accounted for in the mechanical to fluid power conversion process equation. An isentropic compression process is modeled in the blower.

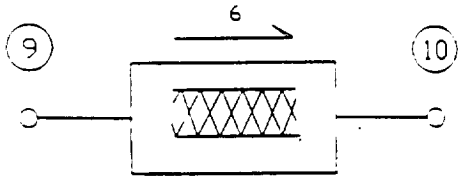

$$P_9 - P_{10} = \frac{K_s}{A_s^2}\left(\frac{R\,T_9}{P_9}\right) MW\ n_s^2$$

Fig. 12. Symbology and sample equation for flow through a porous media. The process is illustrated for flow through the porous filter from point 9 to point 10 on Fig. 2. The formulation of K_s is specific to the porous flow process. Arrows indicate the direction of assigned positive flow.

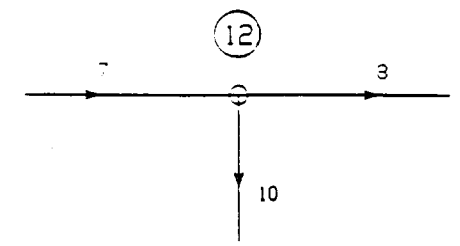

$$n_8 = n_7 - n_{10}$$

$$\dot{H}_8^* = \dot{H}_7^* - \dot{H}_{10}^*$$

Fig. 13. Symbology and sample equations for gas removal. The process is illustrated for gas removal at point 12 on Fig. 2. Arrows indicate the direction of assigned positive flow.

Heat Exchangers – The three heat exchangers (dehumidifying, cooling, and heating) are represented by a generic counterflow model. The processes involved in the heat exchanger model are illustrated in Fig. 15 for the dehumidifier between points 19 and 21 and 18. The processes in the working fluid, whose dynamics are separately controlled, occur between points 38 and 39. The logarithm mean temperature difference method is used. Since condensate is removed in the dehumidifier, a flow path (18) is shown for molar and enthalpy flow. The condensate flow path will not appear for the other two heat exchanger systems. For the dehumidifier the molar flow rates for water vapor and other atmospheric component gases are considered separately. This process is not required for the other heat exchanger systems.

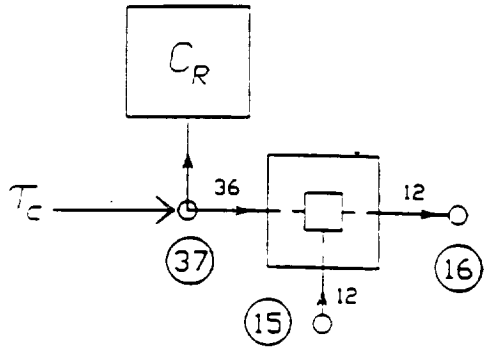

$$\tau_{36}\,\omega_{37} = \frac{\gamma\,R}{\gamma - 1}\,\frac{T_{15}}{\eta_p}\left[\left(\frac{P_{16}}{P_{15}}\right)^{\frac{\gamma-1}{\gamma}} - 1\right] n_{12}$$

$$I\,\dot{\omega}_{37} = \tau_c - \tau_{36}$$

$$\tau_{36} = (P_{16}^* - P_{15}^*)\,K_p$$

Fig. 14. Symbology and sample equations for the blower. The processes occur between points 15, 37 and 16 on Fig. 2. K_p is the pump pressure reaction coefficient. Arrows indicate the direction of assigned positive flow.

Molecular Diffusion – We account for molecular diffusion of gases between the canopy and the chamber air. Fig. 16 illustrates diffusion of water vapor between points 1 and 2 (the substomatal cavity). The diffusion resistance represents the sum of boundary layer and stomatal resistance. Boundary layer resistance varies with wind speed [46]. The stomatal resistance is different for the different molecules in the atmosphere [47] and varies as a function of canopy temperature, ambient relative humidity, canopy carbon dioxide concentration, and canopy water potential [48]. Stomatal and boundary layer resistances are defined as overall canopy level resistances. The molar flow rate (n_2) is proportional to the difference between specific humidity at point 2 and at point 1.

We account for resistance to diffusion through the mesophyll cells for gases and, for carbon dioxide, the resistance associated with the carboxylation reaction [47,

49, 50]. The process is illustrated in Fig. 17 for carbon dioxide. The molar flow rate (n_{39}) is proportional to the difference between carbon dioxide concentration at point 2 and point 46.

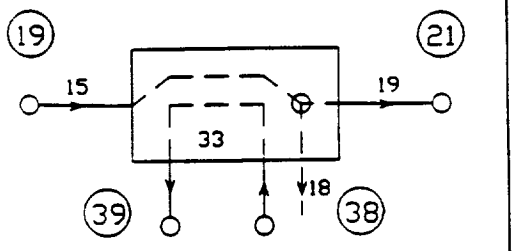

$$\frac{T_{19} - T_{39}}{T_{21} - T_{38}} = \exp\left[\frac{U A_s}{n_{18} c_{p18}} \left(1 - \frac{n_{18} c_{p18}}{n_{33} c_{p33}}\right)\right]$$

$$\dot{H}_{18}^{\circ} = \dot{H}_{19}^{\circ} + \dot{Q}_{33} + \dot{H}_{18}^{\circ}$$

$$n_{19} = n_{19dr} + n_{19A_2^{\circ}}$$

$$n_{18} = n_{18dr} + n_{18A_2^{\circ}}$$

$$n_{18} = n_{18A_2^{\circ}}$$

$$n_{19A_2^{\circ}} = n_{18A_2^{\circ}} - n_{18}$$

$$n_{19dr} = n_{18dr}$$

Fig. 15. Symbology and sample equations for the heat exchanger. The processes are illustrated for the heat exchanger between point 19 and 21 on Fig. 2. Arrows indicate the direction of assigned positive flow.

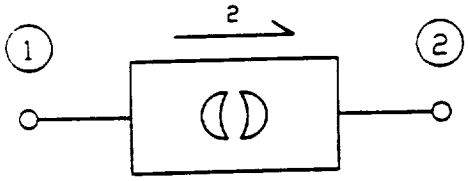

$$n_2 = \frac{\rho_{air,1} A_c (q_1 - q_2)}{MW_{air,1} (r_a^{\circ} + r_s^{\circ})}$$

Fig. 16. Symbology and sample equation for molecular diffusion of gases between the plant canopy and the chamber air. The process is illustrated for water vapor diffusion between point 1 and point 2 on Fig. 2. Arrows indicate the direction of assigned positive flow.

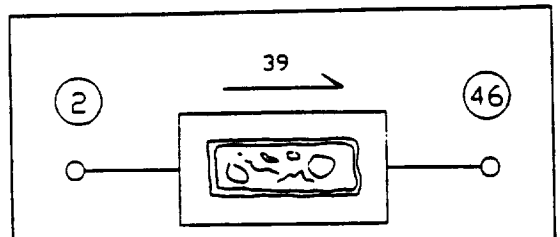

$$n_{39} = \frac{K A_c \rho_{co_2,1} (c_2 - c_{46})}{r_i}$$

Fig. 17. Symbology and sample equation for diffusion through the mesophyll and resistance associated with the carboxylation reaction. The process is illustrated for carbon dioxide between point 2 and point 46. Arrows indicate the direction of assigned positive flow.

Water Transport – We account for water transport through the plant from the point designated as an internal water pool (source) to water vapor in the substomatal cavity. The process is illustrated in Fig. 18. The molar flow rate (n_{38}) is proportional to the water potential difference between points 2 and 44.

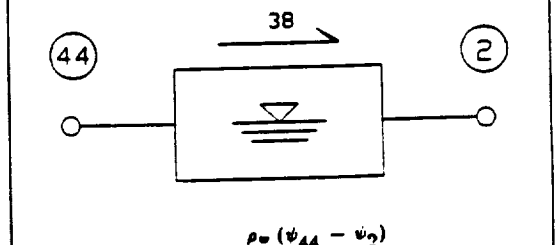

$$n_{38} = \frac{\rho_w (\psi_{44} - \psi_2)}{R_w}$$

Fig. 18. Symbology and sample equation for water transport through the plant. The process is illustrated for transport from point 44 to point 2. Arrows indicate the direction of assigned positive flow.

Convective Heat Transfer – We account for convective heat transfer between surfaces in the chamber and the chamber air. Fig. 19 illustrates convective heat transfer between the plant canopy and the upper chamber air. The convective heat transfer rate ($\dot{Q}_2$) is proportional to the temperature difference between point 1 and point 2. A similar process occurs between points 1 and 4i and points 5 and 7i.

Radiative Heat Transfer – We account for radiative heat transfer between surfaces in the chamber. Fig. 20 illustrates radiative heat transfer between the plant canopy and the upper chamber walls. The radiative heat

transfer rate ($\dot{Q}_{40}$) is proportional to the difference between the fourth power of temperature at point 2 and the fourth power of temperature at point 4i.

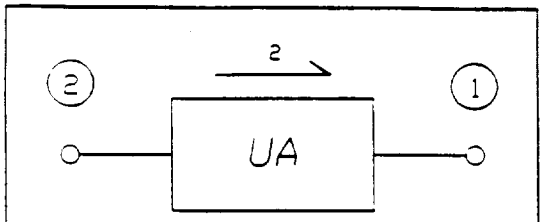

$$\dot{Q}_2 = \dot{h}_c A_c (T_2 - T_1)$$

Fig. 19. Symbology and sample equation for convective heat transfer. The process is illustrated for convective heat transfer between the plant canopy, point 2, and the upper chamber air, point 1. Arrows indicate the direction of assigned positive flow.

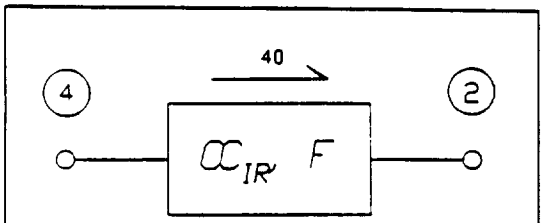

$$\dot{Q}_{40} = K_{r4.2}\ \sigma\ (T_4^4 - T_2^4)$$

Fig. 20. Symbology and sample equation for radiative heat transfer. The process is illustrated for radiative heat transfer between the plant canopy, point 2, and the upper chamber surfaces, point 4. Arrows indicate the direction of assigned positive flow.

Absorption of PAR – We account for absorption of photosynthetically active radiation (PAR) by the plant canopy. Fig. 21 illustrates absorption by the plant canopy (point 2) of PAR from the visible light energy at point 45.

Bound Energy – We account for PAR energy absorbed but not used in photosynthesis, energy present in chemical bonds as a result of photosynthesis and the energy released as a result of respiration. The energy associated with the inorganic materials at point 2 are related to the energy associated with the organic materials at point 46 through the photosynthetic and respiration processes. Some of the PAR absorbed is not used for photosynthesis and becomes part of the energy storage at point 2. The energy released as a function of photorespiration and maintenance respiration becomes part of the energy storage at point 2. Canopy data for wheat in a CELSS can be found in [13]. The process for gross photosynthesis (without photorespiration) is illustrated in Fig. 22.

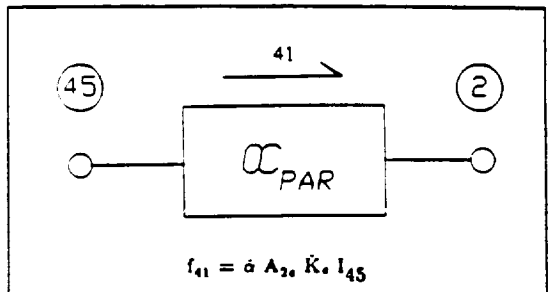

$$f_{41} = \acute{\alpha}\ A_{2e}\ \acute{K}_e\ I_{45}$$

Fig. 21. Symbology and sample equation for absorption rate of photosynthetically active radiation (PAR). Effective canopy area is used since all leaves are not equally illuminated. Average energy content of photosynthetic photons from [13, 42, 51]. Incident PAR above the canopy includes PAR emitted from all sources as well as direct and indirect sources and scattered PAR [44]. Arrows indicate the direction of assigned positive flow.

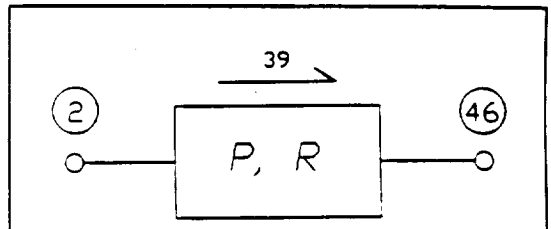

$$f_{39} = \frac{\beta_0\ f_{41}}{\beta + \acute{\alpha}\ \acute{K}_e\ I_{45}}$$

$$\beta_0 = \beta_1 \exp(-\beta_2/T_2)$$

Fig. 22. Symbology and sample equations for rate of transformation of energy to/from organic chemical bonds. The process is illustrated for photosynthesis. Average energy content of photosynthetic photons from [13, 42, 51]. Incident PAR above the canopy includes PAR emitted from all sources as well as direct and indirect sources and scattered PAR [44]. Maximum rate and half saturation constants are functions of carbon dioxide concentration [44]. Arrows indicate the direction of assigned positive flow.

Modulated Sources – We account for modulated sources. Sources are devices which are capable of delivering energy to a system from a location external to it. Sources are considered to deliver a variable to the system in a prescribed manner. A dependent source is one in which that source variable is a function of another independent

variable. The second independent variable is termed the modulating variable [38]. No energy is drawn from the port of the modulating variable. A modulated source is illustrated in Fig. 23. An enthalpy flow rate, $\dot{H}_2^\circ$, occurs between point 1 and 2. The enthalpy flow rate is a function of the modulating variables n_2, the molar flow rate in path 2, and h_2, the specific enthalpy at point 2.

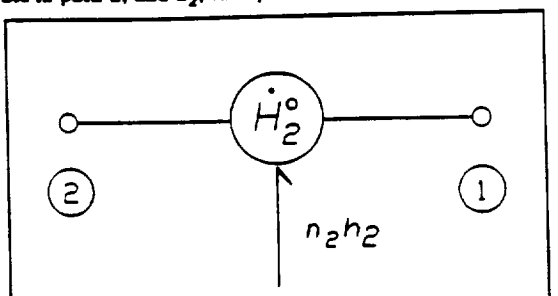

$$\dot{H}_2^\circ = n_2\ h_2$$

Fig. 23. Symbology and sample equation for a modulated source. The process is illustrated for a modulated enthalpy flow rate source between points 1 and 2. The enthalpy flow rate in path 2 is a flow source which depends upon molar flow rate in path 2 and the specific enthalpy at point 2. Arrows indicate the direction of assigned positive flow.

STRUCTURAL RELATIONSHIPS – The symbols for each of the processes which were developed in the previous section are used in the formulation of the modeling diagram for the system. The modeling diagram describes the manner in which those processes which were previously described interact. Whereas the same process may occur at many points and is generic to many physical systems, the structure of the modeling diagram represents a process interaction which is unique to the system being modeled. When the process symbols are linked at the appropriate structural points, two modeling diagrams are produced: one which represents the molar component and one which represents the energy component of the system.

The molar component modeling diagram is shown in Fig. 24. The continuity principle is used to write the equations at each point, i.e. the sum of the molar flow rates into a point is equal to the sum of the molar flow rates out of a point. Examples are:

At point 35,

$$n_3 + n_{31} + n_{32} = n_1$$

At point 3,

$$n_1 = n_1$$

and

At point 1,

$$n_1 + n_2 = n_3 + \dot{n}_{Cn1}.$$

The energy component modeling diagram is shown in Fig. 25. The energy conservation principle is used to write the equations at each point, i.e. the sum of the energy flows into a point is equal to the sum of the energy flows out of a point. Examples are:

At point 35,

$$\dot{H}_{30}^\circ + \dot{H}_{31}^\circ + \dot{H}_{32}^\circ = \dot{H}_1^\circ$$

At point 3,

$$\dot{H}_1^\circ = \dot{H}_1^\circ$$

and

At point 1:

$$\dot{H}_1^\circ + \dot{H}_{22}^\circ + \dot{Q}_2 + \dot{Q}_4 - P_1 \dot{V}_1 = \dot{H}_3^\circ + \dot{E}_{Ca1}.$$

Since we assume that there is no heat transfer, no energy storage, and no work done in the ducts, there is no change in enthalpy through flow paths 5, 6, and 7. Consequently, enthalpy flow rate between points 5 and 12 is designated as $\dot{H}_5^\circ$. Similarly flow path 1, flow paths 16 and 12, path 23, and paths 25 and 31 represent constant enthalpy processes.

CONTROL INPUTS – The variables which are independent of the system and are available to be arbitrarily determined as a function of time or as a function of the system variables are designated control variables. They are chamber lighting, chamber wall temperatures, valve orifice flow areas, gas flow rates out, gas flow rates in, and blower motor torque.

DISTURBANCES – Disturbances may take the form of variables which are independent of the system internal variables but may not be arbitrarily determined (such as chamber volume changes due to glove port use) or changes in system parameters due to aging, etc.

SYSTEM EQUATIONS – The constitutive relationships (processes) and structural equations form the set of algebraic and dynamic primitive equations which together describe the linked thermal and fluid dynamic behavior of the plant growth chamber and the atmospheric control system of the Crop Growth Research Chamber. Pressures and temperatures can be related to the potentials at each point on the molar component and energy component diagrams, respectively. The molar and energy flow and storage process representations shown in the proceeding are symbolic in that in the actual representation accounting for molar flow and storage by species is necessary. The equations can be written in terms of the partial pressures of each atmospheric component, total pressures, mass or molar flow rates (hence velocities, transpiration rates, etc.), air temperatures, plant canopy temperature, etc.

The equations, in state variable form, can be used to analyze system properties such as: (1) location of equilibrium points, (2) stability at equilibrium points, (3) stability robustness at stable equilibrium points, (4) controllability, and (5) observability. The state variable form of the equations, formatted to include system uncertainties and disturbances, can be used to seek robust control algorithms. If analysis of the system model indicates that the properties of the system are unsatisfactory such that robustness cannot be achieved or can only be achieved at unacceptable cost of some other performance measure, a proposed alteration to the system structure may be required. The model of a proposed reconfiguration can developed by reformulating the structural relationships of the process models to conform to structure implied by the altered configuration.

C-2

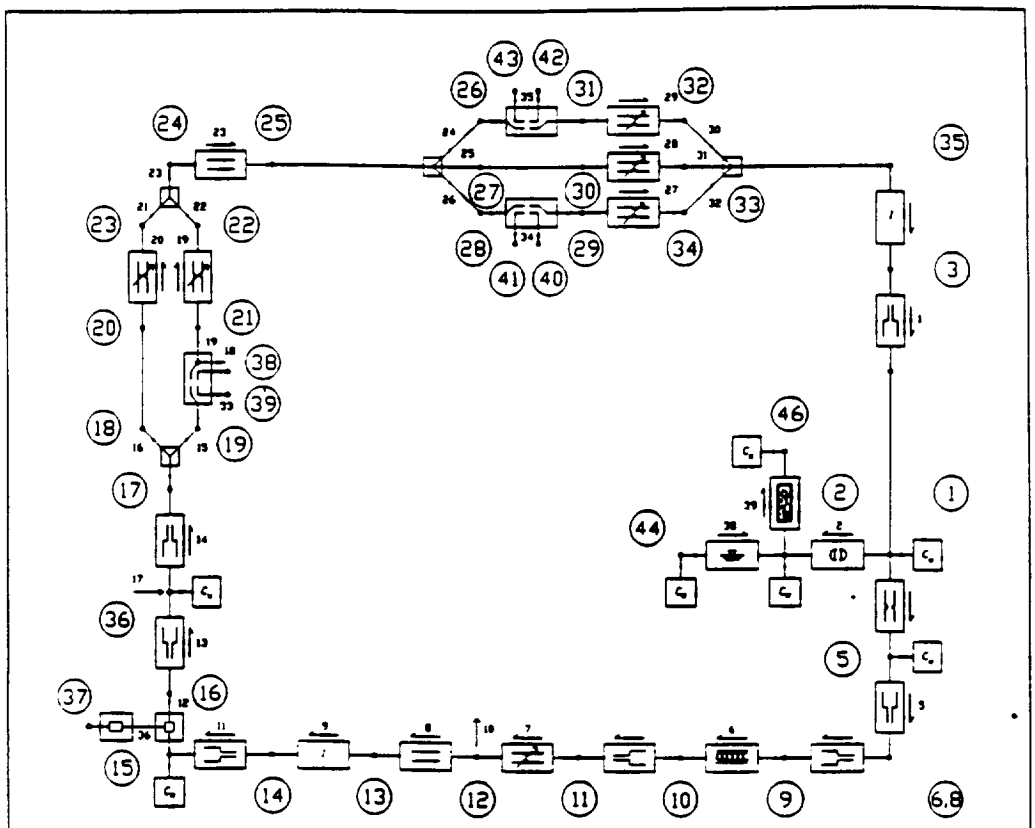

Fig. 24. Molar component of the modeling diagram of the Plant Growth Chamber and atmospheric control system of the Crop Growth Research Chamber. Points and flow paths correspond to those indicated on Fig. 2. Modeling symbols are defined in Figs. 3 through 23.

Additional process models can be added if required by the altered configuration.

CONCLUDING REMARKS

We have presented a symbology for an organized approach to the derivation of the equations which describe the dynamic behavior of a plant growth chamber with closure. We have illustrated the linkage between the model of the physical system components and the model of the biological component. As previously noted, several assumptions were made to reduce the complexity of the system for the purpose of demonstrating the modeling procedure. Additional processes, such as those affecting crop shoot-root interactions, would be added in order to model the behavior of the system in response to root zone environment disturbances and control inputs. Processes which affect longer term phenomena, such as biomass production, would be added to model system behavior over a growth cycle.

It is characteristic of the system control problem to employ simplified models for the purpose of controller synthesis. These models typically (a) employ functionally more simple (linear, usually) representations of process behavior and (b) do not describe all stable dynamics. Historically, this strategy has been remarkably successful because implementation of feedback control can render a system robust to a variety of perturbations. Computer simulations, based on more comprehensive and nearly complete models which at least include the most significant nonlinearities, are most useful to demonstrate controlled system performance. Simulations and the newly emerging perspectives of robust control are crucial for the purpose of assuring performance.

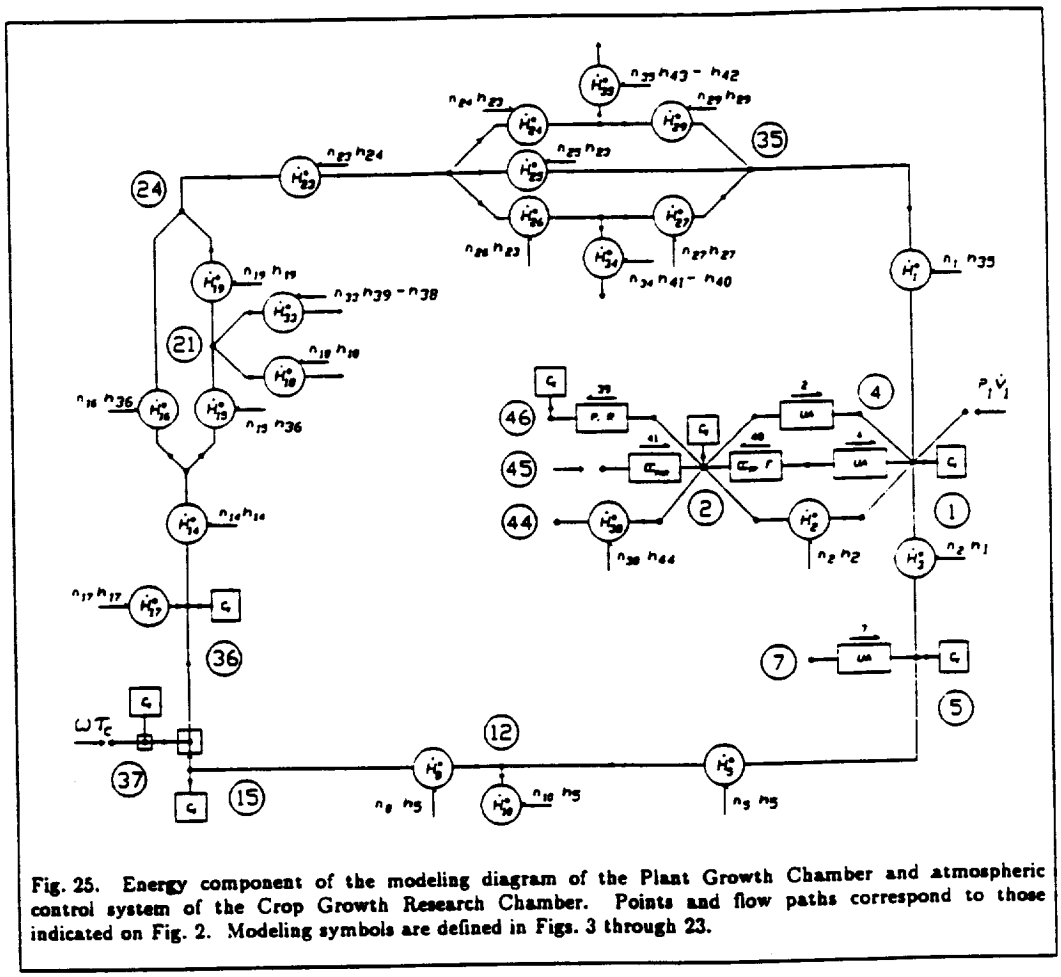

Fig. 25. Energy component of the modeling diagram of the Plant Growth Chamber and atmospheric control system of the Crop Growth Research Chamber. Points and flow paths correspond to those indicated on Fig. 2. Modeling symbols are defined in Figs. 3 through 23.

NOMENCLATURE

A_c	canopy area (m^2)
A_d	effective cross sectional area of the ductwork (m^2)
A_f	duct cross sectional area in flow path i (m^2)
A_i	area of surface i (m^2)
A_s	heat transfer area (m^2)
A_{2c}	total effective canopy area for short wave absorption (m^{-2})
air	dry air
c_j	mole fraction of carbon dioxide at point j
$\bar{c}_{p_i}$	molar specific heat in path i (Joules mol^{-1} K^{-1})
co_2	carbon dioxide
D	duct diameter (m)
$\dot{E}_i$	rate of energy accumulation at point i (watts)
$F_{i,j}$	radiative shape factor between surfaces i and j
f	friction factor
f_{39}	photosynthetic rate (watts)
f_{41}	PAR absorption rate (watts)
$\dot{H}_i^\circ$	total enthalpy flow rate in path i (watts)
$\bar{h}_c$	canopy convective heat transfer coefficient (watts m^{-2} K^{-1})
h_j	specific enthalpy at point j (Joules mol^{-1})
h_2o	water - liquid or vapor (in context)

I	moment of inertia of motor and impeller (kg m^2)
I_{45}	incident PAR above canopy (μmol m^{-2} sec^{-1})
KA_e	effective area for diffusion in the canopy (m^2)
$\dot{K}_e$	average energy content of photosynthetic photons (J μmol^{-1})
K_p	pump pressure reaction coefficient
$K_{r_{ij}}$	radiative heat transfer coefficient (m^{-2}) $K_{r_{ij}} = K_{r_{ij}}(F_{ij}, \epsilon_i, \epsilon_j, A_i, A_j)$
L	effective duct length (m)
$MW_{air,1}$	molecular weight of dry air in chamber (g mol^{-1})
MW_d	molecular weight of air in the ductwork (g mol^{-1})
n_i	molar flow rate in path i (moles sec^{-1})
n_2	nitrogen
o_2	oxygen
$P_1 \dot{V}_1$	work done by the system (watts)
P_j	pressure at point j (Pa)
P_j^*	total pressure at point j (Pa)
PPF	photosynthetic photon flux (μmol m^{-2} sec^{-1})
$\dot{Q}_i$	heat transfer rate in path i (watts)
q_j	humidity ratio at point j
R	universal gas constant (Joules mol^{-1} K^{-1})
R_w	internal fluid resistance (n m sec^{-1})
r_a^w	water vapor boundary layer resistance (sec m^{-1})
r_i	mesophyll resistance (sec m^{-1})
r_s^w	water vapor stomatal resistance (sec m^{-1})
T_j	temperature at point j (K)
U	overall heat transfer coefficient (Joules m^{-2} K^{-1})
V_1	volume of the upper chamber (m^3)
$\dot{\alpha}$	canopy average short wave absorption coefficient
β	PPF half saturation constant (watts m^{-2})
β_0	maximum photosynthetic rate as PPF$\Rightarrow\infty$ for given carbon dioxide concentration (watts m^{-2})
β_1	constant (watts m^{-2})
β_2	constant (K)
γ	ratio of molar specific heats
ϵ_j	emissivity for surface j
η_p	pump efficiency
ψ_j	water potential at point j (Pa)
$\rho_{air,1}$	density of dry air in the chamber (g m^{-3})
$\rho_{co_2,1}$	chamber carbon dioxide molar density (mol m^{-3})
ρ_j	air density at point j (kg m^{-3})
ρ_w	molar density of water
σ	Stephan-Boltzmann constant (watts m^{-2} K^{-4})
τ_e	motor torque input (n m)
ω_i	blower motor speed (rad sec^{-1})

ACKNOWLEDGEMENT

This work was partially supported by a NASA - ASEE Summer Faculty Fellowship at Stanford University - NASA Ames Research Center awarded to A. L. Blackwell.

REFERENCES

[1] MacElroy, R. D., and D. T. Smernoff, eds. 1987. Controlled ecological life support system: regenerative life support systems in space. NASA CP 2480.

[2] Blackwell, A. L. 1989. A perspective on CELSS control issues. In Proceedings of the CELSS '89 Workshop. In press.

[3] CELSS Research Program. (No date). Crop growth research chamber: plan for the development of equipment for research on higher plant growth for the CELSS program: rationale, design, fabrication, testing and utilization. NASA document.

[4] MacElroy, R. D., D. T. Smernoff, and J. D. Rummel, eds. 1987. Controlled ecological life support system: design, development, and use of a ground-based plant growth module. NASA CP 2479.

[5] Tremor, J., and D. L. Bubenheim. In prep. CELSS laboratory scale plant growth equipment design workshop. Tiburon, CA. 14-16 June 1988.

[6] Bubenheim, D. L. 1989. The Crop Growth Research Chamber: a ground based facility for CELSS research. In Proceedings of the CELSS '89 Workshop. In press.

[7] Prince, R. P., W. M. Knott, J. C. Sager, and S. E. Hilding. 1987. Design and performance of the KSC biomass production chamber. Seventeenth Intersociety Conference on Environmental Systems, 13-15 July 1987. Seattle, WA. SAE Paper No. 87-1437.

[8] Prince, R. P., W. M. Knott, J. C. Sager, and J. D. Jones. 1988. Engineering verification of the KSC biomass production chamber. Paper No. LBS-88-096 in Symposium on Lunar Bases and Space Activities in the 21st Century. Houston, TX. 5-7 April 1988.

[9] Jones, P., J. W. Jones, L. H. Allen, Jr., and J. W. Mishoe. 1984. Dynamic computer control of closed environmental plant growth chambers. Design and verification. Transactions of the ASAE 27(3):879-888.

[10] Meyer, G. E., J. A. Lamb, and W. E. Splinter. 1984. Crop moisture stress analysis using computer-controlled environmental chambers and simulated weather sequences. Transactions of the ASAE 27:1862-1870.

[11] Parsons, J. E., J. L. Dunlap, J. M. McKinion, C. J. Phene, and D. N. Baker. 1980. Microprocessor-based data acquisition and control software for plant growth chambers (SPAR system). Transactions of the ASAE 23:589-595.

[12] Phene, C. J., D. N. Baker, J. R. Lambert, J. E. Parsons, J. M. McKinion. 1978. SPAR - a soil-plant-atmosphere research system. Transactions of the ASAE 21(5):924-930.
[13] Bugbee, B. G. 1989. Exploring the limits of crop productivity: a model to evaluate progress. In Proceedings of the CELSS '89 Workshop. In press.
[14] Cole, G. W. 1980a. The application of control systems theory to the analysis of ventilated animal housing environments. Transactions of the ASAE 23:431-436.
[15] Cole, G. W. 1982. A method to predict the performance of mechanically ventilated systems. Transactions of the ASAE 25:419-424.
[16] Hashimoto, Y. 1980. Computer control of short term plant growth by monitoring leaf temperature. Acta Horticulturae 106:139-146.
[17] Willits, D. H., T. K. Karnoski, E. H. Wiser. 1980. A microprocessor-based control system for greenhouse research: Part II - software. Transactions of the ASAE 23:693-698.
[18] Midwest Research Institute. 1981. Solar controlled environment agriculture project. Final report. Volume 2. Battelle Columbus Laboratories System Requirements Definition and System Analysis. MRI/SOL--0800-02. DE86 001286.
[19] Cole, G. W., P. W. McClellan, and J. G. Mannix. 1981. A linear ventilation rate temperature controller for a confined animal housing system. Transactions of the ASAE 23:706-710.
[20] Monteith, J. L., B. Marshall, R. S. Safell, D. Clarke, J. N. Gallagher, P. J. Gregory, C. K. Ong, G. R. Squire, and A. Terry. 1983. Environmental control of a glasshouse suite for crop physiology. J. Exp. Botany 34:309-321.
[21] Mitchell, B. 1986a. Integrated microcomputer-based control system for multiple environmental cabinets. Transactions of the ASAE 29(3):820-823.
[22] Mitchell, B. 1986b. Microcomputer based environmental control system for a disease-free poultry house. Transactions of the ASAE 29(4):1136-1140.
[23] Sager, J. C., C. R. Hargrove, R. P. Prince, and W. M. Knott. 1988. CELSS atmospheric control system. ASAE summer meeting, 26-29 June 1988. Rapid City, SD. Paper No. 88-4018.
[24] Doyle, J. C. 1982. Analysis of feedback systems with structured uncertainty. IEE Proceedings. D-129(6):242-250.
[25] Athans, M. 1986. A tutorial on the LQG/LTR method. Proceedings of the American Control Conference (2):1289-1296. Seattle, WA.
[26] Horowitz, I. 1982. Quantitative feedback theory. IEE Proceedings. D-129(6).
[27] Utkin, V. I. 1984. Variable structure systems: present and future. Automation and Remote Control 44:1105-1120.
[28] Corless, M., and G. Leitmann. 1988. Controller design for uncertain systems via Lyapunov functions. Proceedings of the Automatic Control Conference (4):2019-2024, Atlanta.
[29] Blackwell, A. L., C. C. Blackwell, R. H. Kila, and T. Vecera. 1987. Management strategies under uncertainty: a demonstration of LFGG robust control in a CELSS scenario. pp 8-9 in Space Life Sciences Symposium: Three Decades of Life Science Research in Space. Washington, DC. Office of Space Science and Applications, National Aeronautics and Space Administration. 400 pp.
[30] Blackwell, A. L., and C. C. Blackwell. 1988. A robust control strategy for uncertain plant growth in a CELSS. Abstracts of the Controlled Environmental Life Support Systems Research Conference. College Station, TX.
[31] Fan, L. T., Y. S. Hwang, and C. L. Hwang. 1970. Applications of modern optimal control theory to environmental control of confined spaces and life support systems. Part 1 - Modeling and simulation. Building Science 5:57-71.
[32] Nakanishi, E., N. C. Pereira, L. T. Fan, and C. L. Hwang. 1973. Simultaneous control of temperature and humidity in a confined space. Part 1 - Mathematical modeling of the dynamic behavior of temperature and humidity in a confined space. Building Science 8:39-49.
[33] Bot, G. P. A. 1980. Validation of a dynamical model of greenhouse climate. Acta Horticulturae 106:149-155.
[34] Kindelan, M. 1980. Dynamic modeling of greenhouse environment. Transactions of the ASAE 23:1232-1239.
[35] Cole, G. W. 1980b. The derivation and analysis of the differential equations for the air temperature of the confined animal housing system. Transactions of the ASAE 23:712-720.
[36] Chandra, P., L. D. Albright, and N. R. Scott. 1981. A time dependent analysis of greenhouse thermal environment. Transactions of the ASAE 24:442-449.
[37] Arinze, E. A., G. J. Schoenau, and R. W. Besant. 1984. A dynamic thermal performance simulation model of an energy conserving greenhouse with thermal storage. Transactions of the ASAE 26:508-519.
[38] Shearer, J. L., A. T. Murphy, and H. H. Richardson. 1967. Introduction to system dynamics. Addison-Wesley, Reading, MA. 420 pp.
[39] Dorf, R. C. 1989. Modern control systems. Addison-Wesley, Reading, MA. 603 pp.
[40] Takahashi, Y., M. J. Rabins, D. M. Auslander. 1970. Control and dynamic systems. Addison-Wesley, Reading, MA. 800 pp.
[41] Beaman, J. J., and P. C. Breedveld. 1988. Physical modeling with Eulerian frames and bond graphs. Transactions of the ASME Journal of Dynamic Systems, Measurements, and Control 110:182-188.
[42] Bubenheim, D. L., B. Bugbee, and F. B. Salisbury. 1988. Radiation in controlled environments: influence of lamp type and filter material. J. Amer. Soc. Hort. Sci. 113:468-474.
[43] Reynolds, J. F., and B. Acock. 1985. Modeling approaches for evaluating vegetation responses to carbon dioxide concentration. pp 34-51 in B. R. Strain and J. D. Cure, eds. Direct effects of increasing carbon dioxide on vegetation. DOE/ER-0238. United States Department of Energy, Washington, D. C.

[44] Wann, M., C. D. Raper, Jr., and H. L. Lucas, Jr. 1978. A dynamic model for plant growth: a simulation of dry matter accumulation for tobacco. Photosynthetica 12:121-136.
[45] Cheremisinoff, N. P. 1982. Fluid flow: pumps, pipes, and channels. Ann Arbor Science, Ann Arbor, MI. 702 pp.
[46] Gates, D. M., and L. E. Papian. 1971. Atlas of energy budgets of plant leaves. Academic Press, New York.
[47] Bradley, E. F., and J. J. Finnigan. 1973. Heat and mass transfer in the plant-air continuum. Proceedings of the first Australasian conference on heat and mass transfer. Monash University, Melbourne, Australia.
[48] Jones, H. G. 1983. Plants and microclimate: a quantitative approach to environmental plant physiology. Cambridge Univ. Press, London. 323 pp.
[49] Nobel, P. S. 1983. Biophysical plant physiology and ecology. W. H. Freeman, San Francisco. 608 p.
[50] Charles-Edwards, D. A., D. Doley, and G. M. Rimmington, 1986. Modelling plant growth and development. Academic Press, Sydney.
[51] Bugbee, B. G., and F. B. Salisbury. 1988. Exploring the limits of crop productivity: I. Photosynthetic efficiency of wheat in high irradiance environments. Plant Physiology 88: 869-878.

A2. A brief summary of some of the results obtained in the study; A. L. Blackwell and C. C. Blackwell. 1990. Development of a model for control of the NASA CELSS Crop Growth Research Chamber. *Proceedings of the 1990 American Control Conference*. San Diego, California, USA 23 - 25 May, 3:2113-2114.

DEVELOPMENT OF A MODEL FOR CONTROL OF THE NASA CELSS CROP GROWTH RESEARCH CHAMBER

A. L. Blackwell and C. C. Blackwell

The Center for Dynamic Systems Control Studies, Department of Mechanical Engineering
The University of Texas at Arlington, Arlington TX 76019.

ABSTRACT

In support of development of bioregenerative life support systems for space habitats, a chamber for conducting research on the biophysical response of crop plants in controlled environments is being designed by the National Aeronautics and Space Administration. The imprecision of mathematical descriptions of the behavior of biological systems led to the development of a model which can be used to derive a strategy for control of the chamber environment which is robust to the system uncertainties. The modeling approach and observations of the characteristics of the model are described.

INTRODUCTION

Regenerative life support systems are judged to be essential to success of mission scenarios contemplated by the Office of Exploration of the National Aeronautics and Space Administration (NASA). A higher degree of material closure than that provided by physiochemical life support technology is considered necessary for some scenarios. [1] A means of providing greater closure is through use of a bioregenerative life support system, i.e. one in which the production of food, the replenishment of oxygen and removal of carbon dioxide from the atmosphere and the production of fresh water is provided by higher plants and/or algae in conjunction with physiochemical systems.

To conduct experiments on the biophysical responses of higher plants from seed to maturation in closed environments, a crop growth research chamber (CGRC) [2] is being developed at the NASA Ames Research Center under the Controlled Ecological Life Support System (CELSS) program. [3] Stringent control of all environmental variables (e.g. lighting, temperature, atmospheric oxygen, carbon dioxide concentrations, humidity and pressure, nutrient solution temperature, ion and dissolved oxygen concentrations and pressure) which affect the production of biomass, oxygen, and transpired water vapor, and the consumption of carbon dioxide, liquid water, and nutrients by the plants will be required. Knowledge of the autecology of crop plant populations derived from CGRC research will permit utilization of the CELSS plant growth unit as a multiple input-multiple output life support system component whose function and performance can be varied as required through application of appropriate control strategies.

SYSTEM DESCRIPTION

The CGRC differs from other plant growth chambers (references in [4]) in size, degree of material closure, performance requirements, and number of controlled environmental variables (Table 1). Uncertainties in the CGRC system are most manifest in the living component. The inherent variability of biological systems makes the task of precise mathematical description of their behavior difficult. The bounds set on the required performance of the system, coupled with the uncertainties arising from the imprecision in knowledge of functional forms and parameters describing plant biophysical ecology, have led us to seek a strategy for control of the chamber environment which is robust to the system uncertainties using Lyapunov theory based methods [5]. In this paper we describe the development of a modeling structure consistent with the derivation of such controllers.

MODELING APPROACH

The model includes the linkages between the physical system components and the biological components. Tentative physical component sizes were based upon lighting, pressure, phase and temperature rise constraints and the proposed physical configuration of the chamber (Fig. 1). Assuming that the chamber contained a full canopy of a nearly mature crop of wheat (Yecora Rojo) under fully lighted conditions, essentially all the photosynthetically active radiant energy from the lights was considered absorbed by the plants. A large fraction (5/6) was assumed converted into sensible heat, raising the canopy temperature slightly above that of the nominal ambient chamber air, the remainder used in evaporating water internal to the plant canopy and subsequently transpired. The fraction of energy fixed in photosynthesis or released in metabolism was considered sufficiently small to neglect in the energy balance for short term dynamics. The plant canopy was modeled as temperature and vapor and gas exchange disturbances. A description of the physical system and the modeling system used to derive the constitutive and structural relationships describing the processes occurring in the shoot zone of the plant growth chamber is developed in [4].

The primitive system equations for the nominal model (i.e. without uncertainties)

$$A_1 \dot{\eta} = A_2 \eta + A_3 \sigma + A_4 u + A_5 d$$

$$B_1 \sigma + B_2 \eta + B_3 u + B_4 d = 0 \qquad (1)$$

were derived by linearizing the process equations about an equilibrium point calculated by setting conditions in the chamber at values within the required operating envelope. The nominal linear time invariant state variable form

$$\dot{x} = F x + G u + E d$$

$$y = C x + D u + H d \qquad (2)$$

was derived from (1) according to [6]. The 19 natural variable system states consist of the molar compositions and temperatures of the air in the upper and lower sections of the chamber and in the ducts, blower motor speed, molar flow rate in the ducts and upper chamber volume. The 11 control variables are described in terms of valve loss coefficients, blower motor control torque, and gas injection and extraction rates. The 8 disturbance variables are plant canopy temperature and gas exchange rates, chamber wall temperatures, gas injection temperature and chamber volume changes due to glove port utilization.

PRECEDING PAGE BLANK NOT FILMED

OBSERVATIONS

Some initial observations of the properties of the nominal linear model relevant to control design are discussed below.

a. Utilization of the SVD in MATLAB indicated that, for the scenario modeled, B_1 is poorly conditioned. The values of some eigenvalues of F are quite sensitive to the method used for matrix inversion in the equation reduction procedure. Equation reduction from primitive to state variable form was performed using MATLAB.

b. Of the 19 eigenvalues, 3 are positive real, 5 are negative real, one is zero, the others are complex with negative real parts. All pairs except one have damping ratios (ζ) greater than 0.7.

c. The system was transformed to modal form. Examination of the real Jordan matrix inverse revealed that most modes are primarily influenced by rational groups of natural variables. For example, the molar quantity of water vapor throughout the system (i.e. in the upper chamber, lower chamber, and in the ducts) predominantly influences the most unstable mode and one complex mode; chamber volume predominantly influences the second most unstable mode and a second complex mode; molar quantity of carbon dioxide throughout the system predominantly influences the least unstable mode and a third complex mode. The magnitudes of the three complex modes differ by less than 1%.

d. All modes other than that associated with chamber volume are controllable. All modes are vulnerable to the disturbances.

e. Placement of the largest stable eigenvalue (dominated by system oxygen concentration) from the open loop value of $-0.257E{-}6$ to -1.0 was achieved by linear feedback of only the state variables representing oxygen and system volume without affecting more than the fifth significant figure of any of the other eigenvalues.

CONTINUING DEVELOPMENT

A parameterized linear model is being developed to accommodate potential variations in proposed CGRC design configuration. Bounds on the values for the uncertainties associated with the crop dynamics will be obtained from CELSS crop physiologists. Bounds on the values for the uncertainties associated with the physical system will be obtained from the NASA Ames Research Center CGRC engineering team. Computer simulations of the nonlinear system equations are being developed. The simulations will be used to conduct scenario studies to evaluate system performance with various candidate control strategies.

TABLE 1. Operating ranges and tolerance requirements for the atmospheric variables in the shoot zone of the plant growth chamber of the NASA CELSS Crop Growth Research Chamber.

Air temperature	5-40° C ± 1° C
Relative humidity	35-90% ± 2%*
Carbon dioxide	25-50000 ppm ± 5%*
Oxygen	5-25% ± 5%*
Nitrogen	75-95% ± 5%*
Gage pressure	47 mm Hg ± 5 mm Hg
Air velocity	0.1-1 m sec^{-1} ± .1 m sec^{-1}
Photosynthetic photon flux	0-3000 μmoles m^{-2} s^{-1} ± 10 μmoles m^{-2} s^{-1}
Surface temperatures	Air temperature + 2° C

* tolerance as % of set point value

ACKNOWLEDGEMENT

This research was supported by NASA-ASEE Summer Faculty Fellowships at Stanford University - NASA Ames Research Center awarded to ALB and CCB.

REFERENCES

[1] D. A. O'Handley, "Human pathway to the solar system in the 21st century," SAE Technical Paper 891430. *19th Intersociety Conference on Environmental Systems*, San Diego, CA, 1989.

[2] D. L. Bubenheim, P. M. Luna, M. Haslerud, K. M. Wagenbach, and C. L. Straight, "The Crop Growth Research Chamber: a ground based facility for CELSS research," SAE Technical Paper 891588. *19th Intersociety Conference on Environmental Systems*, San Diego, CA, 1989.

[3] R. D. MacElroy and D. T. Smernoff, eds., "Controlled ecological life support system: regenerative life-support systems in space," NASA CP 2480, 1987.

[4] A. L. Blackwell and C. C. Blackwell, "A modeling system for control of the thermal and fluid dynamics of the NASA CELSS Crop Growth Research Chamber," SAE Technical Paper 891570. *19th Intersociety Conference on Environmental Systems*, San Diego, CA, 1989.

[5] M. Corless and G. Leitmann, "Controller design for uncertain systems via Lyapunov functions," *Proceedings of the Automatic Control Conference*, pp. 2019-2024, Atlanta, GA, 1988.

[6] C. C. Blackwell, "On generating state space equations of a linear constant coefficient system," *Journal of Optimization Theory and Applications*, pp. 65-79, 1986.

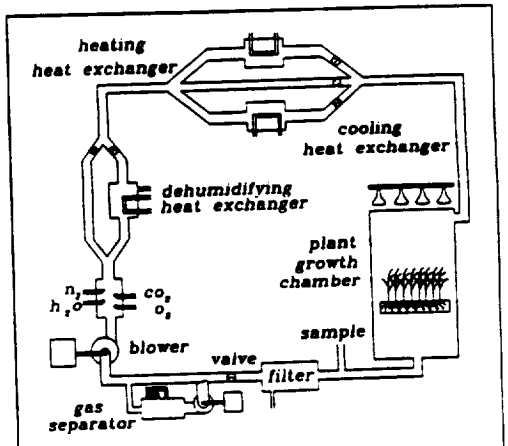

Fig. 1. Plant growth chamber and candidate atmospheric control system for the NASA CELSS CGRC.

APPENDIX A.3:

THE LINEAR STATE VARIABLE REPRESENTATION COEFFICIENT MATRICES

```
APL  =
   1.0D+05 *
    Columns  1 thru  4
  -0.002424541202636  -0.015584615000000  -0.015584615000000  -0.015584615000000
   0.000007428647359  -0.104167521885820  -0.104155231885820  -0.104155231885820
   0.000002400532336  -0.033657271994475  -0.033669561994475  -0.033657271994475
   0.000000012012662  -0.000168286354972  -0.000168286354972  -0.000180581104972
   0.000000158817643  -0.002257842025046  -0.002257842025046  -0.002257842025046
   0.000000886999249  -0.047268854535376  -0.047268854535376  -0.047268854535376
   0.000000000000000   0.104167521885820   0.104155231885820   0.104155231885820
   0.000000000000000   0.033657271994475   0.033669561994475   0.033657271994475
   0.000000000000000   0.000168286354972   0.000168286354972   0.000180581104972
   0.000000000000000   0.002257842025046   0.002257842025046   0.002257842025046
   0.000000000000000  -0.139011870881306  -0.139011870881306  -0.139011870881306
   0.000000000000000   0.000000000000000   0.000000000000000   0.000000000000000
  -0.000007473646694   0.000000000000000   0.000000000000000   0.000000000000000
  -0.000002399467664   0.000000000000000   0.000000000000000   0.000000000000000
  -0.000000012002662   0.000000000000000   0.000000000000000   0.000000000000000
  -0.000000161035711   0.000000000000000   0.000000000000000   0.000000000000000
  -0.000071705926065   0.000000000000000   0.000000000000000   0.000000000000000
   0.000000000000000   0.000000000000000   0.000000000000000   0.000000000000000
   0.000000000000000   0.000000000000000   0.000000000000000   0.000000000000000
    Columns  5 thru  8
  -0.015584615000000  -0.004425979500000   0.000000000000000   0.000000000000000
  -0.104155231885820  -0.029582335980663   0.306365761428881   0.306365761428881
  -0.033657271994475  -0.009559392265193   0.099000649983750   0.099000649983750
  -0.000168286354972  -0.000047796961326   0.000495003249919   0.000495003249919
  -0.002270129825046  -0.000641275897790   0.006641293603077   0.006641293603077
  -0.047268854535376  -0.013465337587892   0.139026042751107   0.139026042751107
   0.104155231885820   0.029582335980663  -0.306375061428881  -0.306338921428881
   0.033657271994475   0.009559392265193  -0.098991976983750  -0.099028119983750
   0.000168286354972   0.000047796961326  -0.000494960009919  -0.000494960009919
   0.002270129825046   0.000641275897790  -0.006640711803077  -0.006640711803077
  -0.139011870881306  -0.039428269392866   0.408858443768547   0.408858443768547
   0.000000000000000   0.000000000000000   0.045837102941176   0.045837102941176
   0.000000000000000   0.000000000000000   0.000009300000000  -0.000026800000000
   0.000000000000000   0.000000000000000  -0.000008673000000   0.000027470000000
   0.000000000000000   0.000000000000000  -0.000000043360000  -0.000000043360000
   0.000000000000000   0.000000000000000  -0.000000581800000  -0.000000581800000
   0.000000000000000   0.000000000000000   0.000000000000000   0.000000000000000
   0.000000000000000   0.000000000000000   0.000000000000000   0.000000000000000
   0.000000000000000   0.000000000000000   0.000000000000000   0.000000000000000
    Columns  9 thru 12
   0.000000000000000   0.000000000000000   0.000000000000000   0.000000000000000
   0.306365761428881   0.306365761428881   0.029593147410898   0.000000000000000
   0.099000649983750   0.099000649983750   0.009562885927852   0.000000000000000
   0.000495003249919   0.000495003249919   0.000047814429639   0.000000000000000
   0.006641293603077   0.006641293603077   0.000641510264327   0.000000000000000
   0.139026042751107   0.139026042751107   0.013429105647768   0.000000000000000
  -0.306338921428881  -0.306338921428881  -0.029593147410898  -0.000007427000000
  -0.098991976983750  -0.098991956983750  -0.009562885927852  -0.000002400000000
  -0.000531103249919  -0.000494960009919  -0.000047814429639  -0.000000012000000
```

APL(continued)

-0.006640711803077	-0.006676853603077	-0.000641510264327	-0.000000161000000
0.408858443768547	0.408858443768547	0.039441678349110	-0.000009894665308
0.045837102941176	0.045837102941176	0.004427597058824	-0.000489255870000
-0.000026840000000	-0.000026840000000	0.000000000000000	0.000007427000000
-0.000008673000000	-0.000008673000000	0.000000000000000	0.000002400000000
0.000036100000000	-0.000000043360000	0.000000000000000	0.000000012000000
-0.000000581800000	0.000035560000000	0.000000000000000	0.000000161000000
0.000000000000000	0.000000000000000	0.000024575432811	0.000071561445609
0.000000000000000	0.000000000000000	0.000000000000000	-0.000003084020638
0.000000000000000	0.000000000000000	0.000000000000000	0.000000000000000

Columns 13 thru 16

0.031773295283869	0.031773295283869	0.031773295283869	0.031773295283869
0.000006330000000	-0.000018260000000	-0.000018260000000	-0.000018260000000
-0.000005901000000	0.000018690000000	-0.000005901000000	-0.000005901000000
-0.000000029530000	-0.000000029530000	0.000024560000000	-0.000000029530000
-0.000000395800000	-0.000000395800000	-0.000000395800000	0.000025090000000
0.000000000000000	0.000000000000000	0.000000000000000	0.000000000000000
0.000000000000000	0.000000000000000	0.000000000000000	0.000000000000000
0.000000000000000	0.000000000000000	0.000000000000000	0.000000000000000
0.000000000000000	0.000000000000000	0.000000000000000	0.000000000000000
0.000000000000000	0.000000000000000	0.000000000000000	0.000000000000000
0.000000000000000	0.000000000000000	0.000000000000000	0.000000000000000
-0.031773295283869	-0.031773295283869	-0.031773295283869	-0.031773295283869
-0.000006220000000	0.000018370000000	0.000018370000000	0.000018370000000
0.000005901000000	-0.000018690000000	0.000005901000000	0.000005901000000
0.000000029510000	0.000000029510000	-0.000024550000000	0.000000029510000
0.000000395800000	0.000000395800000	0.000000395800000	-0.000024180000000
0.000000000000000	0.000000000000000	0.000000000000000	0.000000000000000
0.000000000000000	0.000000000000000	0.000000000000000	0.000000000000000
0.000000000000000	0.000000000000000	0.000000000000000	0.000000000000000

Columns 17 thru 19

0.004429819765695	0.000000000000000	0.648836700000000
0.000000000000000	0.000000000000000	4.336690953038673
0.000000000000000	0.000000000000000	1.401381215469613
0.000000000000000	0.000000000000000	0.007006906077348
0.000000000000000	0.000000000000000	0.094009323204420
0.000012636792617	0.000000000000000	1.967951572080137
0.000000000000000	0.000000000000000	-4.336690953038673
0.000000000000000	0.000000000000000	-1.401381215469613
0.000000000000000	0.000000000000000	-0.007006906077348
0.000000000000000	0.000000000000000	-0.094009323204420
0.000000000000000	0.000000000000000	5.787502839399791
-0.004429819765695	0.000519274000000	0.000000000000000
0.000000000000000	0.000000000000000	0.000000000000000
0.000000000000000	0.000000000000000	0.000000000000000
0.000000000000000	0.000000000000000	0.000000000000000
0.000000000000000	0.000000000000000	0.000000000000000
-0.000024575432811	0.000000822452196	0.000000000000000
0.000000000000000	-0.000001580805758	0.000000000000000
0.000000000000000	0.000000000000000	0.000000000000000

BPL =

1.0D+04 *

Columns 1 thru 4

0.000000000000000	0.000000000000000	0.000000000000000	0.000000000000000
0.000000000000000	0.000000000000000	0.000000000000000	0.000000000000000
0.000000000000000	0.000000000000000	0.000000000000000	0.000000000000000
0.000000000000000	0.000000000000000	0.000000000000000	0.000000000000000
0.000000000000000	0.000000000000000	0.000000000000000	0.000000000000000
0.000000000000000	0.000000000000000	0.000000000000000	0.000000000000000
0.000000000000000	-0.000074270000000	0.000000000000000	0.000000000000000
0.000000000000000	-0.000024000000000	0.000000000000000	0.000000000000000
0.000000000000000	-0.000000120000000	0.000000000000000	0.000000000000000
0.000000000000000	-0.000001610000000	0.000000000000000	0.000000000000000
0.000000000000000	-0.000098946653075	0.000000000000000	0.000000000000000
-1.339113000000000	-0.004591610000000	0.000000000000000	0.000000000000000
0.000000000000000	0.000074270000000	0.000000000000000	0.000100000000000
0.000000000000000	-0.000076000000000	0.000000000000000	0.000000000000000
0.000000000000000	0.000000120000000	0.000000000000000	0.000000000000000
0.000000000000000	0.000001610000000	0.000000000000000	0.000000000000000
0.000000000000000	0.000000000000000	0.000000000000000	0.000717889530091
0.000000000000000	0.000000000000000	0.000017250000000	0.000000000000000
0.000000000000000	0.000000000000000	0.000000000000000	0.000000000000000

Columns 5 thru 8

0.000000000000000	0.000000000000000	0.000000000000000	-0.105145008041067
0.000000000000000	0.000000000000000	0.000000000000000	0.000000850426248
0.000000000000000	0.000000000000000	0.000000000000000	0.000000274811229
0.000000000000000	0.000000000000000	0.000000000000000	0.000000001374056
0.000000000000000	0.000000000000000	0.000000000000000	-0.000001126611533
0.000000000000000	0.000000000000000	0.000000000000000	-0.000027245020290
0.000000000000000	0.000000000000000	0.000000000000000	0.000000000000000
0.000000000000000	0.000000000000000	0.000000000000000	0.000000000000000
0.000000000000000	0.000000000000000	0.000000000000000	0.000000000000000
0.000000000000000	0.000000000000000	0.000000000000000	0.000000000000000
0.000000000000000	0.000000000000000	0.000000000000000	0.000000000000000
0.000000000000000	0.000000000000000	0.000000000000000	0.000000000000000
0.000000000000000	0.000000000000000	0.000000000000000	-0.000000850082734
0.000100000000000	0.000000000000000	0.000000000000000	0.000000274811229
0.000000000000000	0.000100000000000	0.000000000000000	-0.000000001374056
0.000000000000000	0.000000000000000	0.000100000000000	-0.000000018435253
0.000725474031327	0.000911788953009	0.000830173124485	-0.000008208843239
0.000000000000000	0.000000000000000	0.000000000000000	0.000000000000000
0.000000000000000	0.000000000000000	0.000000000000000	0.000000000000000

Columns 9 thru 11

-0.000011567184703	-0.533985494195872	-0.024352741122039
-0.000000004442601	0.000000000000000	0.000000000000000
-0.000000001435605	0.000000000000000	0.000000000000000
-0.000000000007178	0.000000000000000	0.000000000000000
0.000000005885384	0.000000000000000	0.000000000000000
0.000000142327155	0.001232788811738	-0.000138158814227
0.000000000000000	0.000000000000000	0.000000000000000
0.000000000000000	0.000000000000000	0.000000000000000
0.000000000000000	0.000000000000000	0.000000000000000

BPL(continued)

0.000000000000000	0.000000000000000	0.000000000000000
0.000000000000000	0.000000000000000	0.000000000000000
0.000000000000000	0.000000000000000	0.000000000000000
0.000000004440806	0.000000000000000	0.000000000000000
-0.000000001435605	0.000000000000000	0.000000000000000
0.000000000007178	0.000000000000000	0.000000000000000
0.000000000096305	0.000000000000000	0.000000000000000
0.000000042882747	0.000000000000000	0.000000000000000
0.000000000000000	0.000000000000000	0.000000000000000
0.000000000000000	0.000000000000000	0.000000000000000

CPL =

Columns 1 thru 4

0.000000000000000	0.000000000000000	0.000000000000000	0.000000000000000
0.000000000000000	0.000000000000000	0.000000000000000	0.000000000000000
-1.000000000000000	0.000000000000000	0.000000000000000	0.000000000000000
0.000000000000000	-1.000000000000000	0.000000000000000	0.000000000000000
0.000000000000000	0.000000000000000	1.000000000000000	0.000000000000000
-0.374812247255921	-0.428076256499133	-0.428711727325246	2.357019064124783
0.000000000000000	0.000000000000000	0.000000000000000	0.000000000000000
0.000000000000000	0.000000000000000	0.000000000000000	0.000000000000000
0.000000000000000	0.000000000000000	0.000000000000000	0.000000000000000
0.000000000000000	0.000000000000000	0.000000000000000	0.000000000000000
0.000000000000000	0.000000000000000	0.000000000000000	0.000000000000000
0.000000000000000	0.000000000000000	0.000000000000000	0.000000000000000
0.000000000000000	0.000000000000000	0.000000000000000	0.000000000000000
0.000000000000000	0.000000000000000	0.000000000000000	0.000000000000000
0.000000000000000	0.000000000000000	0.000000000000000	0.000000000000000
0.000000000000000	0.000000000000000	0.000000000000000	0.000000000000000
0.000000000000000	0.000000000000000	0.000000000000000	0.000000000000000

Columns 5 thru 8

0.000000000000000	0.000000000000000	0.000000000000000	0.000000000000000
0.000000000000000	0.000000000000000	0.000000000000000	0.000000000000000
0.000000000000000	0.000000000000000	0.000000000000000	0.000000000000000
0.000000000000000	0.000000000000000	0.000000000000000	0.000000000000000
0.000000000000000	0.000000000000000	0.000000000000000	0.000000000000000
0.034662045060659	-0.077007510109763	0.000000000000000	0.000000000000000
0.000000000000000	0.000000000000000	0.000000000000000	0.000000000000000
0.000000000000000	0.000000000000000	0.000000000000000	0.000000000000000
0.000000000000000	0.000000000000000	0.000000000000000	0.000000000000000
0.000000000000000	0.000000000000000	0.000000000000000	0.000000000000000
0.000000000000000	0.000000000000000	0.101936799184506	0.000000000000000
0.000000000000000	0.000000000000000	0.000000000000000	0.000000000000000
0.000000000000000	0.000000000000000	0.000000000000000	0.000000000000000
0.000000000000000	0.000000000000000	0.000000000000000	0.000000000000000
0.000000000000000	0.000000000000000	0.000000000000000	0.000000000000000
0.000000000000000	0.000000000000000	0.000000000000000	0.000070873866447

CPL(continued)

0.000000000000000	0.000000000000000	0.000000000000000	0.000000000000000
0.000000000000000	1.000000000000000	0.000000000000000	0.000000000000000

REPORT DOCUMENTATION PAGE

Form Approved
OMB No. 0704-0188

Public reporting burden for this collection of information is estimated to average 1 hour per response, including the time for reviewing instructions, searching existing data sources, gathering and maintaining the data needed, and completing and reviewing the collection of information. Send comments regarding this burden estimate or any other aspect of this collection of information, including suggestions for reducing this burden, to Washington Headquarters Services, Directorate for information Operations and Reports, 1215 Jefferson Davis Highway, Suite 1204, Arlington, VA 22202-4302, and to the Office of Management and Budget, Paperwork Reduction Project (0704-0188), Washington, DC 20503.

1. AGENCY USE ONLY *(Leave blank)*	2. REPORT DATE	3. REPORT TYPE AND DATES COVERED
	June 1992	Contractor Report

4. TITLE AND SUBTITLE

A Study of the Control Problem of the Shoot Side Environment Delivery System of a Closed Crop Growth Research Chamber

5. FUNDING NUMBERS

NCA2-484

6. AUTHOR(S)

C. C. Blackwell and A. L. Blackwell

7. PERFORMING ORGANIZATION NAME(S) AND ADDRESS(ES)

Department of Mechanical Engineering
The University of Texas at Arlington
Arlington, Texas

8. PERFORMING ORGANIZATION REPORT NUMBER

A-92138

9. SPONSORING/MONITORING AGENCY NAME(S) AND ADDRESS(ES)

Ames Research Center
Moffett Field, CA 94035-1000

10. SPONSORING/MONITORING AGENCY REPORT NUMBER

NASA CR-177597

11. SUPPLEMENTARY NOTES

Point of Contact: R. D. MacElroy, Ames Research Center, MS 239-15, Moffett Field, CA 94035-1000
(415) 604-5573 or FTS 464-5573

12a. DISTRIBUTION/AVAILABILITY STATEMENT

Unclassified-Unlimited
Subject Category – 54

12b. DISTRIBUTION CODE

13. ABSTRACT *(Maximum 200 words)*

The details of our initial study of the control problem of the crop shoot environment of a hypothetical closed crop growth research chamber (CGRC) are presented in this report. The configuration of the CGRC is hypothetical because neither a physical subject nor a design existed at the time the study began, a circumstance which is typical of large scale systems control studies. The basis of the control study is a mathematical model which was judged to adequately mimic the relevant dynamics of the system. The CGRC system hardware which is represented in the model includes a plant growth chamber and those control system components considered necessary to provide acceptable realism in the representation. Control of pressure, temperature, and flow rate of the crop shoot environment, along with its oxygen, carbon dioxide, and water concentration is addressed. To account for mass exchange, the group of plants is represented in the model by a source of oxygen, a source of water vapor, and a sink for carbon dioxide. In terms of thermal energy exchange, the group of plants is represented by a surface with an appropriate temperature. Most of the primitive equations which result from the modeling process are nonlinear. The results of a linearization of the primitive equations about an experimental operating condition and a state variable representation which was extracted from the linearized equations are presented. Next, we present the results of a real Jordan decomposition and the repositioning of an undesirable eigenvalue via full state feedback. The state variable representation of the modeling system is of nineteenth order and reflects the eleven control variables and eight system disturbances. Five real eigenvalues are very near zero, with one at zero, three having small magnitude positive values and one having a small magnitude negative value. A Singular Value Decomposition analysis indicates that these non-zero eigenvalues are not the results of numerical error.

14. SUBJECT TERMS

15. NUMBER OF PAGES
105

16. PRICE CODE
A06

17. SECURITY CLASSIFICATION OF REPORT	18. SECURITY CLASSIFICATION OF THIS PAGE	19. SECURITY CLASSIFICATION OF ABSTRACT	20. LIMITATION OF ABSTRACT
Unclassified	Unclassified		